


2004

Effect Of Source Water Blending On Copper Release In Pipe Distribution System: Thermodynamic And Empirical Models

Weizhong Xiao
University of Central Florida

 Part of the [Civil and Environmental Engineering Commons](#)
Find similar works at: <https://stars.library.ucf.edu/etd>
University of Central Florida Libraries <http://library.ucf.edu>

This Doctoral Dissertation (Open Access) is brought to you for free and open access by STARS. It has been accepted for inclusion in Electronic Theses and Dissertations, 2004-2019 by an authorized administrator of STARS. For more information, please contact STARS@ucf.edu.

STARS Citation

Xiao, Weizhong, "Effect Of Source Water Blending On Copper Release In Pipe Distribution System: Thermodynamic And Empirical Models" (2004). *Electronic Theses and Dissertations, 2004-2019*. 123.
<https://stars.library.ucf.edu/etd/123>

EFFECT OF SOURCE WATER BLENDING ON COPPER RELEASE IN PIPE
DISTRIBUTION SYSTEM:
THERMODYNAMIC AND EMPIRICAL MODELS

By

WEIZHONG XIAO

B.S. Environmental Engineering, Southeast Normal University, P.R.China, 1994
M.S. Environmental Engineering, Johns Hopkins University, US, 2001

A dissertation submitted in partial fulfillment of the requirements
for the degree of Doctor of Philosophy
in the Department of Civil and Environmental Engineering
in the College of Engineering and Computer Science
at the University of Central Florida
Orlando, Florida

Spring Term
2004

Advisor: Dr. James S. Taylor

© 2004 Weizhong Xiao

ABSTRACT

This dissertation focuses on copper release in drinking water. Qualitative and quantitative assessment of Cu and Fe corrosion by process water quality was assessed over one year in a field study using finished waters produced from seven different treatment process and eighteen pilot distribution systems (PDSs) that were made from unlined cast iron and galvanized steel pipes, and lined cement and PVC pipes taken from actual distribution systems. Totally seven different waters were studied, which consisted of three source waters: groundwater, surface, and simulated brackish water designated as G1, S1, and RO. With certain pre-established blending ratios, these three waters were blended to form another three waters designated as G2, G3, and G4. Enhanced surface water treatment was CFS, ozonation and GAC filtration, which was designated as S1. The CFS surface water was nanofiltered, which is S2. All seven finished waters were stabilized and chloraminated before entering the PDSs. Corrosion potential was compared qualitatively and quantitatively for all seven waters by monitoring copper and iron release from the PDSs. This dissertation consists of four major parts.

(1) Copper corrosion surface characterization in which the solid corrosion products formed in certain period of exposure to drinking water were tried to be identified with kinds of surface techniques. Surface characterization indicated that major corrosion products consists of cuprite (Cu_2O) as major underneath corrosion layer and tenorite (CuO), cupric hydroxide ($\text{Cu}(\text{OH})_2$) on the top surface. In terms of dissolution/precipitation mechanism controlling the copper concentration in bulk solution, cupric hydroxide thermodynamic model was developed.

(2) Theoretical thermodynamic models were developed to predict the copper release level quantitatively based on controlling solid phases identified in part (1). These models are compared to actual data and relative assessment is made of controlling solid phases.

(3) Non-linear and linear regression models were developed that accommodated the release to total copper for varying water quality. These models were verified using independent data and provide proactive means of assessing and controlling copper release in a varying water quality environment.

(4) Simulation of total copper release was conducted using all possible combinations of water quality produced by blending finished waters from ground, surface and saline sources, which involves the comparison of copper corrosion potentials among reverse osmosis, nanofiltration, enhanced coagulation, lime softening, and conventional drinking water treatment.

ACKNOWLEDGEMENTS

Doctoral research is an intensely individual journey supported by a tremendous team effort. The individual doctoral candidate pushes his/her intellectual, emotional and, at times, physical limits while scores of people work to guide and rejuvenate each of these faculties as the journey goes further. Without the assistance of others, a dissertation cannot flourish. I have been immensely fortunate to have an excellent group of people nurture me and my research over the past two years, and this dissertation would not be complete without recognizing their efforts.

I have benefited greatly during my time at UCF from the tandem efforts of Dr. Hong and Dr. Taylor. Dr. Hong and Taylor know the importance of allowing students the freedom to find their own way, yet at the same time they are always willing and able to give advice. They are interested not only in the research, but also in cultivating abilities that will allow me to excel long after I graduate from UCF. Thank you.

This research would not have accomplished without the works of all of the members of Tampa Bay Water project, including all of the faculty, staff, post-doc and the graduate students. Committee members Dr. James Taylor, Dr. John Dietz, Dr. Andrew Randall and Dr. Yong-ho Sohn provided valuable technical comments and guidance. And, of course, without the instruction of Dr. Hong, my advisor, this dissertation couldn't have been possible. In particular I will never forget Dr. Norris, every time I face the technical knottiness in the Lab., you are always the first person I seek help for.

I am very grateful to the American Water Works Association Research Foundation and Tampa Bay Water under a Tailored Collaboration Project, "Required Treatment and Water

Quality Criteria for Distribution System Blending of Treated Surface, Ground, and Saline Sources” which support me the finically through my research at UCF.

I would also like to acknowledge my family, friends who provided necessary support and encouragement during, my more than 20-year schooling. Without you, I couldn’t have made it.

TABLE OF CONTENTS

LIST OF FIGUTRES	x
LIST OF TABLES	xii
LIST OF ABBRECIATIONS	xiii
Chapter 1 Literature Survey	1
INTRODUCTION	1
PROBLEM STATEMENT AND STUDY OBJECTIVES.....	2
LITERATURE SURVEY.....	4
Overview of Copper Chemistry	4
Kinetics	19
Surface Characterization	21
Scanning Electron Microscopy (SEM) and Energy Dispersive X-ray Spectroscopy (EDS)	
.....	22
X-Ray Diffraction (XRD) and Grazing Angle X-Ray Diffraction (X’pert) System	25
X-Ray Photoelectron Spectroscopy (XPS)	27
REFERENCES	28
Chapter 2 Surface Characterization and The Theoretical Modeling of Copper Corrosion in Drinking Water Pipe Distribution System	34
INTRODUCTION	34
EXPERIMENTAL METHODS	37
Source Water Production and Blending.....	37
Pilot Pipe Distribution Systems	37
Copper Loop and Coupon Study.....	39
Pipe Surface Characterization.....	40
RESULTS AND DISCUSSIONS.....	41
Observations by SEM/EDS	41
Investigation of Corrosion Products by XRD.....	46
Investigation of Corrosion Products by XPS.....	48
The Theoretical model development	55
CONCLUSION.....	58
REFERENCES	59
Chapter 3 Effect of Blended Water on Copper Corrosion Release in Drinking Water Pipe Distribution System and Empirical Model Development.....	63
INTRODUCTION	63
EXPERIMENT METHODS	66
Source water production and blending	67
Copper corrosion loops.....	69
Water quality monitoring.....	70
RESULTS AND DISCUSSION.....	71

Pilot-Scale Experiment Study	71
Source water blending and water quality variations	71
Copper release under various water qualities	74
Effect of pH.....	74
Effect of Alkalinity	76
Effect of Typical Anions-Chloride and Sulfate	78
Effect of Typical Cation – Calcium.....	80
Other Water Quality Parameter Effects	82
Controlled Experiment Study-Isolation of the Anion Effect	83
Empirical Model Development.....	86
Linear Regression	86
Nonlinear Regression.....	89
CONCLUSIONS.....	91
REFERENCES	93
 Chapter 4 Simulation of Copper Release in Pipe Distribution System and Copper Rule Compliance	96
INTRODUCTION	96
EXPERIMENTS AND METHODS.....	97
Pilot Unit Design.....	97
Lead and Copper Loops.....	99
Statistical Model Development.....	100
RESULTS AND DISCUSSIONS.....	101
Statistical Model Development.....	101
Linear Model.....	102
Non-linear Model.....	102
Verification of Predictive Models.....	106
Simulation of Copper Rule Compliance.....	107
CONCLUSIONS.....	111
REFERENCES	111
 Chapter 5 Comparison of Corrosive Potential by Source and Process.....	114
INTRODUCTION	114
EXPERIMENTAL METHODS	115
Pilot Plant.....	115
Lead and Copper Loops.....	117
RESULTS AND DISCUSSION.....	119
Water Quality of nanofiltration and conventional treatment processes.....	119
Corrosive Effect of Typical Ions on Iron and Copper	120
Group 1 water quality	121
Group 2 water quality	121
Group 3 water quality	122
Corrosion Potential Comparison.....	122
G1, S1 and RO	122

Physical Factor Impact.....	122
Chemical Factor Impact.....	124
Comparison of Nanofiltration and GAC filtration.....	124
Physical Factor Impact.....	126
Chemical Factor Impacts	126
Comparison of Nanofiltration and Softening.....	128
Physical Factor Examination	129
Chemical Factor Consideration.....	129
General Process Comments	130
CONCLUSION.....	131
REFERENCES	132

LIST OF FIGUTRES

Figure 1.1 Simplified Cu (II) hydroxo and carbonate complexes solubility	6
Figure 1.2 Cu(II) E-pH diagram with 10 ⁻⁴ M dissolved Cu(II) concentration copper chemistry ...	7
Figure 1.3 Across-Section Corrosion Product distribution.....	12
Figure 1.4 Copper Level in Short-Term Stagnation Experiment.....	20
Figure 2.1 Pilot-scale pipe distribution system.....	38
Figure 2.2 Eighteen copper loops connected with each PDS	40
Figure 2.3 SEM (JEO-6400) image of a copper coupon that was incubated in a high alkalinity groundwater and covered with black deposits as shown in the upper right corner.	42
Figure 2.4 SEM (JEO-6400) image from a copper coupon incubated in treated surface water (S1) and covered with uniformly distributed and lose green deposits.....	43
Figure 2.5 Representative SEM (JEO-6400) image of copper coupon incubated in desalinated water (RO) and covered with an easily removed green deposit shown in upper right corner	44
Figure 2.6 EDS(JEO-6400) spectra for a copper coupon incubated in desalinated water.....	46
Figure 2.7 X'pert patterns of corrosion products formed on copper coupons in a groundwater environment for varying times of incubation.....	47
Figure 2.8 Representative high-resolution XPS deconvolution Cu2P3/2 peak of corrosion products formed during ground water incubation.....	49
Figure 2.9 Representative high-resolution XPS deconvolution Cu2P3/2 peak of corrosion products formed during with ground water incubation.....	49
Figure 2.10 Cuprite (Cu ₂ O) content percentage variation versus the incubation time	51
Figure 2.11 Copper corrosion products sensitivity analysis –Alkalinity. X axis represent alkalinity as mg/L CaCO ₃ . Y axis represent the scale layer phase contents.....	52
Figure 2.12 Copper corrosion products sensitivity analysis –pH. X axis represent pH value. Y axis represent the scale layer phase contents.	53
Figure 2.13 Thermodynamic models for copper release versus pH and alkalinity for CuO and Cu(OH ₂) controlling solid phases.	58
Figure 3.1:Pilot-scale PDS research site, fourteen hybrid material pipelines and four single material pipelines.	67
Figure 3.2 Copper loops containing separate lead coupons used for corrosion study.	70
Figure 3.3 pH effect on total copper release	75
Figure 3.4 Alkalinity effect on copper release.....	77
Figure 3.5 Chloride effect on total copper release.....	79
Figure 3.6 Sulfate effect on total copper release.....	80
Figure 3.7 Copper release versus calcium and silica	81
Figure 3.8 Normalized calcium effect on total copper release	81
Figure 3.9 Normalized silica effect on total copper release.....	82
Figure 3.10 The effect of alkalinity on total copper release at constant chlorides and sulfates ...	84
Figure 3.11 The effect of chloride on total copper release at constant pH, alkalinity and sulfates	85
Figure 3.12 The effect of sulfates on total copper release at constant pH, alkalinity and chlorides	86

Figure 3.13 Actual and predicted total copper by linear regression	88
Figure 3.14 Actual and predicted total copper by non- linear regression	90
Figure 4.1 Pilot-scale distribution system research site. Left side is the whole site picture, right one is the 18 PDSs consisted of 14 hybrid and four single materials	99
Figure 4.2 Copper loops connecting with individual PDSs effluent for LCR compliance study	100
Figure 4.3 Actual versus predicted ninetyth percentile copper concentrations using linear mode	105
Figure 4.4 Actual versus predicted ninetyth percentile copper concentrations using non-linear model.....	106
Figure 4.5 Verification plot of linear model	106
Figure 4.6 Verification plot of non-linear model.....	107
Figure 4.7 Ternary diagram showing predicted ninetyth percentile copper concentration for blends of finished ground, surface and desalinated water using linear model.....	110
Figure 4.8 Ternary diagram showing predicted ninetyth percentile copper concentration for blends of finished ground, surface and desalinated water using non-linear mo	110
Figure 5.1 Pilot-scale pipe distribution system research site. Fourteen hybrid material pipes and four single material pipelines.....	117
Figure 5.2 Eighteen identical copper loops connecting with eighteen PDSs for LCR study	118
Figure 5.3 G1, S1 and RO total copper release.....	123
Figure 5.4 G1, S1 and RO total iron release	123
Figure 5.5 S1 and S2 iron release	125
Figure 5.6 S1 and S2 copper release	126
Figure 5.7 G3 and G4 iron release	128
Figure 5.8 G3 and G4 copper release.....	129

LIST OF TABLES

Table 1.1 Thermodynamic reactions and corresponding equilibrium constants	8
Table 2.1 Corrosion scale composition during a three month PDS incubation period as determined by XPS analysis.	50
Table 2.2 Aquatic reactions and equilibrium constants involved in model development expressed as logarithm scale. ORP used in monovalent/divalent conversion is 38mV	55
Table 3.1 Pilot-scale experiment water resource, blending scenarios, and related unit processes description.....	68
Table 3.2 Blending scenarios and PDS pipeline influent water distribution	72
Table 3.3 Source water blending ratios and their resultant ten water quality parameters feeding copper loops. Composition symbols refer to as Table 3.1	73
Table 3.4 Linear statistical correlation coefficient matrix of water quality parameters of interest	73
Table 4.1 Treatment systems and blending scenarios.....	98
Table 4.2 Finished groundwater (G1), surface water (S1) and desalinization (RO) water quality	102
Table 4.3 Water quality range and predicted ninetyth percentile copper concentrations	109
Table 5.1 Water source and treatment systems.....	116
Table 5.2 Blending ratios and influent copper loop water quality.....	119
Table 5.3 Relative ranking of processes on copper and iron release for blending project	131

LIST OF ABBREVIATIONS

AAS	Atomic absorption spectrum
Alka.	Alkalinity
AWWA	American Water Works Association
Cond.	Conductivity
DIC	Dissolved inorganic carbon
DICu	Dissolved inorganic copper
DL	Detection limit
DO	Dissolved oxygen
EPA	Environment Protection Agency
MCL	Maximum contamination level
MCLG	Maximum contamination level goal
LCR	Lead and Copper Rule
PDS	Pilot pipe distribution system
RO	Reverse Osmosis
SHE	Standard hydrogen electrode
TBW	Tampa Bay Water
TDS	Total dissolved solid
THM	Trihalomethanes
XPS	X-ray Photoelectron Spectroscopy
XRD	X-Ray Diffraction

Chapter 1 Literature Survey

Introduction

The investigation conducted and presented within this dissertation is part of the research objectives of tailored collaboration project: “Required Treatment and Water Quality Criteria for Distribution System Blending of Treated Surface, Ground, and Saline Sources”, which was supported by the American Water Works Association Research Foundation and Tampa Bay Water (TBW). The major goal of this project is to investigate the drinking water quality changes and resultant impacts on pipe distribution system (PDS) under various blending conditions of different source waters. This research will help TBW to furnish quality drinking water to customers, and avoid detrimental effect on current PDS. The study of copper corrosion by-products release qualitatively and quantitatively is the primary objective of in this dissertation. Four individual parts comprising this dissertation are: (1)surface characterization and theoretical thermodynamic model development; (2)water quality effects on copper release and statistically predictive model development; (3)Lead and Copper Rule (LCR) compliance and its simulation for Florida area; (4)corrosion potential comparison of lime softening, granular activated carbon filtration.

In this chapter, the motivation for this study is presented. This motivation is described in the context of water quality issues facing Tampa Bay Water (TBW). After this presentation, the literature survey is summarized to focus on the basic copper corrosion theory, and surface characterizations of corrosion products. This chapter is concluded with the brief description of pilot-scale experiment research system. Other related issues will be presented in the following chapters.

Problem Statement and Study Objectives

Copper plumbing corrosion by-products release represents one of the highest concerns of drinking water customers nowadays. With increasingly stringent regulation, understanding its release especially in full-scale water utilities has never been more crucial. However, several decades of research to explain these seemingly simple phenomena have not been totally never been accomplished. Until today, the water utilities still in great extent rely on their operating on the experience.

Historically, in Florida about 87 percent of public water supplies were derived from groundwater.[1] However, with the depletion of groundwater, alternative water sources have to be developed to meet the increasing water demand. Except the surface water, brackish water, obviously, will be the one given most concern due to the particular geographical location. Considering this context, the blended water consisting of ground, surface, and desalinated water will compose the primary water supply in the near future. At this moment, the projected blending ratio for TBW will be 62%, 27%, 11%.[2] To make use of the current water treatment facilities, the ideal approaches making this blending water is to treat each kind of water individually, and then blend them together before feeding the municipal pipe distribution systems.

However, the problem accompanying this blending water is the influent water quality would vary depending upon the specific blending ratio and upon the combination of processes utilized for each kind of water treatment. Another fact that the TBW has to consider is the corrosion durability of the old pipe distribution systems which have been serving the water supply for several decades. The corrosion layers accumulated on the pipe surface during history

has to be affected due to the water quality changes. One of possible detriments is the falling off of those corrosion layers because of the impact on their coherence, another possible phenomena is the corrosion rate may accelerate arising from the water quality alteration. For copper, most of usage is customer plumbing in both cold and hot waters. Whether or not the blending water has negative impact on the copper concentration in drinking water is also a highly concern.

All the facing problems need have to be answered immediately with the inception of blending issue. More practically, how much the deviation more or less would be once the previously well-developed in bench-scale models are applied in full-scale operation especially in drinking water circumstance. All of these uncertain factors with blending promote the necessity of large-scale experiment in advance to the realization of conversion from single to mixed waters. Specifically, the following research points are presented in this dissertation.

- Copper corrosion products identification by using surface characterization techniques.
- Determine the controlling solid phases responsible for the copper release level in bulk solution
- Theoretical thermodynamic model development serving as prediction
- Evaluation of water quality impact on copper release
- Statistical regression model develop for prediction purpose.
- Evaluation of potential of LCR compliance with various blending ratios
- With the assistance of statistical models, estimate the copper concentration under projected blending ratios.

- Evaluation of corrosion potential for kinds of processes including nano-filtration, lime softening, and granular activated carbon filtration(GAC).

Literature Survey

Overview of Copper Chemistry

Copper and copper alloy, thanks to their corrosion resistance and ease of installation, have been extensively employed in drinking water pipe distribution systems and utilities, especially in household plumbing materials. Without dissolved oxygen (DO), residual chlorine, or other electron acceptors, copper is very corrosion-resistant because of its noble electrochemical property. The reduction potential of copper is 0.339 volt versus SHE (Standard Hydrogen Electrode) for copper (II), and 0.518 volt versus SHE for copper (I) with respect to pure copper.[3,4] Despite its corrosion resistance, copper corrosion does occur under the normal drinking water conditions, as the existence of DO and residual chlorine creates a general potential range of 0.6 to 1.2 V versus SHE environment.[5,6,7] The copper(III) and copper(IV) oxidation states are known to exist due to their $3d^{10}4s^1$ transition position in periodic table and their much higher ionization enthalpies. However, if no powerful oxidizers exist in the drinking water matrix, they have much smaller roles in corrosion mechanisms.[8] Therefore, the primary concern of this proposal is the corrosion of Cu(0) to copper(I) and copper(II) and their corrosion by-products.

Due to the maximum contamination level goal (MCLG) of copper and lead standards, the promulgation of the LCR (Lead and Copper Rule) by USPEA in 1991 has required approximately 80,000 water utilities nationally to monitor for lead and copper levels.[9,10,11]

For both of round two monitoring, approximately 7% of water utilities exceeded the copper action level.[12] Nonetheless, the copper corrosion still exists as a critical issue, which requires extensive research on how to control this recalcitrant problem in drinking water industry.

With the existence of oxidizer, Copper (0) is oxidized to Cu (I) (cuprous) and Cu (II) (cupric) by following one-electron transfer procedure by tuning mechanism [8,13,14,15] With the immediately formed free cuprous and cupric ions as well as soluble complexes accumulating locally, corresponding insoluble precipitates begins to start up till the precipitation/dissolution reaches equilibrium[3,8]. The overall thermodynamic stability of types of copper complexes are generally depicted in a E-pH diagram in which the electro potential, pH, and solid/liquid phases are correlated delimited pH and electro potential. Another commonly used graphic expression describing this thermodynamics is the solubility diagram in which liquid and solid phases are correlated with pH, solubility products, and dissolved species activities. A simplified example diagram for each expression is given in Figure 0.1 and Figure 0.2, respectively, in which only hydroxo and carbonate complexes are considered. Detailed aquatic reactions probably involved and corresponding thermodynamic constants are listed in Table 0.1.

In drinking water, the primary oxidizer agents are dissolved oxygen and free chlorine species. Following the oxidation, dissolved cuprous or cupric ions form complexes with aqueous anion ligands and other solid phases such as malachite ($\text{Cu}_2(\text{OH})_2\text{CO}_3$), atacamite ($\text{Cu}_4(\text{OH})_6\text{Cl}_2$).[16,17,18,19,20]

The important factors affecting the soluble copper complexes include hydroxide (i.e. pH), carbonate (i.e. Alkalinity or Dissolved Inorganic Carbon (DIC)), sulfate, chloride, ammonia,

orthophosphate, which are the mainly concern in common drinking water environment. Among these, the first four factors are the most important, due to their relative higher activities.

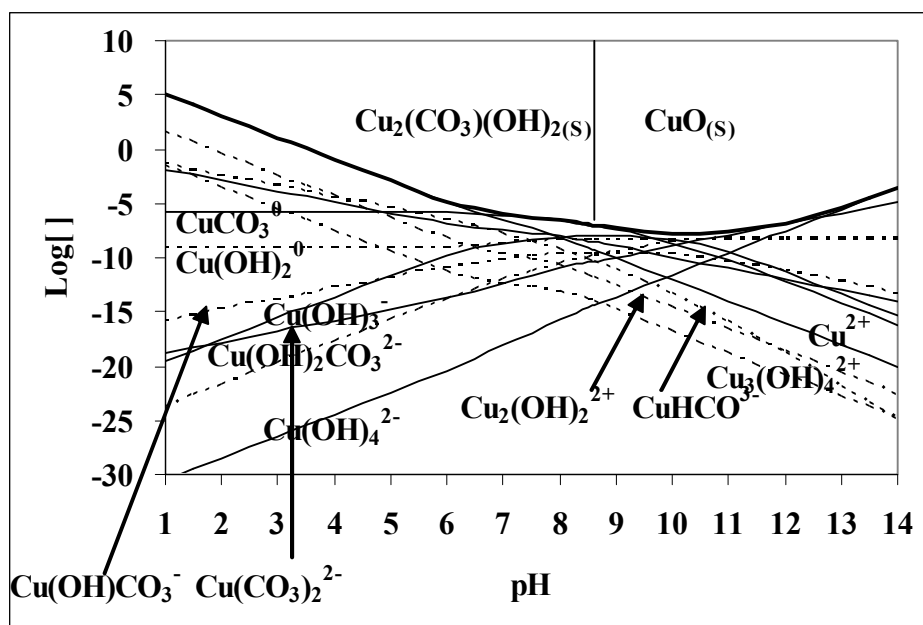


Figure 0.1 Simplified Cu (II) hydroxo and carbonate complexes solubility

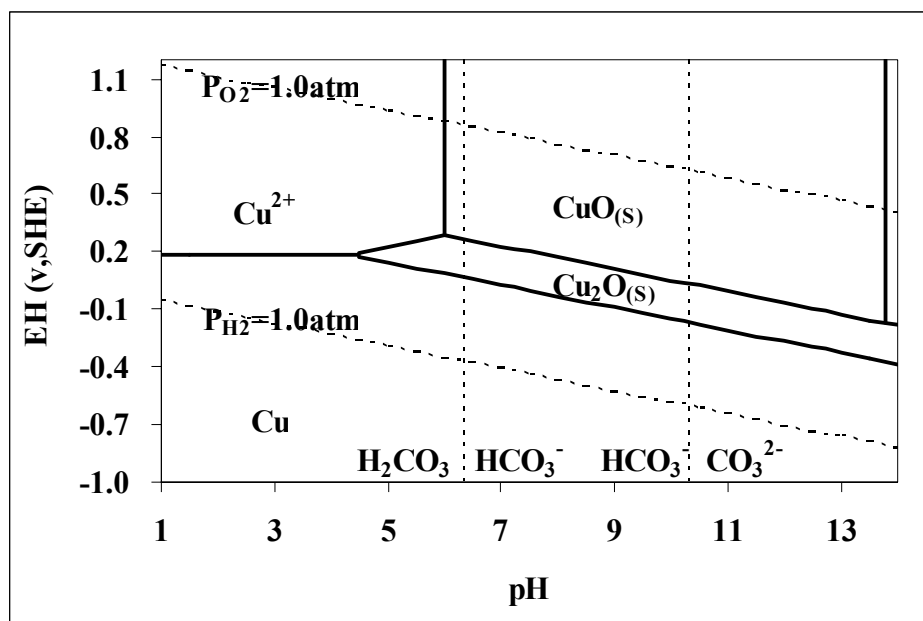


Figure 0.2 Cu(II) E-pH diagram with 10⁻⁴M dissolved Cu(II) concentration copper chemistry

Table 0.1 Thermodynamic reactions and corresponding equilibrium constants

No.	Reactions	Log(K) or log(β) at 25 °C
<i>Hydroxide Species (divalent)</i>		
1	$\text{Cu}^{2+} + \text{H}_2\text{O} \leftrightarrow \text{CuOH}^+ + \text{H}^+$	-7.96
2	$\text{Cu}^{2+} + 2\text{H}_2\text{O} \leftrightarrow \text{Cu}(\text{OH})_2^0 + 2\text{H}^+$	-16.24
3	$\text{Cu}^{2+} + 3\text{H}_2\text{O} \leftrightarrow \text{Cu}(\text{OH})_3^- + 3\text{H}^+$	-26.90
4	$\text{Cu}^{2+} + 4\text{H}_2\text{O} \leftrightarrow \text{Cu}(\text{OH})_4^{2-} + 4\text{H}^+$	-39.56
5	$2\text{Cu}^{2+} + 2\text{H}_2\text{O} \leftrightarrow \text{Cu}_2(\text{OH})_2^{2+} + 2\text{H}^+$	-10.58
6	$3\text{Cu}^{2+} + 4\text{H}_2\text{O} \leftrightarrow \text{Cu}_3(\text{OH})_4^{2+} + 4\text{H}^+$	-20.76
<i>Carbonate Species (divalent)</i>		
7	$\text{Cu}^{2+} + \text{H}^+ + \text{CO}_3^{2-} \leftrightarrow \text{CuHCO}_3^+$	12.13
8	$\text{Cu}^{2+} + \text{CO}_3^{2-} \leftrightarrow \text{CuCO}_3^0$	6.82
9	$\text{Cu}^{2+} + 2\text{CO}_3^{2-} \leftrightarrow \text{Cu}(\text{CO}_3)_2^{2-}$	10.60
10	$\text{Cu}^{2+} + \text{CO}_3^{2-} + \text{H}_2\text{O} \leftrightarrow \text{Cu}(\text{OH})(\text{CO}_3)^- + \text{H}^+$	-4.25
11	$\text{Cu}^{2+} + \text{CO}_3^{2-} + 2\text{H}_2\text{O} \leftrightarrow \text{Cu}(\text{OH})_2(\text{CO}_3)^{2-} + 2\text{H}^+$	-13.14
<i>Chloride, and Sulfate Species (divalent)</i>		
12	$\text{Cu}^{2+} + \text{SO}_4^{2-} \leftrightarrow \text{CuSO}_4^0$	2.36
13	$\text{Cu}^{2+} + \text{Cl}^- \leftrightarrow \text{CuCl}^+$	0.40
14	$\text{Cu}^{2+} + 2\text{Cl}^- \leftrightarrow \text{CuCl}_2^0$	-0.12
<i>Cuprous Species (monovalent)</i>		
15	$\text{Cu}^+ + \text{Cl}^- \leftrightarrow \text{CuCl}^0$	2.70
16	$\text{Cu}^+ + 2\text{Cl}^- \leftrightarrow \text{CuCl}_2^-$	5.48
17	$\text{Cu}^+ + 3\text{Cl}^- \leftrightarrow \text{CuCl}_3^{2-}$	4.81
18	$2\text{Cu}^+ + 4\text{Cl}^- \leftrightarrow \text{Cu}_2\text{Cl}_4^{2-}$	10.32
<i>Conversion between cuprous and cupric copper</i>		
19	$\text{Cu}^+ \leftrightarrow \text{Cu}^{2+} + \text{e}^-$	-2.715

For Cu (I), the predominant solid phases are Cu_2O (cuprite) and $\text{Cu}(\text{OH})$. Thermodynamic calculation indicates the inevitable transformation from $\text{Cu}(\text{OH})$ to Cu_2O , but

the kinetic limitation makes such solid phases coexist, which can be observed by surface techniques. The fate of dissolved Cu (I) species depends on primarily chloride and ammonia among which chloride is much more significant as the activity of chloride is far higher than ammonia, although the cuprous chloride complexes are not as strong as ammine complexes[12]. Cuprous ion also forms very weak hydrolysis species, such as $\text{Cu}(\text{OH})_0$, CuHCO_3^0 , and CuCO_3^- , but no observation of these species are generally reported in the literature. The theoretical formation of such weak complexes have been published to provide the explanation of some trends in rates of oxidation by DO.[21]

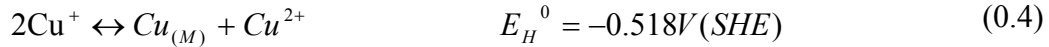
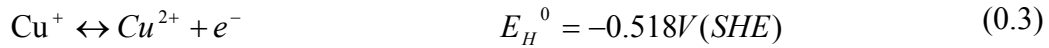
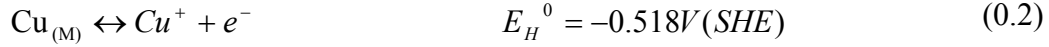
Compared with cuprous, cupric species are much more complicated, because of the higher possible cupric coordinate number[3,22], and the multiple solid phases.[22] Among Cu(II) complexes, inconsistent complexation formation constants (β) can be seen in most publications, particularly for complex $\text{Cu}(\text{OH})_2^0$, the reported $\log \beta$ value ranges from -13.7 to less than -17.3 for the reaction equation (0.1)[12]



Under the typical reduction potential of drinking water condition (range 0.6 to 1.2 volt versus SHE), three possible pathways are responsible for the production of the high oxidation state cupric ion. One is the consecutive single electron transfer in series, another is the simultaneous transfer of two electrons; the last possible approach is the disproportionate transformation of cuprous ion.[3,13]

Evidence in the literature indicates that the first and the third mechanism are more favorable pathways.[13,14] With the electron loss, the ratio of cupric to cuprous ion activity

increases. These variations can be estimated by using Nernst Equation. Equations describing these two favorable redox pathways are listed in equation (0.2) through equation (0.4)



where $\text{Cu}_{(M)}$ is metal copper. More detailed interfacial redox electron transfer are available in the numerous references. [23,24]

The formation of cuprous complexes results from two possible reactions, one is the direct interaction of ligands with Cu(I) specie, another is the reduction of Cu(II) species with metal copper. An example of these reactions between cuprous and cupric species is equation (0.5)



In equation (0.5), octahedral complex $\text{Cu}(\text{NH}_3)_4^{2+}$ (more exactly, it should be written as $\text{Cu}(\text{H}_2\text{O})_2(\text{NH}_3)_4^{2+}$) containing electron-deficient Cu^{2+} tends to seek electron-sufficient species, meanwhile the metal copper surface provides the electron reservoir. Therefore, the copper will lose electrons to form cuprous complexes by obtaining the ammonia ligands from cuprous complexes. It is the large size ammonia and has relatively weak and partial covalent complex bonds in which electron cloud concentrates on nitrogen atom more, making such disproportionation happen.

Another reaction mentioned frequently is chloro complex. Although this complex is not as strong as ammonia complex[25], the concentration of chloride is much higher than ammonia in normal drinking water, and chlorides have higher mobility compared with ammonia, thus the

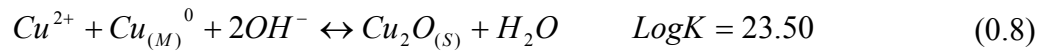
chloro complex is more significant.[26] The ammonia concentration should be higher than chloro complex if these two ligands have same concentration.[27]

Regarding Cu(I) solid phase, there are considerable discrepancies in the literature on the solubility constants for cuprite ($\text{Cu}_2\text{O}_{(s)}$) and cupric hydroxide $\text{CuOH}_{(s)}$. By far, two proposed mechanisms responsible for the formation of $\text{Cu}_2\text{O}_{(s)}$: (i) direct formation of Cu(I) oxide/hydroxide with participation of H_2O and $\text{O}_{2(aq)}$, and (ii) rapid dissolution of $\text{Cu}(\text{OH})_{2(s)}$ followed by the disproportionation reaction.[28] Direct oxidation pathway is shown in equation (0.6)



Unlike traditional electrochemical corrosion procedure, this oxidation is believed not to involve electron transport through metal bulk when immersed in oxygenated aqueous solution,[29] because during the procedure of copper corroding and producing a compact adherent film of cuprite ($\text{Cu}_2\text{O}_{(s)}$), the electrons transferred go through the inner-sphere rather than anodic out-sphere corrosion mechanisms.[29]

Overall reactions of disproportionation pathway of $\text{Cu}_2\text{O}_{(s)}$ formation are shown in equation (0.7) and equation (0.8). By this pathway, electrons follow the outer-sphere mechanisms [22]



Between these two cuprite formation pathways, the first reaction happens very quickly with clear copper surface where oxygen is sufficient, and the resulting scale layer is compact and

may function as semiconductors. The characteristics of semiconductor support the further redox reactions at the film boundary. With the formation of cuprite layer proceeding, oxygen is reduced at the exterior of the adherent layer, therefore the further oxidation produces a porous layer, not so compact as the underlying cuprite layer. Further oxidation of cuprite to cupric species and subsequent cupric precipitation may occur and dominate the outer layer reactions until the equilibrium is achieved.[29] Illustration of uniform corrosion scale layers and their distribution are presented Figure 0.3

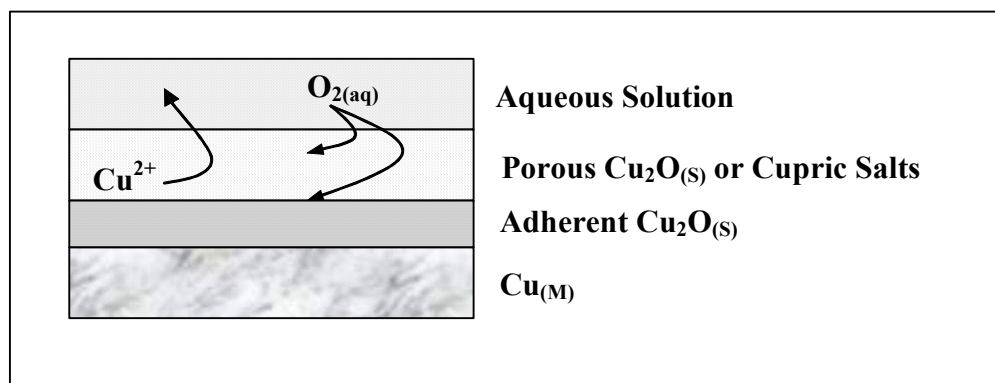


Figure 0.3 Across-Section Corrosion Product distribution

Cu(II) ions formed from oxidation of Cu(I) enter the aqueous solution, interact with ligands, and increase the solubility considerably. Among ligands, the most important species include hydroxo and carbonate, which are responsible for the high level copper in drinking water.[12] The concentration of complexes strongly depends on ligand availability, in other words, pH, DIC, chloride, sulfate concentration and their diffusion coefficients. With stagnant

state, theoretical calculation indicates the DICu(II) is around 0.025ppm with pH 8.0 for hydroxo complex control. Thus it is believed that hydroxo complex is not the only factor affecting the copper level, carbonate complex also contributes significantly to the overall copper level.

Important Cu(II) solid phases formed include tenorite ($\text{CuO}_{(s)}$), cupric hydroxide ($\text{Cu}(\text{OH})_{2(s)}$), cupric carbonate ($\text{CuCO}_{3(s)}$), and malachite ($\text{Cu}_2\text{CO}_3(\text{OH})_{2(s)}$). Mechanisms responsible for these solid phase formation could be inferred from the solubility theory if we assume that (i) copper surface is clean, (ii) particles of solid phase is big enough and (iii) dissolved copper concentration gradient is zero. Unfortunately, such strict assumptions are not suitable to be used in the practical case to predict the tap water copper level, because the passivation film would be formed on the metal surface either loosely or tightly, meanwhile the dissolved copper gradient is not zero, and oxygen going through the passivation film could be the rate limiting step.[30].

The transformation from $\text{Cu}(\text{OH})_{2(s)}$ to $\text{CuO}_{(s)}$ is exothermic ($\Delta G^0 = -5.23 \text{ KJ/mol}$), and supports that the controlling solid phase should be $\text{CuO}_{(s)}$ if only hydroxo ligands exist. [12] However, evidences in the literature implicate that the predominant phase should be $\text{Cu}(\text{OH})_{2(s)}$ instead of $\text{CuO}_{(s)}$ in pure water condition with short-term period. The reason is the particle of $\text{CuO}_{(s)}$ formed is much finer compared with $\text{Cu}(\text{OH})_{2(s)}$ so that the $\text{CuO}_{(s)}$ is less stable than coarse $\text{Cu}(\text{OH})_{2(s)}$ according Ostwald Step Rule.[24]

Extensive publications stated the predominant solid phase in aged drinking water pipe at neutral pH is malachite ($\text{Cu}_2\text{CO}_3(\text{OH})_{2(s)}$). [29,30] However, in the new copper pipe, $\text{Cu}(\text{OH})_{2(s)}$ would be the predominant solid phase.[31]. The detailed reason controlling the transformation between the new and aged corrosion by-product, unfortunately, are not well-understood.

With copper entering in the liquid phase after losing electron, the concentration of ions oxidized near the solid-liquid interface is higher than the bulk body if no strong hydraulic shear occurs. Such accumulation makes the Ion Activity Product (IAP) higher until the critical cluster is formed and provides the basis of nucleation and the consequent crystal growth and ripening in terms of carbonate and hydroxo complexes. Such diffusion, adsorption, and nucleation for precipitation would happen simultaneously[24,32]. Therefore, the final solid phase under potable water environment is a mixture of passivation layer and precipitate, not a single solid phase and without clear boundary among these solid phases. Here, by passivation layer, we mean the, while precipitate, we mean the resultant species when IAP is greater than their K_{sp} .

The effect of water chemistry on the copper dissolution is understood based on their IAP value. Their effects on the formation of passivation layer is not studied well based on the literature review. The combination of these factors may either change the passivation film formation pathways or vary the film formation kinetics.

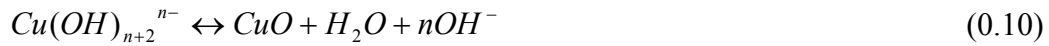
An important consideration with respect to copper level in tap water is the control of copper solubility, thus the minimum potential dissolved copper activity. The dissolved Cu (I) species, however, does not occupy the important position in the entire copper contaminants, therefore, the cuprosolvency regarding cupric species is the central concern.[12] Based on this view of point, most of recent studies focus on the impact of water quality on copper corrosion, in other words, the composition of corrosive surroundings.

Precipitation of copper differs from dissolution in many respects, especially the formation of precipitate and of soluble complexes.[33,34,35,36,37,38,] In most cases, the complexation equilibrium between central ion and ligands are more or less rapid, the composition and

constants are easier to measure or calculated. Precipitation, however, is much more complicated, many processes are involved such as the induction of supersaturation, nucleation, particle growth, Ostwald ripening, recrystallization, and agglomeration. Each of these procedures is heavily sensitive to chemical features such as pH, alkalinity, anion species and physical factor such as temperature of water as well as aging duration time. The combined interactions contribute the poor reproducibility of ill-defined solid phases and consequent inconsistent solubility constants.

In drinking water, possible controlling solid phases could be basic cupric carbonate $\text{Cu}_2\text{CO}_3(\text{OH})_2$ (malachite), cupric hydroxide $\text{Cu}(\text{OH})_2$, and cupric oxide CuO (tenorite) in descending solubility sequence. The formation of malachite however requires exceedingly intense carbonate/bicarbonate anion concentration which seldom happens in typical drinking water conditions even through the appearance of malachite has been recorded in literatures. Tenorite and cupric hydroxide both could show up and control the copper release in terms of precipitation/dissolution mechanism depending the aging period. Evidences indicated that the freshly precipitated solid phase very probably be metastable cupric hydroxide. In the following aging processes of $\text{Cu}(\text{OH})_2$ in water, each of the below four mechanisms could be predominant: (1) ordering of the hydroxide structures, that is the procedure of converting the amorphous status to crystalline substance, (2) growth of the particle, in this procedure, the crystalline structure may not form, the amorphous structure still continue, this is also called Ostwald ripening. (3) dehydration of hydroxide, this mechanism is rather water quality sensitive, especially the pH sensitive; (4) hydration. Because those four mechanisms may be involved simultaneously other than subsequently due to the continuously changed water quality, thus the resultant solid phases modifications are poorly predicted and non-homogeneous. With the formation of the initial

amorphous and unstable active crystalline $\text{Cu}(\text{OH})_2$, they undergo deactivation to be more stable (Ostwald ripening) or direct dehydration to be tenorite (CuO). Before dehydration happens, some researchers suggested the hydration occurs first, in other words, complexation then following dehydration as following reactions (0.9) and (0.10).[33,35]



Thermodynamically, controlling solid phases cannot coexist since the inevitable transformation of one to another-Solid phase rule. The kinetics, however, limits this application, in other words, those solid phases do coexist and the composite phases may determine the characteristics of the system. Intermediate species as active $\text{Cu}(\text{OH})_2$, freshly formed CuO and so on make the correct determination of appropriate solubility constants not possible. Many literatures build up their models on $\text{Cu}(\text{OH})_2$ control due to the closest prediction magnitude, and some of them demonstrated their conclusion from the existence of X-ray peaks of $\text{Cu}(\text{OH})_2$. In our study, however, the X-ray peak of $\text{Cu}(\text{OH})_2$ never showed up, that indicated the $\text{Cu}(\text{OH})_2$ layer is really thin on the substrate interface.

With precipitation/dissolution chemistry as determinative model of copper release in drinking water, substantial researches have been made to find out the primary factors of water quality affecting the copper level. It is now widely accepted that alkalinity, pH are the most important factors, other inorganic anions such as chloride, phosphate, neutral dissolved oxygen, chlorine residual, natural organic matter as well as temperature, microorganisms also have their influence at specific case, but not significant comparing with those two factors. Edward et. al. proposed a linear function describing increasing soluble copper versus higher alkalinity at

constant pH from their pipe-rig test experiment, and they found the linear coefficients change with varying pH. Such similar trends also were published in other literatures. pH, on the other hand, has the opposite effect from alkalinity, that is increasing pH reduce copper release. The cooperated effect by alkalinity and pH sometimes confuses water utilities the general trend plots in which there is no obvious relationship could be concluded even during long term investigation. Most of literature illustrate the principles explaining alkalinity and pH effects as solubility models in which (1)soluble carbonate complexes dominate the soluble copper species, (2)the free cupric ion concentration is controlled by cupric hydroxide assuming the thermodynamic equilibrium has been reached.

Although these single factor effects have been investigated exhaustively, there still exists difficulty to make accurate prediction of copper level even with clearly known water quality. Literature review indicates that there are at least five reasons responsible for this discrepancy except for those mentioned earlier (1)kinetic limitation, that is the hypothetical equilibrium may not be established or be damaged among soluble and solid phases during the investigation period; (2)the actual controlling solids may consist of several intermediate phases due to asynchronous transformation of phases such as the coexistence of fresh, aged precipitated cupric hydroxide and cuprite (CuO), the latter is believed to be dehydration product of cupric hydroxide or the products of further oxidation of cuprite; (3)inconsistent equilibrium constants have been used in different researches, this uncertainty even could create conflict prediction with each other. (4)confounding effect. Alkalinity, like described above, is proportional to the copper level at he most cases, but some research suggested the opposite result if the water is soft, that is the copper

concentration would be higher with low alkalinity in soft water. Consequently, in order to evaluate the alkalinity effect, the hardness has to be known. (5)particulate interference.

All these facts make the actual prediction based on theoretical consideration more difficult, and in most cases, only wide range and general trends could be estimated. In great extent, water utilities still rely on empirical experience to estimate the copper concentration. Therefore, pilot scale experiments are strongly recommended in order to supply satisfactory water into pipe distribution system.

Although there is no an appropriate index indicating the corrosion potential of copper in drinking water chemistry by far, several semi-empirical and mathematical models coupling important factors have been developed. Such an example is shown in the following equation (0.11), which emphasizes the pH, DIC, and sulfate: [12]

$$Cu_{Max} = 0.5DIC - 1.37pH + 2[SO_4^{2-}] + 10.2 \quad (0.11)$$

Where Cu_{Max} is the maximum stagnation copper level by unit mg Cu/L; DIC and sulfate concentrations are mmol/L.

The solid phase most likely controlling the Cu (II) solubility according to previous corrosion and natural water modeling studies is malachite ($Cu_2(OH)_2CO_3$) which can be identified by its blue-green color through visual inspection. However, the cupric hydroxysulfate and hydroxychloride solid phases also can be shown as a shade of blue-green, especially in pitting corrosion case, which limits the accuracy of this claim. So the particular corrosion products should be determined by the sophisticated surface analytical techniques.

Commonly, the accurate prediction regarding the composition of corrosion products are somewhat complicated because of the uncertainty of published thermodynamic equilibrium

constants for most of copper-containing solid phases, which are partially determined under different water qualities. The solubility constants also depend on the particle size formed.

Except for the inorganic ligands, organic and biological factors also exert the impact on cuprosolvency. The effect of microbial on copper results from its attack on copper by exopolymers and deteriorates the passivation film. One of the aggregative parameters characterizing the organics is the NOM (Natural Organic Matter) which are primarily composed of humic or fulvic substances. Cu(II) may bind with adsorbed organic material containing appropriate functional groups. This binding reducing the copper concentration may be caused by adsorbed organic acting as either a diffusion barrier, or as a less soluble corrosion film.

Kinetics

The overall oxidation potential range in drinking water seems favoring the formation of Cu(II) ion more. However, the fact that $\text{Cu}_2\text{O}_{(s)}$ layer does exist, implying that the redox kinetic of Cu(I) to Cu(II) is a rate-limiting step. With the formation of compact $\text{Cu}_2\text{O}_{(s)}$ layer, the availability of Cu(I) on the exterior of film surface is limited, which mainly comes from the defect of compact $\text{Cu}_2\text{O}_{(s)}$ layer lattice and the disproportionation reactions. Due to the reduction of Cu(I) availability, the overall formation rate of $\text{Cu}_2\text{O}_{(s)}$ slows down away from metal-scale interface. Meanwhile, the oxygen diffusion through the interior compact film is much slower than the exterior loose film layer. The combination of theses two factors explains the composition of solid phase layer.[39]

A long-term stagnant experiment conducted by Merkel et al[30] indicated that the copper level would reach a maximum level after several hours when immersing into synthesized

drinking water, then going down to final equilibrium concentration. The characteristic curve is shown in Figure 0.4.[30] Using experiment data and mechanism assumptions, Merkel et al[30] proposed a kinetic model describing the varying levels of dissolved copper and this mathematical model is shown in equation (0.12)

$$[Cu]_t = S_0 \sigma \left(\frac{k_1}{k_2 - k_1} [e^{-k_1 t} - e^{-k_2 t}] \right) + [Cu]_{t \rightarrow \infty} \quad (0.12)$$

where, $[Cu]_t$ is the predicted dissolved copper level after t time of immersion period; S_0 is the average oxygen concentration of influent; σ is the fraction of copper oxidized entering the solution phase of oxidized copper; k_1 and k_2 are integrative kinetic rate constants of oxidation and incorporation into scale, respectively; $[Cu]_{t \rightarrow \infty}$ is the equilibrium copper level. Although this model is only be used to predict the pure distilled water environment, but it still gives insight to develop the model applicable to practical potable water where anion ligands play the important role with oxygen oxidizer.

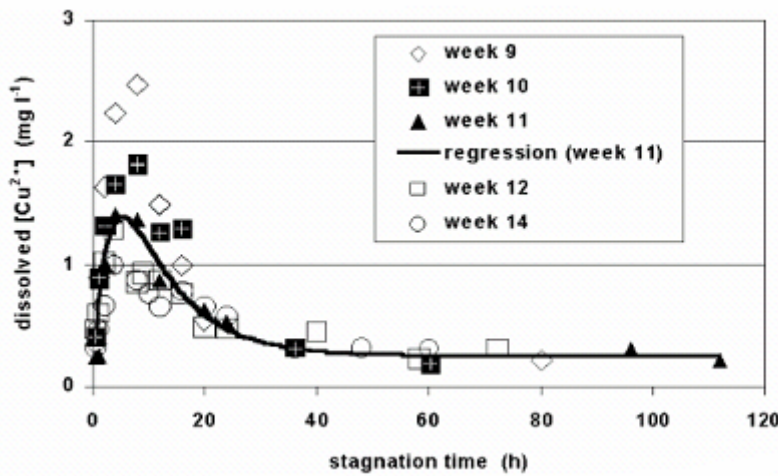


Figure 0.4 Copper Level in Short-Term Stagnation Experiment

For Cu(I) species, the transformation from $\text{Cu}(\text{OH})_{(\text{s})}$ to $\text{Cu}_2\text{O}_{(\text{s})}$, thermodynamically, is favorable, since the ΔG^0 for such a reaction is -19.56KJ/mol . No literatures are available to discuss the specific transformation rate between these two solid phases, but the fact that no $\text{Cu}(\text{OH})_{(\text{s})}$ were observed in medium- or long-term indicates that the reaction rate may not be the rate-limiting step, even the transformation is carried out in solid-solid phase.

Under stagnant state, oxygen or other electron sink species concentration decrease at the interface continuously, meanwhile the copper level increases within short-term, then decreases until the equilibrium. However, their kinetic rates are not simple first or second order. Principle behind these phenomena is that reactions involved are very complicated. With the reactions proceeding, mass transfer coefficients decreases, not a constant. Meanwhile, the hydraulic shearing may affect the layer formed. By far, there is no empirical equation describing kinetics of copper corrosion under actual drinking water conditions.

Surface Characterization

As mentioned earlier, the first step of developing theoretical model is the determination of controlling solid phases. Thermodynamically, the solid phases will not coexist if the final equilibrium has been reached, in practical application, however, this assumption need to be considered carefully. With many cases, various factors will retard this hypothetical equilibrium being reached. Thus, the more realistically circumstances are the coexistence of several interim solid phases. For copper, the most possible solid phases showing the corrosion layer could be tenorite (CuO) and cupric hydroxide ($\text{Cu}(\text{OH})_2$), malachite ($\text{Cu}_2\text{CO}_3(\text{OH})_2$). Among these three

phases, the first two are more possible to exist due to the fact that the formation $\text{Cu}_2\text{CO}_3(\text{OH})_2$ requires extremely high alkalinity of drinking water context and/or long-term incubation.

Within the possibilities of coexisting solid phases, one or two of them will take the controlling function with respect to the copper level. Several approaches might be proposed to identify the controlling phases including chemistry analysis, spectroscopy, kinetic experiment control and so on. Considering this particular case, spectroscopy is more applicable in this study primarily based on the feature of metal corrosion products.

For surface characterization analysis, two techniques mainly employed were X-ray diffraction (XRD) and X-ray Photoelectron Spectroscopy (XPS). With the assistance of other two instrumental analysis by Raman Spectroscopy and Scanning Electron Microscopy/ Energy Dispersive Spectroscopy, the major components of solid phase corrosion products formed along interface and their distributions along cross-section were identified, thus provided the help to work out how the surface characters affect the metal release. Generally speaking, pattern of XPS spectra extracts out the chemical component of top surface of corrosion layer, XRD explores what chemical exists in the bulk sample. SEM magnify visually the physical structure of sample surface. EDS spectra specify what elements are in the sample. Raman variation spectra focusing on the functional groups of chemical works as complement approach with XRD and XPS together address the entire world of corrosion layer. [40,41,42,43]

Scanning Electron Microscopy (SEM) and Energy Dispersive X-ray Spectroscopy (EDS)

The Scanning Electron Microscope (SEM) is one of the most versatile and widely used tools of modern science, which is capable of providing information about the topography

(surface features of a material or "how it looks", its texture); morphology (the shape and size of the particles making up the material), composition (the elements and compounds from which the material is made of and their relative amounts) and crystallographic features (how the atoms are arranged in the object) of both the physical and biological materials. This information are then used for determining materials' properties.[44,45,46]

By scanning an electron probe across a specimen, high-resolution images of the morphology or topography of a specimen, with great depth of field, at very low or very high magnifications can be obtained. Compositional analysis of a material may also be obtained by monitoring X-rays produced by the electron-specimen interaction. Thus detailed maps of elemental distribution can be produced from multi-phase materials or complex, bio-active materials. Characterization of fine particulate matter in terms of size, shape, and distribution as well as statistical analyses of these parameters, may be performed.

In the scanning electron microscope (SEM) a very fine 'probe' of electrons with energies up to 40 keV is focused at the surface of the specimen in the microscope and scanned across it in a 'raster' or pattern of parallel lines. A number of phenomena occur at the surface under electron impact: most important for scanning microscopy are the emission of secondary electrons with energies of a few tens eV and re-emission or reflection of the high-energy backscattered electrons from the primary beam. The intensity of emission of both secondary and backscattered electrons is very sensitive to the angle at which the electron beam strikes the surface, i.e. to topographical features on the specimen. The emitted electron current is collected and amplified; variations in the resulting signal strength as electron probe is scanned across the specimen are used to vary the brightness of the trace of a cathode ray tube being scanned in synchronism with

the probe. There is thus a direct positional correspondence between the electron beam scanning across the specimen and the fluorescent image on the cathode ray tube.

The magnification produced by scanning microscope is the ratio between the dimensions of the final image display and the field scanned on the specimen. Usually magnification range of SEM is between 10 to 200000 X and the resolution (resolving power) is between 4 to 10 nm (40 -100 Angstroms). There are many different types of SEM designed for specific purposes ranging from routine morphological studies, to high-speed compositional analyses or to the study of environment - sensitive materials.

Chemical analysis (microanalysis) in the scanning electron microscope (SEM) is performed by measuring the energy or wavelength and intensity distribution of X-ray signal generated by a focused electron beam on the specimen. With the attachment of the energy dispersive spectrometer (EDS) or wavelength dispersive spectrometers (WDS), the precise elemental composition of materials can be obtained with high spatial resolution. When we work with bulk specimens in the SEM very precise accurate chemical analyses (relative error 1-2%) can be obtained from larger areas of the solid (0.5-3 micrometer diameter) using an EDS or WDS.

In practical application, however, the magnification which can be reached to produce readily interpretable images is limited by the sample analyzed. For example, under the case that the sample presents well-developed crystal, clear and well-defined picture can be obtained and is easy to interpret. Once the sample, however, doesn't form any well-developed crystal structure, the identification of corresponding compound is difficult and may not provide any informative message. Another example is the oxide species. Due to the nonconductive feature of oxide, the

image may not provide useful information except the rough topography and/or morphology even though the sample is coated. For EDS, the quantitative content may not be reliable according to the preliminary study. The interference of carbon tape on the sample hold as well as the contaminants from vacuum chamber distorts the carbon content of sample. Thus, the EDS application is primarily used to explore the elemental composition qualitatively.

X-Ray Diffraction (XRD) and Grazing Angle X-Ray Diffraction (X'pert) System

X-rays can be used to reveal detailed information about the chemical composition and physical nature of all kinds of natural and manufactured materials- from metals, minerals, oils and other liquids, to plastics, pharmaceuticals and semiconductors. When an X-ray beam bombards a crystalline lattice in a given orientation, the beam is scattered in a definite manner characterized by the atomic structure of the lattice. This phenomenon, known as 'X-ray diffraction', occurs when the wavelength of X-rays and the interatomic distances in the lattice have the same order of magnitude. X-ray diffraction is a versatile, non-destructive analytical technique for identification and quantitative determination of the various crystalline compounds, known as 'phases', present in solid materials and powders. Identification is achieved by comparing the x-ray diffraction pattern or 'diffractogram' obtained from an unknown sample with an internationally recognized database containing reference patterns for more than 70,000 phases. Modern computer-controlled diffractometer systems use automatic routines to measure, record and interpret the unique diffractograms produced by individual constituents in even highly complex mixtures.[47,48,49]

A crystal lattice is a regular three-dimensional distribution (cubic, rhombic, etc.) of atoms in space. These are arranged so that they form a series of parallel planes separated from one another by a distance d , which varies according to the nature of the material. For any crystal, planes exist in a number of different orientations - each with its own specific d -spacing. Bragg's Law was used to describe this phenomena and produce the pattern interpretable. When a monochromatic x-ray beam with wavelength λ is projected onto a crystalline material at an angle θ , diffraction occurs only when the distance traveled by the rays reflected from successive planes differs by a complete number n of wavelengths. By varying the angle θ , the Bragg's Law conditions are satisfied by different d -spacing in polycrystalline materials. Plotting the angular positions and intensities of the resultant diffracted peaks of radiation produces a pattern, which is characteristic of the sample. Where a mixture of different phases is present, the resultant diffractogram is formed by addition of the individual patterns.

One of the features of XRD lies in that XRD can detect the bulk crystalline structure of sample of interest, the penetration depth ranges from 50 to 10,000 (μm) depending on the specific conditions. Another particular advantage of this diffraction analysis is that it discloses the presence of substance as that substance actually exists in the sample, not in terms of its constituent chemical elements. Most important in this application is its capability of phase identification. The rule governing this is that any given substance always produces a characteristic diffraction pattern, whether the substance is present in the pure state or as one constituent of a mixture of substances. For any specific substance, three pattern lines were used in identification. Within certain shift variation range, the sample shows the three lines if it has the same crystal. Depending on the specific samples, two kind of XRDs were used in this

project, one is powder XRD, another is grazing angle XRD which is called as X'pert. The former is used once the powder sample can be collected, the later is used when the sample can not be collected by powder and the sample is planar, both of them produce the same type X-ray pattern.

Like SEM/EDS, XRD has its inherent disadvantage. The interested application of XRD in TBW project is phase identification, which utilizes the characteristic pattern produced by the crystal. The corrosion products formed in designed incubation period, however, may not presents as crystals, but amorphous, which presents as broad bump, not sharply distinguishable peaks. Another disadvantage is that XRD is not a surface sensitive technique, which can not be used to identify the phases right on the top layer along with several atomic layer thickness. In this TBW project, the corrosion products formed was continuously covering the old products, XRD technique alone, however, can not distinguish them, the identification of top surface component has to rely on the XPS.

X-Ray Photoelectron Spectroscopy (XPS)

XPS was developed in the mid 1960s by K. Siegbahn and his research group. The phenomenon is based on the photoelectric effect outlined by Einstein in 1905 where the concept of the photon was used to describe the ejection of electrons from a surface when photons impinge upon it. For XPS, Al Kalpha (1486.6eV) or Mg Kalpha (1253.6eV) are often the photon energies of choice. Other X-ray lines can also be chosen such as Ti Kalpha (2040eV). The XPS technique is highly surface specific due to the short range of the photoelectrons that are excited from the solid. The energy of the photoelectrons leaving the sample are determined using a

concentric hemispherical analyzer (CHA) and this gives a spectrum with a series of photoelectron peaks. The binding energy of the peaks are characteristic of each element. The peak areas can be used (with appropriate sensitivity factors) to determine the composition of the materials surface. The shape of each peak and the binding energy can be slightly altered by the chemical state of the emitting atom. Hence XPS can provide chemical bonding information as well. XPS is not sensitive to hydrogen or helium, but can detect all other elements. [50,51,52].

References

- (1) Fernald, E.A., and D.J. Patton. 1985. *Water Resources Atlas of Florida*, Florida State University, Institute of Science and Public Affairs.
- (2) Dietz, J.D., J.S. Taylor, L.A. Mulford, C.J. Cullen., and C.A. Owen. 2002. Assessment of Source Water Blends on Distribution System Water Quality. *In Proc. of 31st annual AWWA Water Quality Technology Conference. Seattle, Wash: AWWA.*
- (3) Pankow, J.F. 1991. *Aquatic Chemistry Concept*. Chelsea, Mich.: Lewis Publishers.
- (4) Wagman D.D., W. H. Evans, V.B. Parker, R. H. Schumm, I. Halow, S. M. Bailey, K. L.Churney, and R. L. Nuttall. 1982 *The NBS Tables of ChemicalThermodynamic Properties, J. Phys. Chem. Ref. Data*, Vol. 11, Suppl. 2
- (5) Reiber, S.H. 1989. Copper Plumbing Surfaces: An Electrochemical Study. *Jour. AWWA*, 81(7):114-122.
- (6) Eilbeck, W.J. 1984. Redox Control in Breakpoint Chlorination of Ammonia and Metal Ammine Complexes. *Water Research*, 18:1:21.
- (7) Stone, A., D. Spyridakis, M. Benjamin, J. Ferguson, and S. Osterbus. 1987. The Effect of Short-term Changes in Water Quality on Copper and Zinc Corrosion rate. *Jour. AWWA*, 79(2):75-82.

- (8) Cotton, F.A., and G. Wilkinson. 1988. *Advanced Inorganic Chemistry. Fifth.* New York: John Wiley and Sons, Inc.
- (9) Lead and Copper. Final Rule Correction. 1991. *Federal Register*. 56:135:32112.
- (10) Lead and Copper. Final Rule. 1991. *Federal Register*. 56:110:26460.
- (11) Lead and Copper. Final Rule Correction. 1992. *Federal Register*. 57:125:28785.
- (12) Schock, M.R., and J.A. Clement. 1995. *Effect of pH, DIC ,Orthophosphate and Sulfate on Drinking Water Cuprosolvency.* Cincinnati, Ohio. EPA/600/R-95/085.
- (13) Hamann, C.H., A. Hammett, and W. Vielstich. 1998. *Electrochemistry.* New York: Wiley-VCH
- (14) Lowe, J.P. 1993. *Quantum Chemistry, Second Edition.* New York: Academic Press.
- (15) Wieckowski, A., *Interfacial Electrochemistry: Theory, Experiment, and Applications,* Marcel Dekker Inc., New York, NY, (1999)
- (16) Marani, D., J.W. Patterson, and P.R. Anderson. 1995. Alkaline Precipitation and Aging of Cu(II) in the Presence of Sulfate. *Water Research*, 29(5) 1317-1326.
- (17) Stumm, W., and R.L. Champlin. 1967. Comment on Technical and Legal Aspects of Copper Tube Corrosion. *Jour. AWWA*, 59(3):401-406.
- (18) Adeloju , S.B., and H.C. Hughes. 1986. The Corrosion of Copper Pipes in High Chloride-Low Carbonate Mains Water. *Corrosion Science*, 26(10):851-870.
- (19) Atlas , D.C., and O.T. Zajicek. 1982. The Corrosion of Copper by Chlorinated Waters. *Water Research*, 16(5):693-658.
- (20) Edwards, M., S. Jacobs, and R.J. Taylor. 2000. The blue Water Phenomenon. *Jour. AWWA.*, 92(7):72-82.

- (21) Miltero, F.J., M. Izaguirre, and V.K. Sharma. 1987. The Effect of Ionic Interaction on the rates of Oxidation in Natural Waters. *Marine. Chemistry*, 22(2-4):179-191.
- (22) Stumm, W., and J.J. Morgan. 1996. *Aquatic Chemistry*. New York: John Wiley & Sons, Inc.
- (23) Wieckowski, A. 1999. *Interfacial Electrochemistry: Theory, Experiment, and Applications*. New York: Marcel Dekker
- (24) Stumm, W. 1992. *Chemistry of the Solid-Water Interface*. New York: John Wiley & Sons, Inc.
- (25) Carroll, F.A. 1998 *Perspectives on Structure and Mechanism in Organic Chemistry*. Pacific Grove, Calif. Brooks/Cole Publishing Company
- (26) Bockris, J.O'M., and A.K.N. Reddy. 1970. *Modern Electrochemistry, Vol. I*. New York: Plenum Press
- (27) De, Zoubov, N., C.C., Vanlengenhagle, and M. Poubiax 1974 Atlas of Electrochemical Equilibria in Aqueous Solutions, Houston, Texas
- (28) Shoesmith, H.M., and W. Lee. 1977. The dissolution of Cupric Hydroxide Films from Copper Surface. *Electrochimica Acta*, 22(12):1411-1417.
- (29) Ives, D.J.G., and A.E. Rawson. 1962. Copper Corrosion I (Thermodynamic Aspect), II (Kinetic Studies), III (Electrochemical Theory in General Corrosion), IV (Effects of Saline Addition). *Jour. Electrochemical Society*, 109:447-466.
- (30) Merkel, T.H., H.J. Gross, W. Werner, T. Dahlke, S. Reicherter, G. Beuchle, and S.H. Eberle. 2002. Copper Corrosion By-product Release in Long-term Stagnation Experiments. *Water Research*, 36(6):1547-1555.
- (31) Edwards, M., and N. Sprague. 2001. Organic Matter and Copper Corrosion By-product: a mechanistic study. *Corrosion Science*, 43(1):1-18.

- (32) Kash, P.W., M.X. Yang, A.V. Teplyakov, G.W. Flynn, and B.E. Bent. 1997. Chemical Displacement of Molecules Adsorbed on Copper Surfaces: Low-Temperature Studies with Applications to Surface Reactions. *Jour. of Physical Chemistry*, 101(40):7908-7918.
- (33) Ugorets, M.Z., E.A. Buketov, and K.M. Akhmetov. 1968. Thermographic Study of the Dehydration of Copper Hydroxide in Alkaline Solutions. *Russ. Jour. of Inorganic Chemistry*, 13(6):1525-1529.
- (34) Chalyi, V.P. 1963. Mechanism of Aging of Individual Metal Hydroxides and Hydroxide Systems. *Russ. Jour. of Inorganic Chemistry*, 8(2):269-273.
- (35) Feitknecht, W., P. Schindler. 1963 Solubility Constants of Metal Oxides, Metal Hydroxides, and Metal Hydroxide Salts in Aqueous Solution *Pure and Applied Chemistry* (6):130-199
- (36) Isaac, R.A.; L. Gil, A.N. Cooperman, K. Hulme, B. Eddy, M. Ruiz, K. Jacobson, C. Larson, and O.C. Pancorbo. 1997. Corrosion in Drinking Water Distribution Systems: A Major Contributor of Copper and Lead to Wastewater and Effluent. *Environmental Science and Technology*, 31(11):3198-3203.
- (37) Hidmi, L., and M. Edwards. 1999. Role of Temperature and pH in $\text{Cu}(\text{OH})_2$ Solubility. *Environmental Science and Technology*, 33(15):2607-2610.
- (38) Patterson, J.W., E.B. Richard, and D. Marani. 1991. Alkaline Prediction and Aging of Copper from Dilute Cupric Nitrite. *Environmental Science and Technology*, 25(10):1780-1787.
- (39) Stumm, W. 1990. *Aquatic Chemical Kinetics: Reaction rate if Processes in Natural Waters*. New York: John Wiley & Sons, Inc.
- (40) Townsend, H.E., T.C. Simpson, and G.L. Johnson. 1995. Structure of Rust on Weathering Steel in Rural and Industry Environments. *Corrosion*, 50(7):546-554.

- (41) Oh, S., D.C. Cook, and H.E. Townsend. 1999 Atmospheric corrosion of different steels in marine, rural and industrial environments. *Corrosion Science* 41(9):1687-1702
- (42) Bonin, P.M.L., W. Jedral, M.S. Odziemkowski, R.W. Gillham 2000 Electrochemical and Raman Spectroscopic Studies of the Influence of Chlorinated Solvents on the Corrosion Behavior of Iron in Borate Buffer and in Simulated Groundwater. *Corrosion Science*. 42(11):1921-1939
- (43) Baek, W.C., T. Kang, H.J. Sohn, and Y.T. Kho. 2001. In-Situ Surface Enhanced Raman Spectroscopic Study on the Effect of Dissolved Oxygen on the Corrosion Film on Low Carbon Steel in 0.01 M NaCl Solution. *Electrochemical Acta.*, 46(15):2321-2325.
- (44) Coulthard, I., and T.K. Sham. 1998. Morphology of Porous Silicon Layers: Image of Active Sites from Reductive Deposition of Copper onto the Surface. *Applied Surface Science*, 126(3/4):287-291.
- (45) Zhu, H.H., L. Lu, and J.Y.H. Fuh. 2003. Development and Characterization of Direct Laser Sintering Cu-based Metal Powder. *Jour. of Materials Processing Technology*, 140(1-3):314-317.
- (46) Barbra, G.L. 1985. *SEM: a user's manual for materials science*. Metals Park, Ohio: American Society for Metals.
- (47) Warren, B.E. 1990. *X-ray diffraction*. New York: Dover Publications.
- (48) Cullity, B.D., and S.R. Stock. 2001. *Elements of X-Ray Diffraction*. Upper Saddle River, N.J.: Prentice Hall.
- (49) Sathiyarayanan, S., M. Sahre, and W. Kautek. 1999. In-situ grazing incidence X-ray diffractometry observation of pitting corrosion of copper in chloride solutions. *Corrosion Science*, 41(10):1898-1909.

- (50) Briggs, D. 1998. Surface analysis of polymers by XPS and static SIMS. New York: Cambridge University Press.
- (51) Czanderna, A.W., and M.D. Hercules. 1991. *Ion Spectroscopes for Surface Analysis*. New York: Plenum Press.
- (52) Wagner, D.C. 1991. *The NIST X-ray photoelectron spectroscopy (XPS) database*. Gaithersburg, Md.:U.S. Dept. of Commerce, National Institute of Standards and Technology.

Chapter 2 Surface Characterization and The Theoretical Modeling of Copper Corrosion in Drinking Water Pipe Distribution System

Introduction

Mitigation of copper release in drinking water plumbing system has been a major challenge because the Lead and Copper Rule (LCR) and the associated toxicity. In the past several decades, extensive research has been done to determine the mechanisms controlling metal release in drinking water systems and association of those mechanisms with water quality in order to control metal release. Electrochemical oxidation and aquatic precipitation/dissolution have been the primary mechanisms associated with metal release [1-8]. In electrochemical corrosion process, metallic copper is oxidized by one electron transfer mechanism [9], which couples the consumption of oxidants in drinking water such as dissolved oxygen and/or residual chlorine with an oxidized metal (copper). Two electron transfer pathways are proposed for copper. One proposed pathway is that electrons transport through metal bulk requiring random movement of anodic and cathodic sites that move rapidly over a large surface area on the oxidized metal[10]. If this transfer is relatively stable the corrosion is uniform over the copper surface and is described as "uniform corrosion". The other proposed pathway is electron transport through a rapidly formed compact cuprous oxide scale layer (cuprite Cu_2O) as opposed to the bulk metal[11]. In either pathway a cupric layer forms and covers the entire metal surface, which provides a copper source for electron transfer. As the cupric layer ages cupric ion accumulate and precipitate as cupric species because they are so insoluble. Thus aquatic precipitation/dissolution replaces electrochemical oxidation as the mechanism controlling copper release, and is the common view in the literature regarding copper release.

Precipitation of copper differs from dissolution of copper in many respects, especially regarding the formation of precipitates and soluble complexes. In most cases, the formation of complexes between central ion and ligands reaches equilibrium rapidly[12]. The composition and measurement of the formed complexes are easy to measure or calculate. Precipitation is much more complicated and involves many processes such as the induction of super saturation, nucleation, particle growth, Ostwald ripening, recrystallization, and agglomeration[1,2,3]. Each of these processes is very sensitive to chemical features such as pH, alkalinity, anion species and physical factors such as water temperature and aging time. The combined interactions contribute to the poor reproducibility of ill-defined solid phases and inconsistent solubility constants[3].

In drinking water, possible controlling solid phases in ordered by solubility are basic cupric carbonate $\text{Ca}_2\text{CO}_3(\text{OH})_2$ (malachite), cupric hydroxide $\text{Cu}(\text{OH})_2$, and cupric oxide CuO (tenorite)[12,13]. The formation of malachite however requires exceedingly intense carbonate and bicarbonate concentrations, which seldom happens in drinking water even through the appearance of malachite has been recorded in literature[13,14]. Tenorite and cupric hydroxide could be present and control the precipitation and dissolution of copper given adequate aging period. Evidence indicates the freshly precipitated copper solid phase is very probably metastable cupric hydroxide[1,2,3]. Each of four mechanisms could dominant aging of $\text{Cu}(\text{OH})_2$ in water:

1. Ordering of the hydroxide structures, which is the procedure of converting the amorphous status to crystalline substance
2. Particle Growth, an amorphous structure is dominant and crystalline structures do not form, which is known as Ostwald ripening.

3. Dehydration of hydroxide, this mechanism is water quality sensitive, and especially pH sensitive
4. Hydration.

Solid phase's modifications are poorly predicted and are non-homogeneous because those four mechanisms may be involved simultaneously not subsequently because of continuously changing water quality. With the formation of the initial amorphous and unstable active crystalline $\text{Cu}(\text{OH})_2$, these reactions cease and Ostwald ripening or direct dehydration to tenorite (CuO) occurs. Before dehydration, some researchers suggest hydration occurs first, as shown in the following reactions[1].



Thermodynamically, controlling solid phases cannot coexist since the inevitable transformation of one to another-Solid Phase Rule- different solid phases can coexist thermodynamically, but there is only one controlling solid phase[12]. Kinetics limits this application, and different solid phase were observed in practical experiments, which may result in composite phases that determine system characteristics. Determination of appropriate solubility constants is not possible because of formation of intermediate species such as active $\text{Cu}(\text{OH})_2$, freshly formed CuO and so on. Many $\text{Cu}(\text{OH})_2$ models are created because a $\text{Cu}(\text{OH})_2$ model most accurately predicts copper concentrations from field data and $\text{Cu}(\text{OH})_2$ has been confirmed by the existence of associated X-rays[13,15]. In this work, however, the X-ray peak of $\text{Cu}(\text{OH})_2$ was never seen, which indicated the $\text{Cu}(\text{OH})_2$ layer is very thin on the substrate interface.

The purpose of this work was to develop a theoretical model for the copper scales based on surface characterization of copper coupons that were aged in a pilot-scale pipe distribution systems (PDSs) after exposure to different water qualities. Varying quality was created in the PDSs by blending finished waters that were produced from ground, and surface waters. Hence, the compositions of the copper scales were correlated to composition bulk water in the PDSs. This method provided a practical approach to develop theoretical models for copper release. The theoretical models were modified to compensate for the many mechanisms and accompanying aging processes affecting the copper scales. Consequently semi-empirical predictive models for copper release as a function of water quality were developed.

Experimental Methods

Source Water Production and Blending

Three conventional water sources used for this study were, groundwater (G1) treated by aeration; surface water (S1) treated by coagulation, flocculation with ferric sulfate, then sedimentation, ozonation, sand filtration, biologically activated carbon absorption; and desalinated water (RO) processed by reverse osmosis. Post treatment for all of these waters was pH stabilization and chloramination prior to PDS distribution. Finished waters were stored in tanks and blending was achieved by controlling pumping to the PDSs.

Pilot Pipe Distribution Systems

The PDSs consisted of fourteen hybrid lines and four single material lines as shown in Figure 0.1. Hybrid PDSs consisted of PVC, lined cast iron, unlined cast iron, and galvanized

steel pipes that had been removed from actual distribution systems. The four single materials PDSs were made entirely of PVC, lined cast iron, unlined cast iron and galvanized pipe. All of pipes were taken from municipal distribution systems that were exposed to only groundwater for decades. The nominal length of each line was 100 feet. All pipe diameters were six inches with the exception of the galvanized steel pipe diameter which was two inches. Blended water was distributed to each pipe using peristaltic pumps. Influent and effluent PDS samples were analyzed for dissolved and total iron, pH, alkalinity, chloride, sulfate, calcium, magnesium, sodium, silica, dissolved oxygen, and chlorine residuals for more than a year. The data set used for this work was collected over five three-month phases totaling 15 months. Phases were determined by blend change, which occurred every three months. All water quality analysis followed EPA standard procedures [22]



Figure 0.1 Pilot-scale pipe distribution system

Copper Loop and Coupon Study

Copper and lead corrosion loops as shown in Figure 0.2 followed each PDSs and were monitored as required for LCR compliance. Each copper loop consisted of 25 feet of copper tubing and contained a lead coupon. A one liter sample was drawn from the first 22 feet of the copper loop. The additional three feet in the copper loop compensated for mixing. The lead coupon was a pre-weighed 50:50 tin:lead coupon and was placed within the copper tubing at the same location in each loop system. All fittings were made of PVC or some other insert polymer. The lead coupons were commonly used for corrosion studies and were identical. The size of the coupons was determined by assuming a 1/8th inch solder bead on the interior of each 0.5 inch diameter joint was exposed to drinking water in home plumbing systems under a sink that had 8 fittings, which lead to 3.38 square inches and was a reasonable simulation of lead exposure under a kitchen sink. Hence, all coupons had a surface area of 3.38 square inches.

Weekly samples were collected after a 6 hour standing period. During the first phase of the study influent and effluent loop samples were collected and found to be identical except for copper and lead. pH, dissolved oxygen, alkalinity, calcium, magnesium and inhibitor functional group analysis ($\text{PO}_4\text{-P}$) were monitored weekly. Weight change of the lead coupons was determined at the end of each phase.

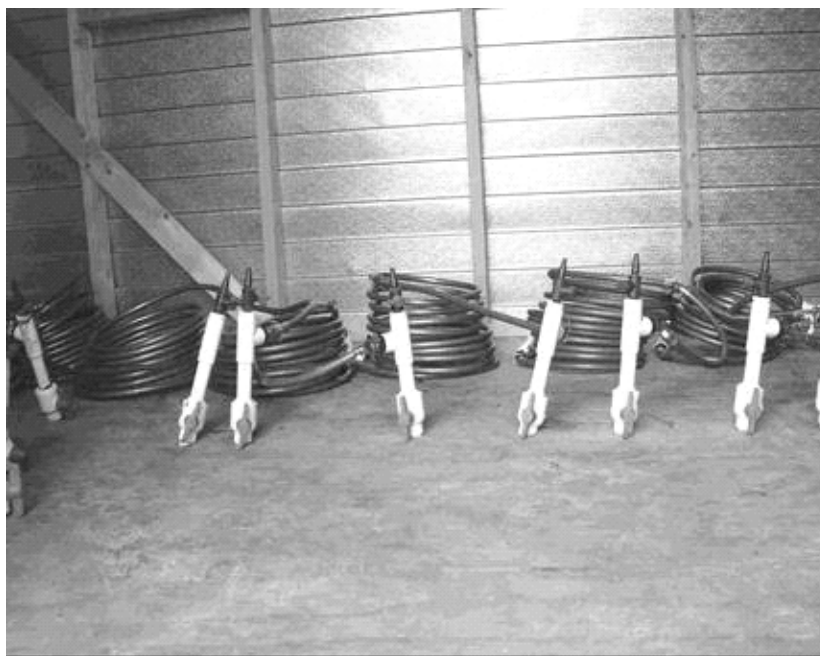


Figure 0.2 Eighteen copper loops connected with each PDS

Pipe Surface Characterization

XRD and XPS were major surface characterization techniques used in this investigation. Preliminary information was also collected using SEM and EDS. The copper coupons were harvested and cut into two 5×5 mm section using a hand saw and stored in the desiccators to remove any adsorbed moisture. The XRD analysis was conducted using a grazing X'pert machine (Philips), which consisted of a X-ray diffractometer with a fine structure air-insulated X-ray tube with a copper anode ($\text{Cu K}_{\alpha 1}$ 1.5406 Å). Full X-ray diffraction patterns were recorded for the scan angles (2θ) from 10° to 80° to identify copper phases, 0.01° scanning step, scanning time step was 2.00 scans per second?. Using the ICDD-PDF database, individual crystalline phases were identified from their XRD patterns. The XPS scan was performed using a 5400 PHI ESCA. The base pressure during analysis was 10^{-9} torr and the power for Mg- $\text{K}\alpha$ X-

radiation (1253.6 eV) was 350 watts. Both survey and high-resolution narrow spectra were recorded with electron pass energy of 44.75 eV and 35.75 eV respectively to achieve the maximum spectral resolution. Any charging shift produced by the samples was carefully removed by using a B.E. scale referred to C(1s) B.E. of the hydrocarbon part of the adventitious carbon line at 284.6 eV. Non-linear least square curve fitting was performed using a Gaussian/Lorentzian peak shape after background removal.

Results and Discussions

Observations by SEM/EDS

Powder deposits on coupons that had been exposed for 1, 2 and 3 months PDS water were inadequate for sample collection. The most distinct visual change was the color of the scale, which varied depending on water quality. The color of coupons incubated in groundwater (G1) were light red to yellow, brown, black as shown in upper right corner of Figure 0.3 (typical color of $\text{Cu}_2\text{O}/\text{CuO}/\text{CuCO}_3$). The coupons incubated in treated surface water (S1) were unevenly and slightly colored green-blue as shown in upper right corner of Figure 0.4 (typical color $\text{Cu}(\text{OH})_2/\text{Cu}_2\text{CO}_3(\text{OH})_2$). The deposits on copper coupons incubated in desalinated RO water as shown in Figure 0.5 were a porous, loose blue-green substance that could be easily removed. The light red and brown-black deposits on G1 coupons indicated that part of corrosion products were oxides. The blue-green deposits on S1 coupons were hydroxides and/or carbonate corrosion products. The S1 oxides indicated S1 was less corrosive than G1 because $\text{Cu}(\text{OH})_2$ is less stable than CuO , and the later is believed to be the dehydration of $\text{Cu}(\text{OH})_2$ [1,2]. In comparison to G1 and S1 coupon corrosion products, the more porous loose blue-green deposits on RO coupons

seems to be freshly formed and most unstable, which indicate that RO produced the least corrosive water.

There was no white-grey color on the coupon surface, which indicated cuprous sulfate and chloride salts were not present. There was no change in the thickness of copper coupons after exposure to the PDS water, which indicated that the corrosion rate is quite slow in a drinking water environment.

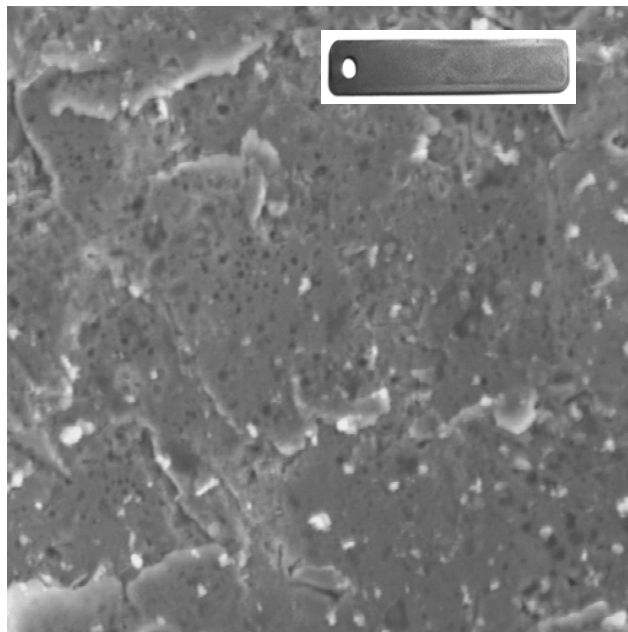


Figure 0.3 SEM (JEO-6400) image of a copper coupon that was incubated in a high alkalinity groundwater and covered with black deposits as shown in the upper right corner.

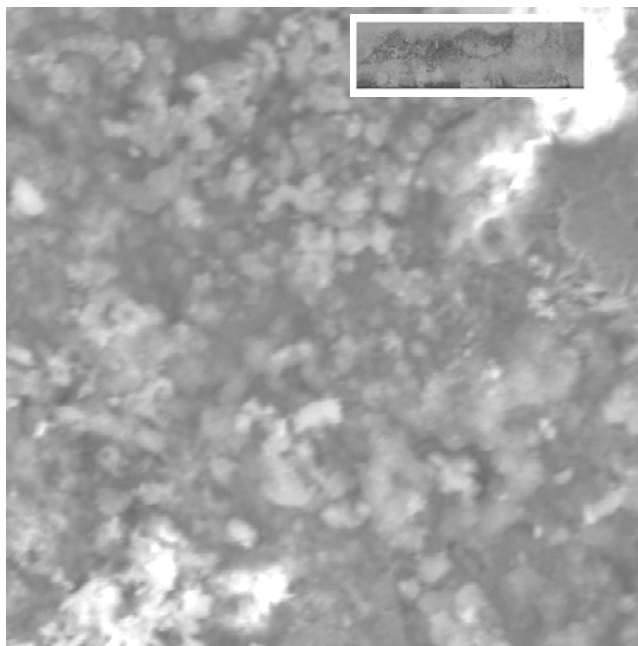


Figure 0.4 SEM (JEO-6400) image from a copper coupon incubated in treated surface water (S1) and covered with uniformly distributed and loose green deposits

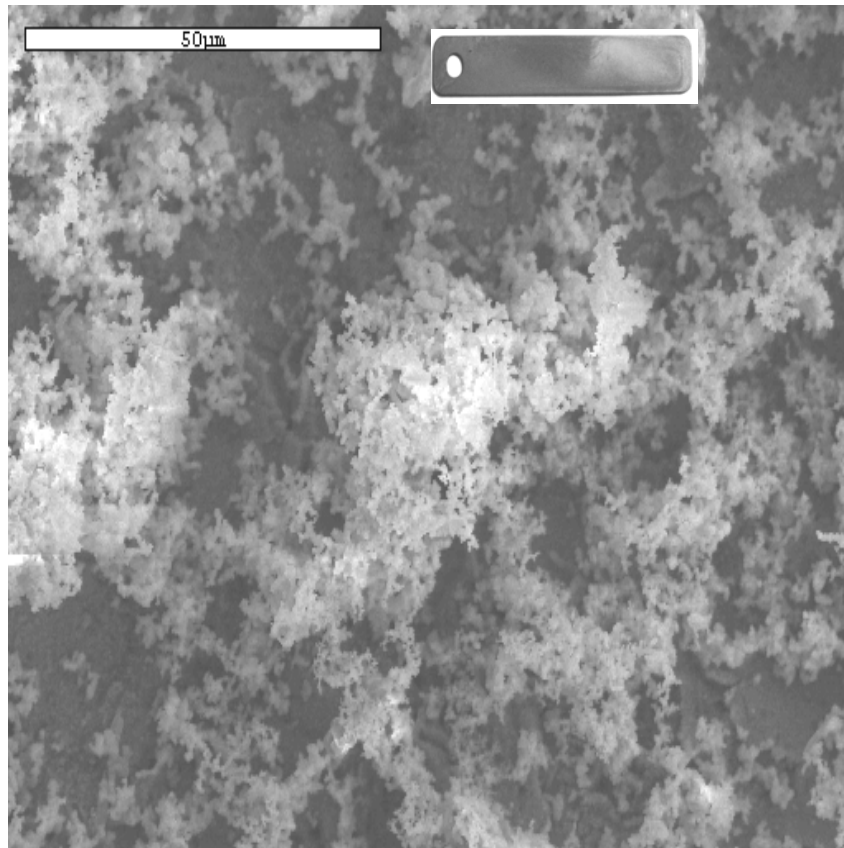


Figure 0.5 Representative SEM (JEO-6400) image of copper coupon incubated in desalinated water (RO) and covered with an easily removed green deposit shown in upper right corner

Other than visual examination, SEM photographs of copper coupons that were exposed to finished ground, surface, and RO waters are shown in Figure 0.3, Figure 0.4, and Figure 0.5. The morphologies shown in these figures are obviously different. The blue-green scale formed in the S1 and RO environment as shown in Figure 0.4 and Figure 0.5 was porous, loose, and readily removed by swabbing with a paper towel. However the scale on the coupon shown in Figure 0.3 is quite compact, dark brown to black and tightly bound on the coupon surface. Corresponding EDS spectra of the copper coupon that was exposed to the RO environment is

presented in Figure 0.6 which shows chlorine and sulfur were present in the scale composition but at low ratios relative to other major elements. Some chloride/sulfate copper salts were in the samples which were incubated in the RO environment. There was more chloride in the RO finished water, and hence more chloride on the RO coupon surface. In finished S1 water, sulfate is major anion affecting the scale, as shown, there were some blue-green deposits on S1 coupon, but less porous and less loose than that on RO coupon, The associated porous, loose blue-green scale products probably consisted of sulfate salts as opposed to chloride salts. The major components of the compact dark brown black top layer on the copper coupon scale from the groundwater environment were expected to be copper oxides. The high chloride and sulfate concentration in the RO and S1 environment more readily form less compact scale products than copper oxide or hydroxide scales. The porous blue-green scale on the copper coupons in the RO environment could have been deposited from the bulk solution as opposed to a formed oxide or hydroxide scale, which would explain their ease of removal. Sulfur, phosphorus, silica, aluminum, calcium, and iron were found on the coupon surface through other EDS spectra. Calcium, silica and iron were thought to be deposited from the bulk solution and were present in the finished water or could have come from the unlined PDS metal pipes. Sulfur and phosphorus are components of new copper pipes or formed scales, which could not be differentiated and identified.

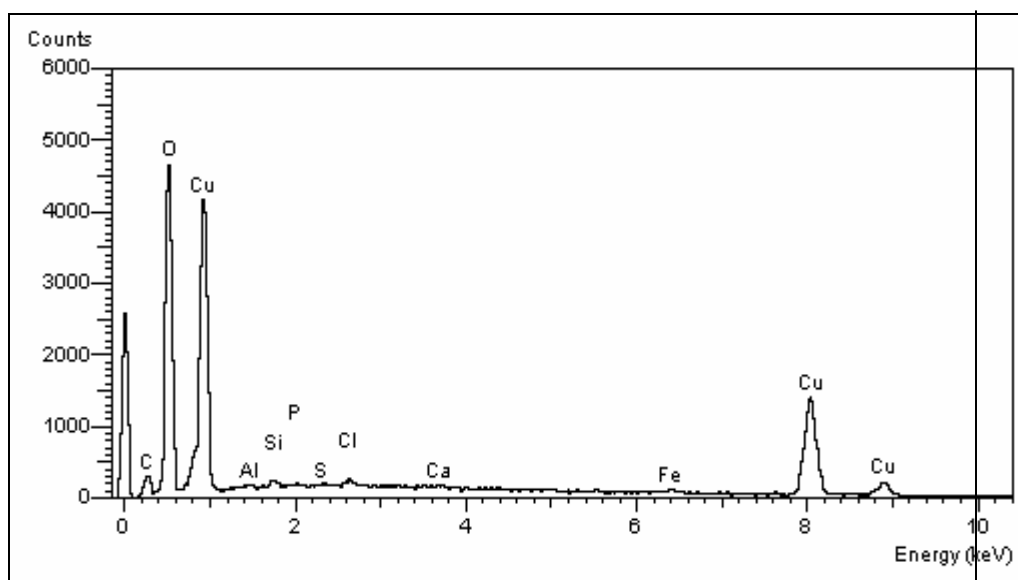


Figure 0.6 EDS(JEO-6400) spectra for a copper coupon incubated in desalinated water

Investigation of Corrosion Products by XRD

Grazing XRD system X'pert was used to characterize the scale layers formed on the copper coupons after incubation. The XRD patterns were superimposed following incubation for all coupons. The two, three, and six month intensities were shifted by 2500 and 5000 intensity units for pattern differentiation. As shown Figure 0.7, Cu_2O was the only detectable crystal corrosion product that formed on the copper substrate (coupon). No Cu(II) phases were identified, some minor peaks were identified as CaCO_3 , especially in the one month pattern. The missing of CuO/Cu(OH)_2 is partially due to two main factors. First, the Cu(II) crystal phases were not adequately formed during incubation to allow detection by XRD, which is a bulk identification technique that has a detection depth approximately between 50\AA and $10,000\text{\AA}$. Any phases existing prior to the detection depth can not be detected by XRD. Such phases have

to be explored using other more surface sensitive approaches. Second, the Cu(II) phases were formed as amorphous phases, not crystalline structures. Amorphous phases create “noise” in XRD patterns that do not show sharp peaks. There were no obvious humps in Figure 0.7, which indicated amorphous Cu(II) species was not present..

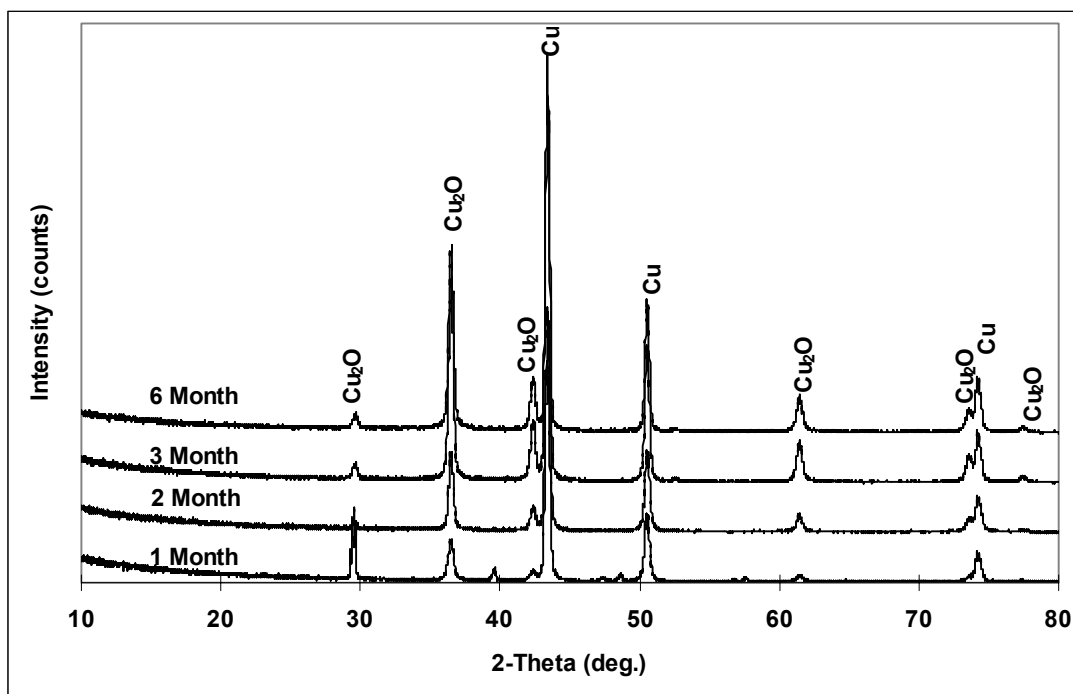


Figure 0.7 X’pert patterns of corrosion products formed on copper coupons in a groundwater environment for varying times of incubation..

Although the XRD study focused on qualitative analysis more than quantitative analysis, the approximate trends shown in Figure 0.7 are obvious. The ratio of $\text{Cu}/\text{Cu}_2\text{O}$ is decreasing as time of incubation increases, which indicates the thickness of Cu_2O is increasing. This shows that the one electron transfer mechanism for formation of copper scale in the loop environment

might be a controlling mechanisms. Metallic copper was oxidized to be Cu_2O , then oxidized to Cu(II) species and not directly transformed from substrate copper to Cu(II) .

Investigation of Corrosion Products by XPS

XRD results found the Cu(II) corrosion product layers formed in the three-month incubation periods were not thick enough to be identified. Hence, a more surface sensitive technology, XPS, was utilized. A detailed XPS scan and a deconvolution of $\text{Cu}2\text{P}3$ peak from a copper coupon that was incubated in ground water (G1) are shown in Figure 0.8. The deconvolution peak revealed Cu_2O , CuO , and Cu(OH)_2 existed in the coupon scale layer and were major peaks. Typically, the penetration depth of XPS is 0.5 to 1.0\AA which is the approximate thickness of several atoms. The appearance of Cu_2O in such a thin layer verified that the longitudinal distribution of corrosion products beginning from the scale surface was Cu(II) , Cu_2O , and substrate copper, which was consistent with published laboratory study results[11,13,15], and explained the absence of Cu(II) in XRD analysis. Similar results were observed in Figure 0.9 which is the deconvolution $\text{Cu}2\text{P}3$ from a copper coupon that was incubated in RO water for three months.

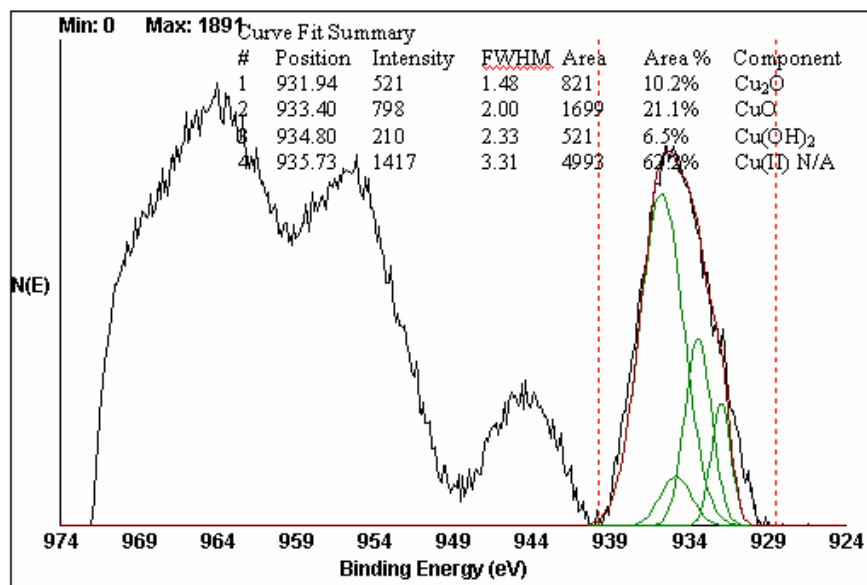


Figure 0.8 Representative high-resolution XPS deconvolution Cu₂P_{3/2} peak of corrosion products formed during ground water incubation.

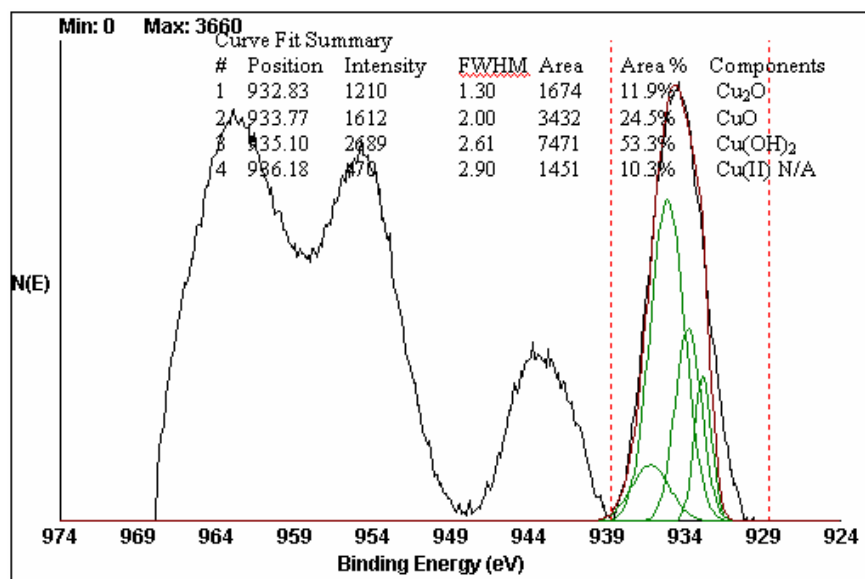


Figure 0.9 Representative high-resolution XPS deconvolution Cu₂P_{3/2} peak of corrosion products formed during with ground water incubation.

The significance of aging and water quality to composition of corrosion layers was investigated by analyzing the XPS scans of the copper coupons that were incubated for one, two, three, and six-month periods. Solid phase composition and associated water quality are shown in

Table 0.1. The Cu(I) ratio to total Cu versus exposure time is presented in Figure 0.10. The relative percentage of cuprite in the surface scale decreased for two or three months and then increased. The common trends of cuprite compositions versus incubation time in each of the four environments indicate cuprite formation is not closely correlated to water quality, however there were exceptions. These XPS scans indicate the surface composition depends on time and water quality unlike the underlying Cu_2O layer. Another information could be obtained is the coexistence of CuO and $\text{Cu}(\text{OH})_2$. The amount of stable CuO and metastable $\text{Cu}(\text{OH})_2$ in the scale was not clearly correlated to time in the XPS scans, however there was correlation to water quality. The relative abundance of CuO versus $\text{Cu}(\text{OH})_2$ varied with blending for the three month exposures as shown in

Table 0.1. The relative abundance of $\text{Cu}(\text{OH})_2$ was generally less than CuO except in RO water, which was due to the continuous transformation of $\text{Cu}(\text{OH})_2$ to CuO . Hence, CuO gradually accumulated and $\text{Cu}(\text{OH})_2$ was consumed and formed simultaneously. The compositions shown in

Table 0.1 are based on analyses of ten copper coupons. CuCl_2 and CuSO_4 were found on the surface by XPS analyses but are not shown in

Table 0.1 because they were deposited on the surface when the coupon was dried in air and not in the corrosion layer.

Table 0.1 Corrosion scale composition during a three month PDS incubation period as determined by XPS analysis.

Blending	Ratio	Cu_2O	CuO	$\text{Cu}(\text{OH})_2$	$\text{Cu}(\text{mg/L})$
G1	100	27.0	55.8	17.2	0.49
S1	100	52.4	47.6	0.0	0.70
G1/S1/RO	62/27/11	6.1	53.1	40.8	0.98
RO	100	13.3	27.3	59.4	0.52

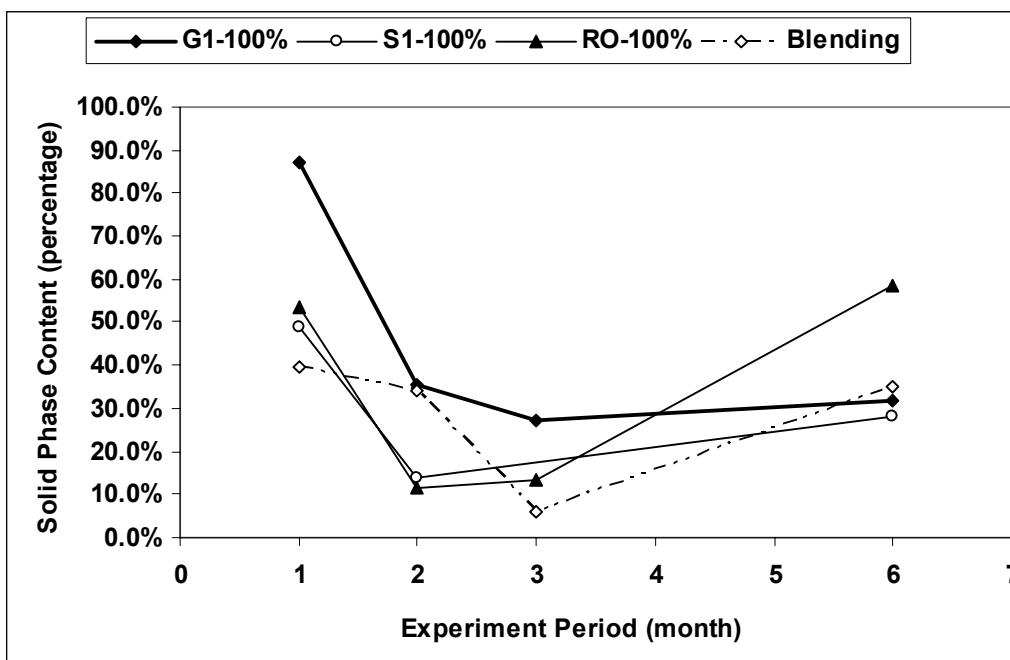


Figure 0.10 Cuprite (Cu_2O) content percentage variation versus the incubation time

The copper corrosion loops utilized in the field study provided total copper data that was correlated to water quality by statistical regression. Linear and non-linear models were created that related alkalinity, pH, sulfates and chlorides to total copper. Consequently the impact of alkalinity, pH, temperature, sulfate, and chloride on the formation of Cu_2O , $\text{Cu}(\text{OH})_2$ and CuO in surface scales over time of incubation was investigated. The ranges of water quality involved in this study were 52 to 211 mg/L as CaCO_3 for alkalinity, 7.61 to 8.12 for pH, 18.4 to 28.3°C for temperature, 20 to 93 mg/L chloride, and 3 to 228mg/L for sulfate. The relative composition of Cu_2O , $\text{Cu}(\text{OH})_2$ and CuO in surface scales of coupon exposed to different environments for a 1, 2, 3 and 6 month incubation period is presented in Figure 0.11 for varying alkalinity of each

environment. The composition of Cu_2O , $\text{Cu}(\text{OH})_2$ and CuO was normalized to 100% and the relative composition is shown in the associated histograms in Figure 0.11.

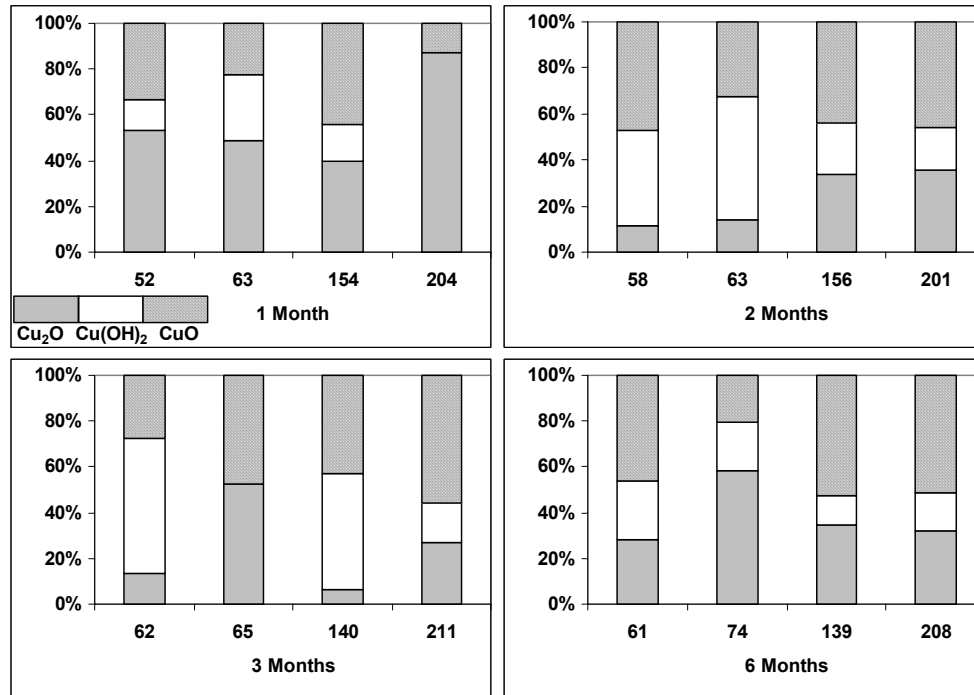


Figure 0.11 Copper corrosion products sensitivity analysis –Alkalinity. X axis represent alkalinity as mg/L CaCO_3 . Y axis represent the scale layer phase contents.

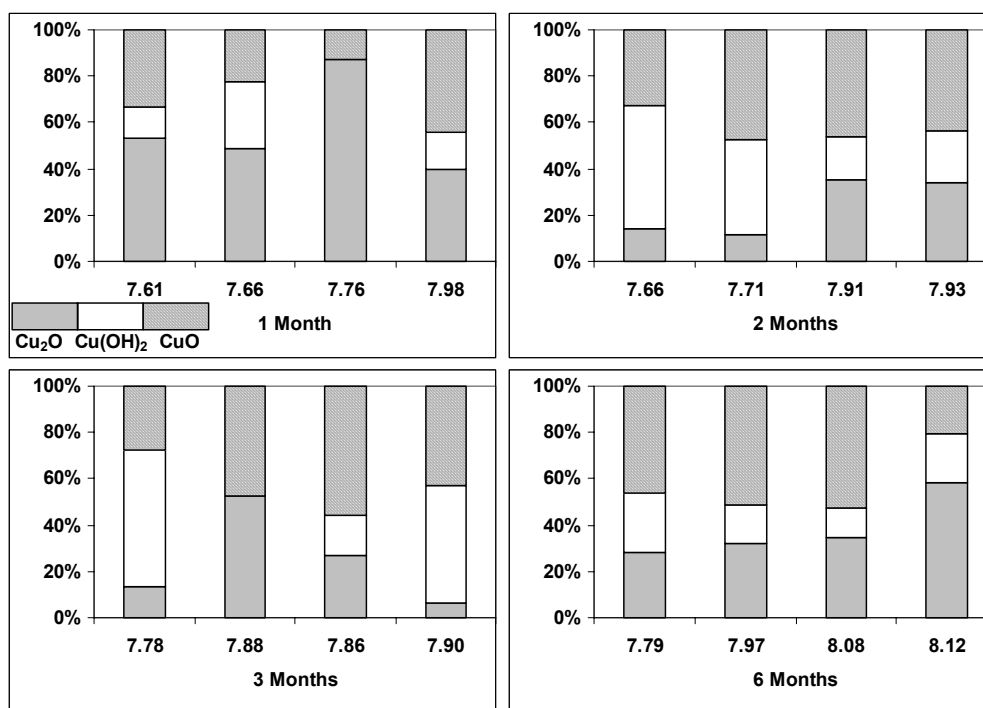


Figure 0.12 Copper corrosion products sensitivity analysis –pH. X axis represent pH value. Y axis represent the scale layer phase contents.

As shown in Figure 0.11, the variation of solid phase composition was not sensitive to variations in alkalinity. For the one month coupon, the relative percent Cu₂O decreased as alkalinity increased, but increased with alkalinity increasing till the maximum alkalinity environment, 204 mg/L as CaCO₃. In the second month the relative percent Cu₂O increased as alkalinity increased. The variation in Cu₂O relative composition does not appear to be related to alkalinity in the three and six month samples.

The relative composition of Cu₂O, Cu(OH)₂ and CuO in surface scales of coupon exposed to different environments for a one, two, three and six month incubation period is presented in Figure 0.12 for varying pH of each environment. The pH range is relatively tight,

but pH is a log term and the variation of pH from 7.61 to 7.98 represents a 43 % variation in protons shown in the one month sample. Copper release is reduced as pH increases due to the solubility of the controlling solid phase and free copper ion and the associated dissolved copper complexes. The relative composition of Cu_2O , $\text{Cu}(\text{OH})_2$ and CuO was independent of pH variations over time for the conditions of this study. The relative composition for each of three solid components did vary from month to month but in no discernable relation to pH. The relative percentage of cupric hydroxide percentage did stabilize in the sixth month.

Temperature, unlike other water qualities, can not be controlled in field studies. Thus the sensitivity analysis of temperature on surface characterization includes time and temperature. As expected, water temperature increased steadily with time during the field investigation. The 95% confidence intervals for temperature by time of samples are 18.4 to 19.0°C for month one, 22.7 to 23.1°C for month two, 24.9 to 25.4°C for month three, and 27.3 to 28.4°C for month six. Temperature was significantly less variable within monthly intervals. The average temperature the one, two, three and six month coupons were 18.7, As with pH and alkalinity, there was no discernable correlation between the relative composition of Cu_2O , $\text{Cu}(\text{OH})_2$ and CuO in surface scales and temperature. The same trend was observed for chlorides and sulfates, there was no discernable correlation between the relative composition of Cu_2O , $\text{Cu}(\text{OH})_2$ and CuO in surface scales for either sulfates or chlorides.

No significant relationship was found between the relative composition of Cu_2O , $\text{Cu}(\text{OH})_2$ and CuO in surface scales and any of the significant water quality variables in the linear and non-linear models that related total copper to alkalinity, pH, sulfates or chlorides. This may have been due to the length of investigation as the six month period of incubation was not long

enough to show trends that are dependent on approaching equilibrium. The lack of correlation of soluble water quality parameter to total copper may also have been due to the impact of particulate copper on total copper, and the dependence of copper particulate release with hydraulic conditions and other variables than water quality.

The Theoretical model development

Thermodynamic modeling was conducted for several combinations of water quality and controlling solid phases for copper. One fundamental assumption for thermodynamic modeling is that equilibrium and speciation are well-defined. This may have not been the case in the six month study period, which limits application of thermodynamic models. There are some issues with developing thermodynamic models to accurately describe field systems. The coexistence of CuO and Cu(OH)₂ and the difficulty of identifying their cross-sectional distribution in surface scales limited the identification of the controlling phase. There was some discrepancy among published values for equilibrium constants and the impact of the release of particulate copper is not considered by thermodynamic modeling. However, theoretical models can be developed and adjusted to field data, which is a meaningful and valuable tool for analyzing and controlling copper release in drinking water distribution systems. Major anions, ligands, and complexation reactions are listed in

Table 0.2. The total dissolved copper calculation is shown in equation (0.3), where the subscript “T” stands for the total copper, and the “OH”, “CO₃”, “Cl”, “SO₄” represents the associated hydroxide, carbonate, chloride, and sulfate complexes. Phosphate and ammonia complexes contribute significantly at certain conditions, but these conditions are not achieved in drinking water distribution systems and their impact on total soluble copper is insignificant.

$$[Cu]_T = [Cu_{T,OH}] + [Cu_{T,CO_3}] + [Cu_{T,Cl}] + [Cu_{T,SO_4}] \quad (0.3)$$

Table 0.2 Aquatic reactions and equilibrium constants involved in model development expressed as logarithm scale. ORP used in monovalent/divalent conversion is 38mV

No.	Reactions	Log(K) or log(β) at 25 °C
<i>Hydroxide Species (divalent)</i>		
1	$\text{Cu}^{2+} + \text{H}_2\text{O} \leftrightarrow \text{CuOH}^+ + \text{H}^+$	-7.96
2	$\text{Cu}^{2+} + 2\text{H}_2\text{O} \leftrightarrow \text{Cu}(\text{OH})_2^0 + 2\text{H}^+$	-16.24
3	$\text{Cu}^{2+} + 3\text{H}_2\text{O} \leftrightarrow \text{Cu}(\text{OH})_3^- + 3\text{H}^+$	-26.90
4	$\text{Cu}^{2+} + 4\text{H}_2\text{O} \leftrightarrow \text{Cu}(\text{OH})_4^{2-} + 4\text{H}^+$	-39.56
5	$2\text{Cu}^{2+} + 2\text{H}_2\text{O} \leftrightarrow \text{Cu}_2(\text{OH})_2^{2+} + 2\text{H}^+$	-10.58
6	$3\text{Cu}^{2+} + 4\text{H}_2\text{O} \leftrightarrow \text{Cu}_3(\text{OH})_4^{2+} + 4\text{H}^+$	-20.76
<i>Carbonate Species (divalent)</i>		
7	$\text{Cu}^{2+} + \text{H}^+ + \text{CO}_3^{2-} \leftrightarrow \text{CuHCO}_3^+$	12.13
8	$\text{Cu}^{2+} + \text{CO}_3^{2-} \leftrightarrow \text{CuCO}_3^0$	6.82
9	$\text{Cu}^{2+} + 2\text{CO}_3^{2-} \leftrightarrow \text{Cu}(\text{CO}_3)_2^{2-}$	10.60
10	$\text{Cu}^{2+} + \text{CO}_3^{2-} + \text{H}_2\text{O} \leftrightarrow \text{Cu}(\text{OH})(\text{CO}_3)^- + \text{H}^+$	-4.25
11	$\text{Cu}^{2+} + \text{CO}_3^{2-} + 2\text{H}_2\text{O} \leftrightarrow \text{Cu}(\text{OH})_2(\text{CO}_3)^{2-} + 2\text{H}^+$	-13.14
<i>Chloride, and Sulfate Species (divalent)</i>		
12	$\text{Cu}^{2+} + \text{SO}_4^{2-} \leftrightarrow \text{CuSO}_4^0$	2.36
13	$\text{Cu}^{2+} + \text{Cl}^- \leftrightarrow \text{CuCl}^+$	0.40
14	$\text{Cu}^{2+} + 2\text{Cl}^- \leftrightarrow \text{CuCl}_2^0$	-0.12
<i>Cuprous Species (monovalent)</i>		
15	$\text{Cu}^+ + \text{Cl}^- \leftrightarrow \text{CuCl}^0$	2.70
16	$\text{Cu}^+ + 2\text{Cl}^- \leftrightarrow \text{CuCl}_2^-$	5.48
17	$\text{Cu}^+ + 3\text{Cl}^- \leftrightarrow \text{CuCl}_3^{2-}$	4.81
18	$2\text{Cu}^+ + 4\text{Cl}^- \leftrightarrow \text{Cu}_2\text{Cl}_4^{2-}$	10.32
<i>Conversion between cuprous and cupric copper</i>		
19	$\text{Cu}^+ \leftrightarrow \text{Cu}^{2+} + \text{e}^-$	-2.715

Complete models were develop for total copper considering CuO or Cu(OH)₂ as the controlling solid phase in equilibrium with all species shown in

Table 0.2. The relative contribution of each species was determine and insignificant contributing species were discarded. The most significant species are shown in equation (0.4) and account for 99.1% of the dissolved total copper.

$$\begin{aligned}
[Cu]_T = & [Cu^{2+}] + [CuOH^+] + [Cu(OH)_2^0] + [Cu(OH)_3^-] + [CuHCO_3^-] \\
& + [CuCO_3^0] + [Cu(CO_3)_2^{2-}] + [Cu(OH)_2CO_3^{2-}]
\end{aligned}
\tag{0.4}$$

Within 7.5-8.5 pH and 50-200mg/L $CaCO_3$ alkalinity, it is clear that aqueous $Cu(CO_3)^0$, $CuHCO_3^+$, and $CuOH^+$ dominate the composition of total copper, thus pH and alkalinity are important and sensitive factors. Other anions such as sulfates and chlorides are not included in equation (0.4) because the water quality conditions in drinking water significantly reduce their impact on copper concentrations. The predicted total dissolved copper species is eight times higher with $Cu(OH)_2$ as the controlling solid phase as opposed to CuO as the controlling solid phase. Predicted and actual copper concentrations versus field alkalinity and pH from the field data are illustrated in Figure 0.13. The model based on $Cu(OH)_2$ as the controlling solid phase slightly underestimates copper release. Given the field copper release consisted of dissolved and particulate species, the $Cu(OH)_2$ model accounting for dissolved species is acceptable. $Cu(OH)_2$ may not be the controlling solid phase as the particulate contribution to total copper release is unknown. As shown, copper release is more sensitive to alkalinity when pH decreases and to pH when alkalinity increases, thus the appropriate approach preventing copper problem is to keep pH high and alkalinity low as defined by the conditions of this investigation.

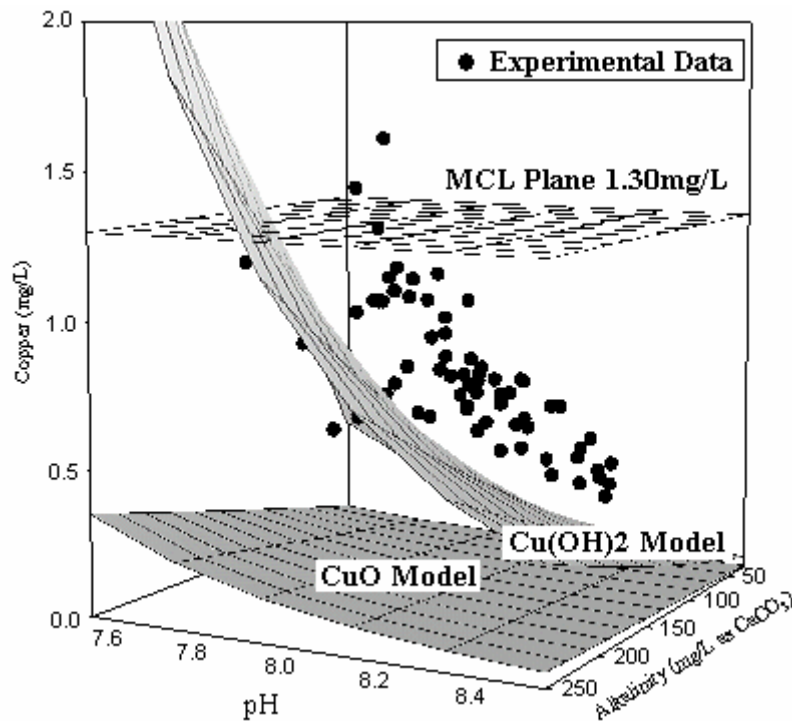


Figure 0.13 Thermodynamic models for copper release versus pH and alkalinity for CuO and Cu(OH)₂ controlling solid phases.

Conclusion

- Six months of exposure to drinking water environments was inadequate to form enough divalent corrosion products on copper coupons for XRD detection. For all samples taken at one, two, three and six months the major corrosion scale layer on the copper coupons consisted of cuprite (Cu₂O) as no consistent formation of Cu(II) species was observed in the scale.
- The morphology of the top of the surface scale varied with water quality. A high alkalinity and low chloride finished groundwater environment produced a more compact top scale layer than a low alkalinity and high chloride finished water environment.

- Tenorite (CuO) and $\text{Cu}(\text{OH})_2$ were the major cupric component on the very top of the copper layer. Other $\text{Cu}(\text{II})$ species could exist given the right environment. Cuprite (Cu_2O) is present in the very top layer, which indicated a continuous disappropriation reaction.
- Cuprite (Cu_2O) variation in the top layer was dependent on aging. $\text{Cu}(\text{II})$ species were not dependent on aging.
- Theoretical approach is useful qualitatively, but is limited quantitatively due to the impact of particulate copper. However the trend of total copper release with pH and alkalinity is consistent with the trend predicted by the $\text{Cu}(\text{OH})_2$ solid phase equilibrium model..

References

- (1) Ugorets, M.Z., E.A. Buketov, and K.M. Akhmetov. 1968. Thermographic Study of the Dehydration of Copper Hydroxide in Alkaline Solutions. *Russ. Jour. of Inorganic Chemistry*, 13(6):1525-1529.
- (2) Chalyi, V.P. 1963. Mechanism of Aging of Individual Metal Hydroxides and Hydroxide Systems. *Russ. Jour. of Inorganic Chemistry*, 8(2):269-273.
- (3) Feitknecht, W., P. Schindler. 1963 Solubility Constants of Metal Oxides, Metal Hydroxides, and Metal Hydroxide Salts in Aqueous Solution *Pure and Applied Chemistry* (6):130-199
- (4) Isaac, R.A.; L. Gil, A.N. Cooperman, K. Hulme, B. Eddy, M. Ruiz, K. Jacobson, C. Larson, and O.C. Pancorbo. 1997. Corrosion in Drinking Water Distribution Systems: A Major Contributor of Copper and Lead to Wastewater and Effluent. *Environmental Science and Technology*, 31(11):3198-3203.

- (5) Hidmi, L., and M. Edwards. 1999. Role of Temperature and pH in $\text{Cu}(\text{OH})_2$ Solubility. *Environmental Science and Technology*, 33(15):2607-2610.
- (6) Patterson, J.W., E.B. Richard, and D. Marani. 1991. Alkaline Prediction and Aging of Copper from Dilute Cupric Nitrite. *Environmental Science and Technology*, 25(10):1780-1787.
- (7) Matijevic, E. 1978 Preparation and Properties of Monodispersed Colloidal Metal Hydrous Oxides *Pure Applied Chemistry* (50):1193-1210
- (8) Feng, Y., W.K. Teo, K.S. Siow, K.L. Tan, and A.K. Hsieh. 1996 The Corrosion Behaviour of Copper in Neutral Tap Water Part I: Corrosion Mechanisms *Corrosion. Sci.* 38(3) 1996 369-385
- (9) Hamann, C.H., A. Hammett, and W. Vielstich. 1998. *Electrochemistry*. New York: Wiley-VCH
- (10) Jones D.A. 1995 *Principles and Prevention of Corrosion* 2nd edition New Jersey Prentice Hall
- (11) American Water Works Association Research Foundation 1996 *Internal Corrosion of Water Distribution Systems* 2nd Edition DVGW-TZW
- (12) Pankow, J.F. 1991. *Aquatic Chemistry Concept*. Chelsea, Mich.: Lewis Publishers.
- (13) Michael R.S., A.L. Darren 1995 Effect of pH, DIC,, Orthophosphate and Sulfate on Drinking Water Cuprosolvency *EPA report EPA/600/R-95/085*
- (14) Edwards, M., M. Schock, and T.E. Meyer. 1996. Alkalinity, pH, and Copper Corrosion By-product Release. *Jour. AWWA.*, 88(3):81-94.
- (15) Hidmi, L., and M. Edwards. 1999. Role of Temperature and pH in $\text{Cu}(\text{OH})_2$ Solubility. *Environmental Science and Technology*, 33(15):2607-2610

- (16) Marani, D., J.W. Patterson, and P.R. Anderson. 1995. Alkaline Precipitation and Aging of Cu(II) in the Presence of Sulfate. *Water Research*, 29(5) 1317-1326.
- (17) Merkel, T.H., H.J. Gross, W. Werner, T. Dahlke, S. Reicherter, G. Beuchle, and S.H. Eberle. 2002. Copper Corrosion By-product Release in Long-term Stagnation Experiments. *Water Research*, 36(6):1547-1555
- (18) Chmielova, M., J. Seidlerova, and Z. Weiss. 2002 X-Ray Diffraction Phase Analysis of Crystalline Copper Corrosion Products after Treatment in Different Chloride Solutions *Corrosion Science* 45(5):883-889
- (19) Boulay, N., and M. Edwards. 2001 Role of Temperature, Chlorine, and Organic Matter in Copper Corrosion By-product Release. *Water Research*. 35(3):683-690
- (20) Nassau, K., A.E., Miller, and T.E. Garedel 1987 The Reaction of Simulated Rain With Copper, Copper Patina, and Some Copper Compounds. *Corrosion Science*. 27(7):703-719
- (21) Reiber, S.H. 1989 Copper Plumbing Surfaces: An Electrochemical Study *Journal of AWWA*. 81(7):114-122
- (22) Broo, A.E., B. Berghult, and T. Hedberg. 1997 Copper Corrosion in Drinking Water Distribution Systems-The Influence of Water Quality *Corrosion Science*. 39(6):1119-1132
- (23) Edwards, M., L. Hidmi, and D. Gladwell 2002 Phosphate Inhibition of Soluble Copper Corrosion By-product Release *Corrosion Science* 44(5):1057-1071
- (25) Cotton F.A., and G. Wilkinson. 1999 *Advanced Inorganic Chemistry* New York Sixth. John Wiley & Sons.

- (26) Froning, M.H., M.E. Shanley, E.J. Jr. Verink. 1976 An Improved Method for Calculation of Potential-pH Diagrams of Metal-Ion-Water System by Computer *Corrosion Science*. 16(6):371-377
- (27) Edwards, M., S. Jacobs, R.J. Taylor. 2000 The blue Water Phenomenon *Journal of AWWA*. 92(7):72-82
- (28) Standard Methods for the Examination of Water and Wastewater 1999 18th Edition APHA-AWWA-WPCF

Chapter 3 Effect of Blended Water on Copper Corrosion Release in Drinking Water Pipe Distribution System and Empirical Model Development

Introduction

Cuprosolvency enhances copper corrosion in drinking water distribution systems and generates regulatory and consumer issues for many water suppliers, even though copper is relatively corrosion resistant. Violations in excess of the 1.30 mg/L total copper action level specified by the LCR (Lead and Copper Rule) are not uncommon, and blue and green water have been observed in tap water at homes [1-7]. Consequently, the water community needs to understand the physical-chemical factors controlling copper release in home plumbing systems in order to develop a proactive strategy for prevention of excessive copper release. Extensive research has been conducted on copper release in the past [1, 3, 4]. These works have indicated precipitation and dissolution of cupric hydroxide ($\text{Cu}(\text{OH})_2$) was the controlling solid phase for the release of dissolved copper, and associated cupric hydroxide ($\text{Cu}(\text{OH})_2$) solubility models were descriptive of this mechanism. Although these models apply to restrictive environments, they are not universal to drinking water environments in distribution systems due to the relationship and confounding effects of common water quality parameters in drinking water on copper release.

Copper is not thermodynamically stable in drinking because of equilibrium with a controlling solid phase and the presence of oxidizers such as dissolved oxygen and chlorine. A one-electron transfer mechanism dominates the initial release of copper to drinking water. Elemental copper is oxidized to a cuprous ion, which is followed by the precipitation of cuprite (Cu_2O)[8]. Further oxidation of cuprous ions and cuprite produces cupric ions that will

accumulate at the local point of oxidation due to the limited mass transfer associated with diffusion and the resulting stagnation [3]. Although interactions between cupric ion and common anions in drinking water coupled with stagnation reduce the free cupric ion concentration near the copper pipe material surface, cupric ion eventually become supersaturated and precipitation controls the soluble copper concentration in water [7,9]. Like other metals, the copper precipitation involves formation of a precipitate followed by aging as two distinct phases. The first phase consists of supersaturating, nucleation, and particle growth, while the second growth phase involves Ostwald ripening, recrystallization, and agglomeration. These mechanisms occur simultaneously or in series and present a complex reactionary environment. The final precipitate modifications significantly depend on specific water quality parameters such as temperature, pH, anions, and aging time [10,11,12,13,14]. Slight variations of water quality could lead to a number of different solid compounds morphologies and modifications. Prediction models based on the controlling precipitation/dissolution theories, however, are constructed assuming the equilibrium constants are in fact constant and do not vary with water quality and aging. Consequently, it is not unusual to obtain different actual and predicted copper using equilibrium models.

It is now widely accepted that alkalinity and pH are two most important factors affecting copper release in drinking water based on the current precipitation and dissolution equilibrium model. Chlorides, sulfates, phosphates, neutral dissolved oxygen, chlorine residual, natural organic matter, temperature, microorganisms also influence copper release in drinking but far less than alkalinity and pH [1-7]. Most literature illustrated the principles pertaining to alkalinity and pH effects on copper release by assuming (1) soluble carbonate complexes dominate the

soluble copper species [3,8], and (2) the free cupric ion concentration is controlled by cupric hydroxide given thermodynamic equilibrium has been reached. Some researchers using a pipe-rig in field studies published a linear relationship between soluble copper and higher alkalinity at constant pH. The slope of the linear coefficient relating copper release to alkalinity decreases with increasing pH [4]. Similar trends also were published in the literature. pH and alkalinity have opposite effects on copper release. Increasing pH reduces copper release, whereas increasing alkalinity increases copper release and vica-versa.

Although the effects of individual factors have been investigated extensively, accurate predictions of copper concentrations are difficult to make in known water quality. Literature indicates that there are several reasons affecting accurate predictions of copper in known water quality[15]: (1) Kinetics limit copper predictions as equilibrium may not be achieved during the contact periods. There may be several controlling solids and intermediate phases due to asynchronous transformation such as the coexistence of fresh, aged precipitated cupric hydroxide ($\text{Cu}(\text{OH})_2$) and cuprite (CuO). The latter is believed to be a dehydration product of cupric hydroxide or the products of further oxidation of cuprite. The true equilibrium constants may not be known. Several researchers have reported different equilibrium constants for the same reaction. There are significant confounding effects that are not represented by equilibrium constants. Increasing alkalinity is generally thought to increase soluble copper but some researchers reported higher copper concentrations at lower alkalinity in soft waters. Consequently, known hardness is necessary to evaluate the effect of alkalinity on soluble copper. Finally, the concentration of copper can be affected by particle release, which is affected by water quality variation and hydraulic forces in the distribution system.

As noted, there are many factors affecting copper release and accurate prediction of copper is difficult in drinking water distribution systems. In most cases, only wide ranges and general trends can be estimated. Water utilities rely on operational experience to control copper concentrations in distribution systems. Therefore, pilot scale investigations are strongly recommended for controlling copper in drinking water distribution systems.

Experiment Methods

Using data from a large field study, this work correlates varying water quality and the associated confounding effects to copper release. The site of the field study shown in Figure 0.1 was at the Cypress Creek Drinking Water Facility in Pasco County Florida. Ground, surface and desalinated finished waters were produced on site and blended before discharge to pilot distribution systems (PDSs). The blending variations produced water quality variations that are common in distributions systems receiving different finished waters. Specific water quality parameters include alkalinity, pH, TDS, silica, calcium, sulfate, chloride, dissolved oxygen, and temperature. Linear and non-linear models were developed by regression of released copper to water quality and can be used for prediction of total copper for any given water quality, which provide a predictive means of copper control in drinking water distribution systems.



Figure 0.1: Pilot-scale PDS research site, fourteen hybrid material pipelines and four single material pipelines.

Source water production and blending

The field site contained seven different pilot plants that produced drinking water by desalinization, enhanced surface water treatment, surface and ground water nanofiltration, softening and conventional ground water treatment. A brief description and associated acronyms for the seven water treatment processes is presented in Table 0.1. Four waters were produced from groundwater and are denoted G1, G2, G3 and G4, which represents conventional, softening, softening of blended water and nanofiltration of blend waters. Two waters were produced from surface water and are identified as S1 and S2, which represents enhanced coagulation, ozonation and biological activated carbon (BAC) filtration. The RO water was produced using reverse

osmosis. Aeration, pH stabilization, and chloramination post treatment was common to all waters.

Table 0.1 Pilot-scale experiment water resource, blending scenarios, and related unit processes description

No.	I. D.	Source Water	Unit Processes
1	G1	Groundwater	Aeration, Disinfection, pH stabilization
2	G2	Groundwater	Softening, Sedimentation, Sand Filtration, Disinfection, pH stabilization
3	G3	Groundwater, RO and S1	Softening, Sedimentation, Sand Filtration and Disinfection, pH stabilization
4	G4	Groundwater, RO and S1	Nano-filtration, pH stabilization
5	S1	Surface Water	Coagulation, Flocculation, Sedimentation, Ozone, GAC bio-reactor, Disinfection, sand filtration, pH stabilization
6	S2	S1 after sedimentation	Nano-filtration, pH stabilization
7	RO	Groundwater	5 um cartridge pre-filtration, RO, Disinfection, pH stabilization

The blended waters were discharged to eighteen different PDSs that were made from actual distribution system PVC, unlined cast iron (UCI), lined cast iron (LCI), and galvanized steel (GS) pipe. Fourteen PDSs were hybrid lines and consisted of 25 feet of 6-inch PVC, 18 feet of 6-inch UCI, 25 feet of 6-inch LCI and 40 feet of 2-inch diameter galvanized steel. The segments were coupled using flexible interconnects made from organic polymers known as

speedies. Four PDSs were made totally of PVC, UCI, LCI and GS. All pipes were excavated from existing distribution systems.

The discharges from the pilot distribution systems were routed (in parallel) to separated copper loops and cradles that houses coupons made of the four different pipe materials. The cradles were constructed of 4-inch PVC, with interior trays cut from 3-inch diameter PVC. The total length of cradle required to house the coupons was 12 feet. Flows into the cradle were manipulated to maintain similar velocities and residence times in all units.

Copper corrosion loops

Each PDS was followed by a copper loop shown in Figure 0.2 to simulate monitoring kitchen tap water quality as required by the Lead and Copper Rule (LCR). All copper loops were identical and 30 feet long. The first 27 feet in the loop contained 1 L, which was the required LCR sample volume. The additional 3 feet compensated for mixing of water that was not in contact with copper pipe. All other fittings and materials were inert polymers. Copper coupons were installed in each loop for surface characterization. The coupons were commonly used for weight loss studies and identification. These coupons had a surface area of 3.38 square inches, which was determined by assuming 17 joints in the copper plumbing under a typical consumer sink with each having a 1/8th inch bead on the inside of each 0.5 inch diameter joint, which seemed rational for a typical home sink.

The field study was conducted in six phases. A phase was defined as every time the blends were changed to the PDSs. Blends were changed every three months. The field study lasted for eighteen months and consisted of six different phases.

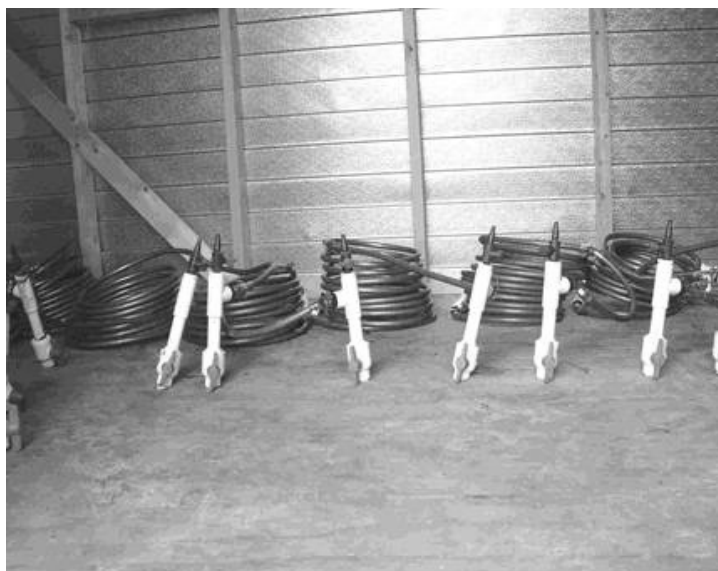


Figure 0.2 Copper loops containing separate lead coupons used for corrosion study.

Water quality monitoring

The copper loops were flushed daily. However the water in the loops was stagnant for six hours before samples were collected for analyses. Approximately 2~3 gallons of water from the PDSs were flushed through each loop for 5 minutes, which amounted to a 3 loop volume. Samples were preserved at 4 °C before analyses. Samples were analyzed bimonthly in phase I/II and weekly in phase III-IV. Initial testing demonstrated PDS effluent water quality did not change in the copper loop except for copper and lead concentrations, thus PDS effluents were monitored for all other water parameters than copper and lead.

Results and Discussion

Pilot-Scale Experiment Study

Source water blending and water quality variations

The blends of finished waters used for the first four phases of the project are shown in

Table 0.2. The water quality composition of the blends is shown in Table 0.3. The coefficients of determination (R^2) for solutes from all finished waters (PDS influents) are shown in

Table 0.4. Except for R^2 of 1, all R^2 greater than 0.30 are underlined and bolded in order to highlight interrelated source water quality. G1 was groundwater that contained relatively high alkalinity, calcium, conductivity, silicates, and UV_{254} to other sources. Conductivity was relatively high because of the relatively high TDS. G1 had moderate, sulfates, dissolved oxygen, and low chlorides to the other waters. As shown in Table 4, the R^2 are relatively high for an alkalinity relationship with calcium, UV_{254} and silicate. R^2 is also relatively high for a calcium-conductivity correlation. S1 and RO were somewhat similar and were a low alkalinity, low UV_{254} waters with moderate calcium, dissolved oxygen. Sulfates and TDS were only high in S1. Consequently, sulfates are not correlated to any other water quality parameter and are a good indicator of surface water in any blend. Chlorides, sodium were only high in RO waters and are relatively highly correlated as shown in

Table 0.4. Chlorides, silica and sodium are good indicators of the relative amount of blended RO water in this work. However, the major point from

Table 0.4 is that the source of each finished waters leaves a chemical indicators which can be used to identify the relative amount of finished waters in the blends used in this work, and also in the blends in an actual distribution system.

Table 0.2 Blending scenarios and PDS pipeline influent water distribution

PDS – Material	Phase 1/3							Phase 2/4						
	G1	G2	G3	G4	S1	S2	RO	G1	G2	G3	G4	S1	S2	RO
01 – hybrid	100								100					
02 – hybrid		100						100						
03 – hybrid					100								100	
04 – hybrid			100							100				
05 – hybrid							100					100		
06 – hybrid	55				45			68						32
07 – hybrid	68						32	55				45		
08 – hybrid	23				45		32	60					30	10
09 – hybrid	60				30		10	23				45		32
10 – hybrid		50			50			62				24		14
11 – hybrid		62			24		14		50			50		
12 – hybrid			100								100			
13 – hybrid						100								100
14 – hybrid	62				27		11	62				27		11
15 – unlined iron	23				45		32	60				30		10
16 – lined iron	23				45		32	60				30		10
17 – PVC	23				45		32	60				30		10
18 – galvanized	23				45		32	60				30		10

Table 0.3 Source water blending ratios and their resultant ten water quality parameters feeding copper loops. Composition symbols refer to as Table 0.1

Blending Composition	Blending Ratio	Copper (mg/L)	Alkalinity (mg/L)	pH [-]	Cl ⁻ (mg/L)	SO ₄ ²⁻ (mg/L)	DO (mg/L)	TDS (mg/L)	Ca ²⁺ (mg/L)	Silica (mg/L)	Temp. (°C)	UV-254 (cm ⁻¹)
G1	100	0.92	207	7.87	28.9	26.1	6.5	421	84.8	13.7	24.2	0.060
S1	100	0.63	60	7.92	37.1	190.2	6.3	423	56.5	10.0	24.0	0.024
RO	100	0.61	69	8.06	91.7	5.8	5.2	267	28.7	3.5	24.1	0.028
G2	100	0.66	89	7.92	23.0	26.0	6.9	227	34.1	13.7	24.2	0.057
G3	100	0.45	61	8.13	49.7	79.0	6.2	306	35.4	10.4	23.9	0.043
G4	100	0.52	88	8.17	43.9	6.8	6.3	233	35.0	10.0	24.0	0.028
S2	100	0.52	66	8.13	68.5	12.7	5.6	239	28.0	8.8	23.9	0.029
G1-RO	68-32	1.11	158	7.94	49.4	19.4	5.6	367	69.2	9.8	23.8	0.048
G1-S1-RO	62-27-11	1.14	147	7.91	40.1	77.4	5.5	394	66.4	10.8	24.2	0.046
G1-S2-RO	60-30-10	0.77	151	7.99	45.9	19.9	6.0	348	66.1	10.9	24.0	0.048
G1-S1	55-45	1.15	139	7.94	35.0	105.9	6.2	422	70.3	11.9	24.1	0.041
G1-S1-RO	23-45-32	0.78	104	8.01	53.5	93.4	6.5	389	56.1	8.8	24.0	0.034
G2-S1-RO	62-24-14	0.61	77	8.03	39.7	73.4	6.1	296	40.8	10.9	23.8	0.040
G2-S1	50-50	0.59	73	8.02	32.7	112.6	6.5	328	45.0	11.2	23.9	0.037

Table 0.4 Linear statistical correlation coefficient matrix of water quality parameters of interest

Parameter	pH	Alkalinity.	Cl ⁻	SO ₄ ⁻²	Na ⁺	Ca ⁺²	Silicate	Cond.	UV254	DO	Temp.
pH	1.00	-0.16	0.11	0.00	0.00	-0.06	0.00	-0.24	-0.09	0.19	-0.15
Alkalinity	-0.16	1.00	-0.13	-0.06	0.23	0.60	0.16	0.21	0.31	0.00	0.00
Cl ⁻	0.11	-0.13	1.00	-0.04	0.34	-0.10	-0.56	-0.01	-0.21	-0.01	0.00
SO ₄ ⁻²	0.00	-0.06	-0.04	1.00	0.02	0.10	0.03	0.27	-0.08	0.02	-0.01
Na ⁺	0.00	0.23	0.34	0.02	1.00	-0.22	-0.65	0.06	-0.27	-0.12	0.04
Ca ⁺²	-0.06	0.60	-0.10	0.10	-0.22	1.00	0.24	0.38	0.09	0.05	-0.04
Silicate	0.00	0.16	-0.56	0.03	-0.65	0.24	1.00	0.00	0.16	0.08	0.00
Cond.	-0.24	0.21	-0.01	0.27	0.06	0.38	0.00	1.00	0.00	-0.04	0.02
UV-254	-0.09	0.31	-0.21	-0.08	-0.27	0.09	0.16	0.00	1.00	0.05	0.00
DO	0.19	0.00	-0.01	0.02	-0.12	0.05	0.08	-0.04	0.05	1.00	-0.40
Temp.	-0.15	0.00	0.00	-0.01	0.04	-0.04	0.00	0.02	0.00	-0.40	1.00

Copper release under various water qualities

Water quality was correlated with copper release by linear regression. Alkalinity and pH, were highly correlated and exerted a significant impact on released copper. Chloride and sulfate are the major anions in drinking water, while DO is a major oxidant. Although sodium is major cation, it varies with chloride almost always and in this work and has a similar effect. Calcium may have a significant effect on copper release because of the associated effect of CaCO_3 precipitation on corrosion. UV_{254} represents a major fraction of organic matter and like silica could significantly inhibit copper release. Finally conductivity is a direct measure of electron transfer, is directly related to TDS and could have a significant impact on copper release in this work. The effects of all of these water quality parameters on copper release are considered in the following sections.

Effect of pH

The average copper release for the eighteen PDSs for the first four phases versus pH is shown in Figure 0.3 by average range of alkalinity. PDS pH ranged between 7.71 and 8.28 during the field study. Alkalinity was grouped by determining the smallest Euclidean distance standard within each group that contained 36.1 % and 66.7 % percentile of the alkalinity population for delimitation. This method of determining confounding effects of independent variables is in the literature [16, 17]. These three groups corresponded to low, moderate, and high alkalinity as defined by 51 to 67 mg/L, 68 to 127 and 128 to 212 as CaCO_3 . The average copper release associated with these groups was 0.50, 0.67 and 0.94 mg/L respectively. Clearly, two qualitative trends are evident. Copper release decreases as pH increases and the slope for copper release versus pH increases as alkalinity increases. Similar observations were referenced

in the literature review. The pH effect may be caused by the associated decrease of free cupric ions and relevant soluble hydroxyl complexes with decreased proton activity. Even through the pH effect is rather obvious at lower pH, the pH range is narrow in drinking water and the associated effects are more difficult to observe. However this interpretation shows copper release is affected by both alkalinity and pH, and pH impacts the affect of alkalinity on copper release.

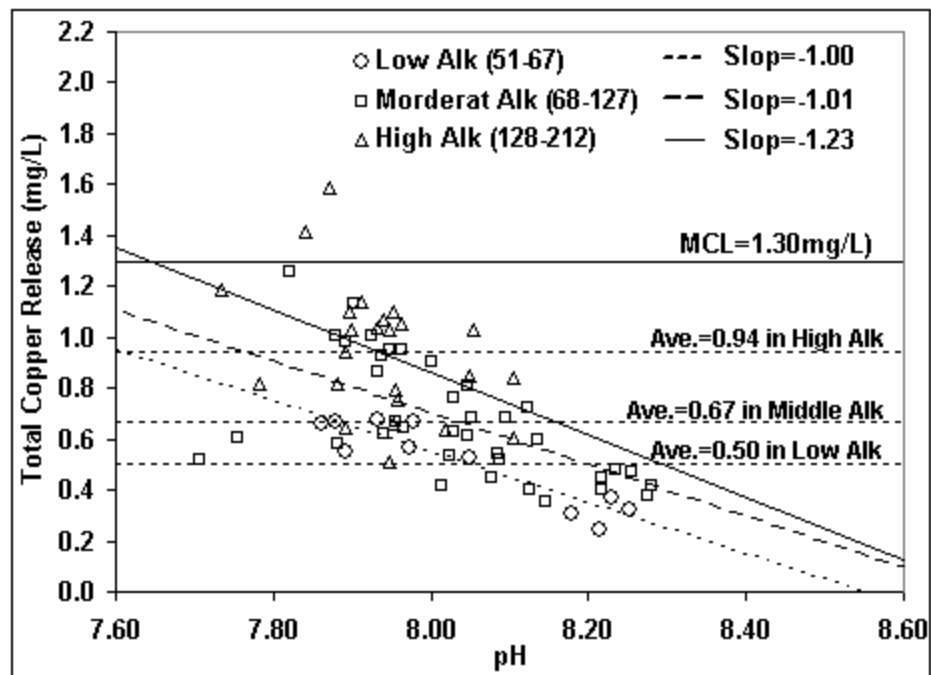


Figure 0.3 pH effect on total copper release

Effect of Alkalinity

The average phase copper release for all PDS loops versus average alkalinity is shown in Figure 0.4. Alkalinity ranged between 51 and 212 mg/L as CaCO_3 during the field study, which is representative of the expected variation caused by blending finished ground, surface and desalinated waters. Copper release clearly increases as alkalinity increases. In drinking water, alkalinity is essentially all bicarbonate, which combines with free cupric ions to form CuCO_3^0 , a dissolved complex accounting for more than 80% of the total soluble copper. Even though the impact of other confounding factors can not be eliminated, alkalinity produced a very significant correlation to released copper. Copper release is slightly more scattered at high alkalinity than at low alkalinity. The probable reason is higher alkalinity releases more copper due to the soluble complexes, which in turn increases free copper ions and enhances confounding effects.

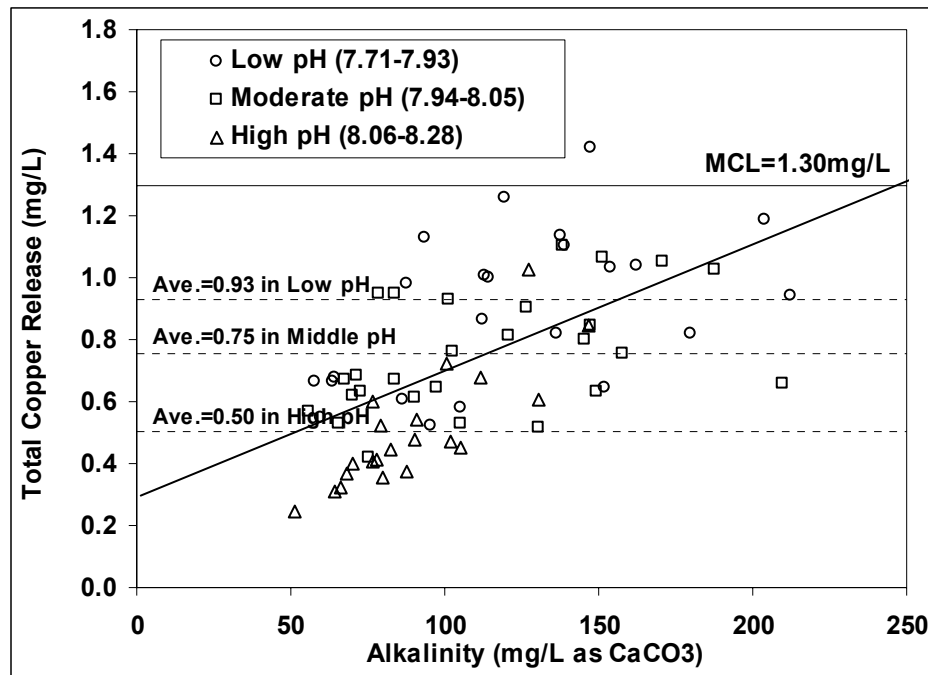


Figure 0.4 Alkalinity effect on copper release

The confounding effects of pH on the effect of alkalinity on copper release were investigated using groups as shown in Figure 0.4. Low, moderate and high pH groups were created using Euclidean distances, which were pH 7.71 to 7.93, pH 7.94 to 8.05 and pH 8.06 to 8.28. In our experimental environments, finished waters were stabilized before blending and discharge to the PDSs. Noting that alkalinity was directly correlated to calcium, waters low in alkalinity were low in calcium and a higher pH was required for stabilization. So, high pH was casually correlated to low calcium and alkalinity.

Clearly, as shown in Figure 0.4, copper release increases as alkalinity increases. The effect of pH on the relationship between total copper release and alkalinity is similar to the effect of alkalinity on the relationship between total copper release and pH. As seen in Figure 0.4, the

total copper released from the low pH group is higher than the total copper released from the high pH group. Hence, the same conclusion can be drawn from Figure 0.3 and Figure 0.4, which is both alkalinity and pH effect copper release. Increasing alkalinity increases copper release, increasing pH decreases copper release.

Effect of Typical Anions-Chloride and Sulfate

Conflicting conclusions have been published regarding the effect of chloride on copper release. Some researchers suggested that the chloride would increase the dissolved copper concentration due to soluble chloro-complexes formation [3], but some researchers concluded that chloride have increased and decreased copper release on occasion and the relationship is not clear [18]. Sulfate, forms a dissolved copper complex (CuSO_4^0), which may slightly enhance copper release, but the complex is quite weak and unlikely to make a significant contribution to the total copper release at sulfate concentrations common to drinking water.

The insignificant effects of chlorides and sulfates on copper release are illustrated in Figure 0.5 and Figure 0.6. As previously noted, alkalinity ranged from 212 and 51 mg/L as CaCO_3 , and pH ranged from 7.71 to 8.28 in the field study. At the first glance, high concentrations of chloride appear to reduce copper release. However the five data points corresponding to Cl concentration greater than 80 mg/L (the high Cl concentrations) corresponded to low alkalinity and high pH (77mg/L as CaCO_3 and 8.07). Hence, the lower copper concentrations were not due to only chlorides. The effect of sulfate on copper release is shown in Figure 0.6. Similarly, two copper release data points at the highest sulfate concentrations corresponded to low alkalinity and moderate pH (68, and 56 mg/L as CaCO_3 and

7.98 and 7.97 respectively). Moreover, there is no relationship between sulfate or chloride and copper release shown by general trends or Euclidean distance trend analyses.

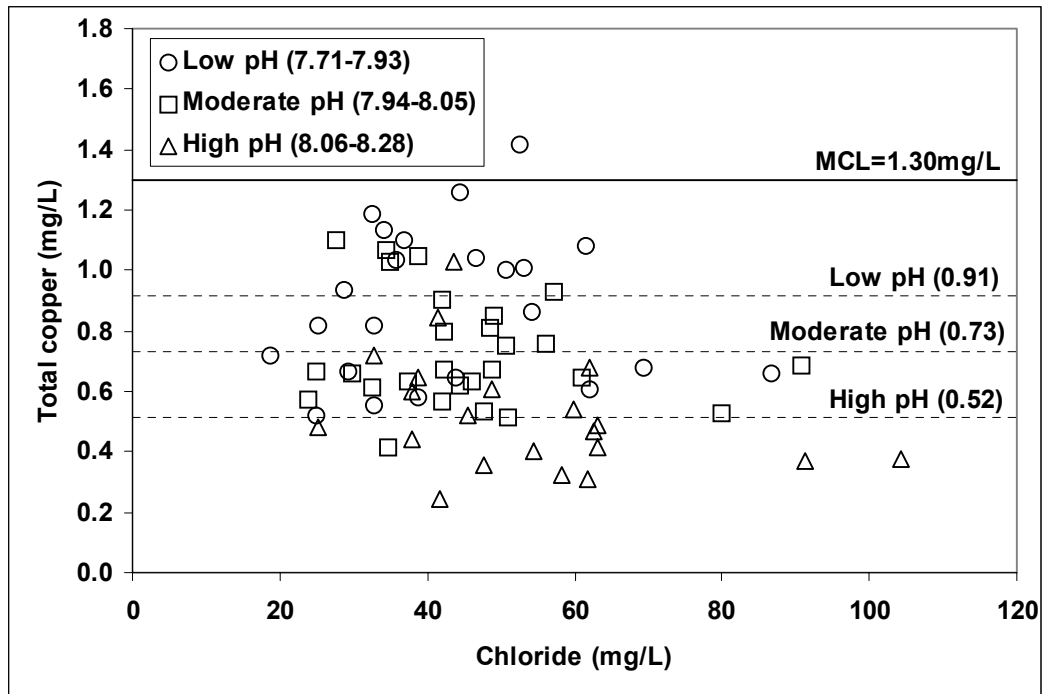


Figure 0.5 Chloride effect on total copper release

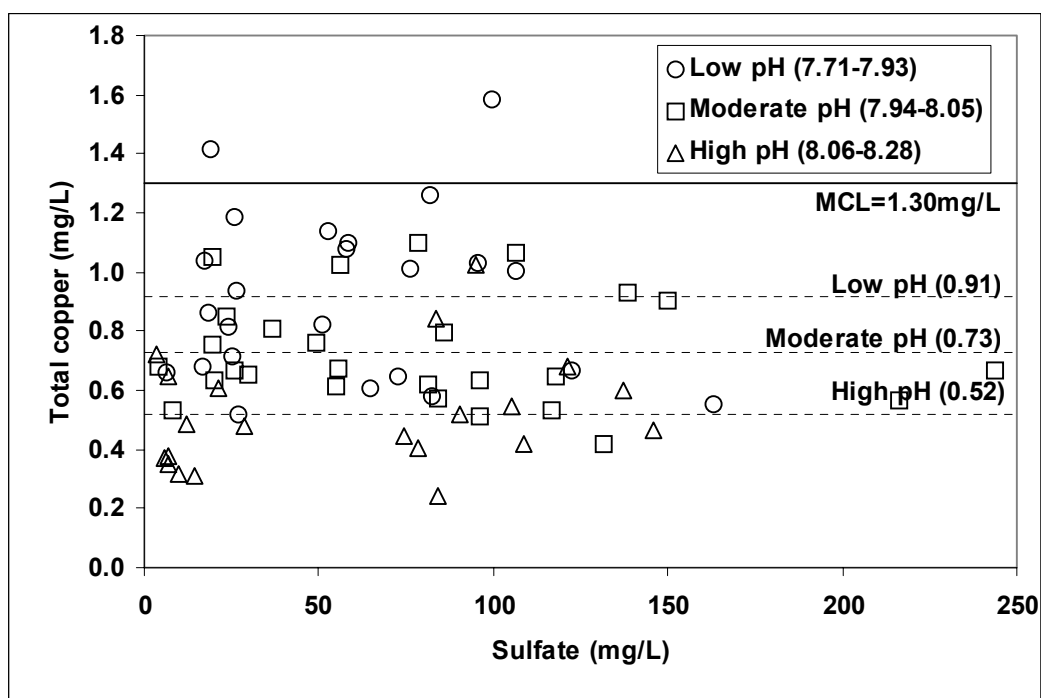


Figure 0.6 Sulfate effect on total copper release

Effect of Typical Cation – Calcium

Conventionally, calcium is thought to form a protective layer with carbonate on metals and isolate (short-circuit) the electron transport pathway. Consequently a plot of released copper versus calcium would be expected to have a negative slope, which is seen in Figure 0.7. However high calcium came from groundwater in this work and was always accompanied by high alkalinity. The true effect of calcium on copper is shown by normalizing calcium with respect to alkalinity as in Figure 0.8. There is no relationship between the calcium/alkalinity ratio and released copper. Consequently calcium had no effect on copper release..

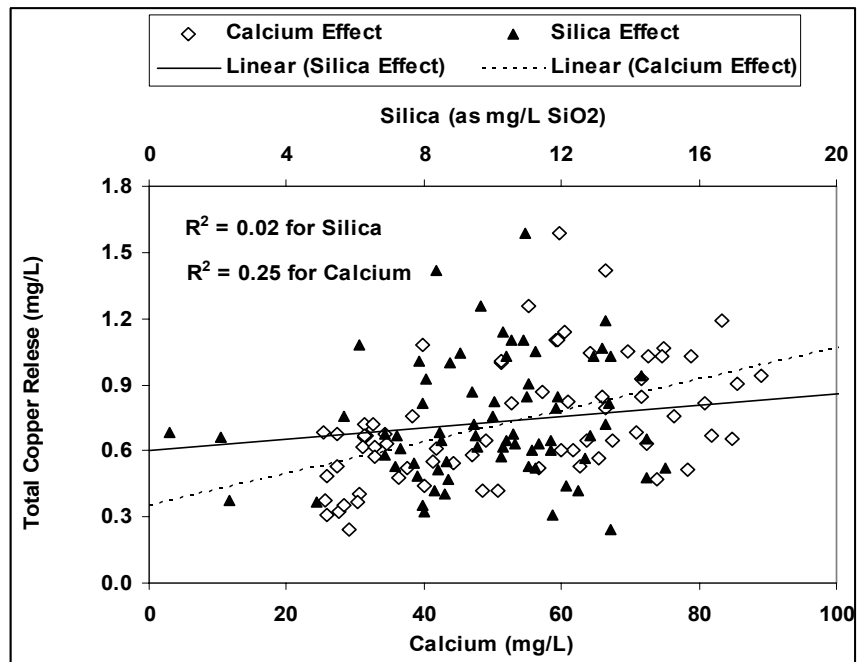


Figure 0.7 Copper release versus calcium and silica

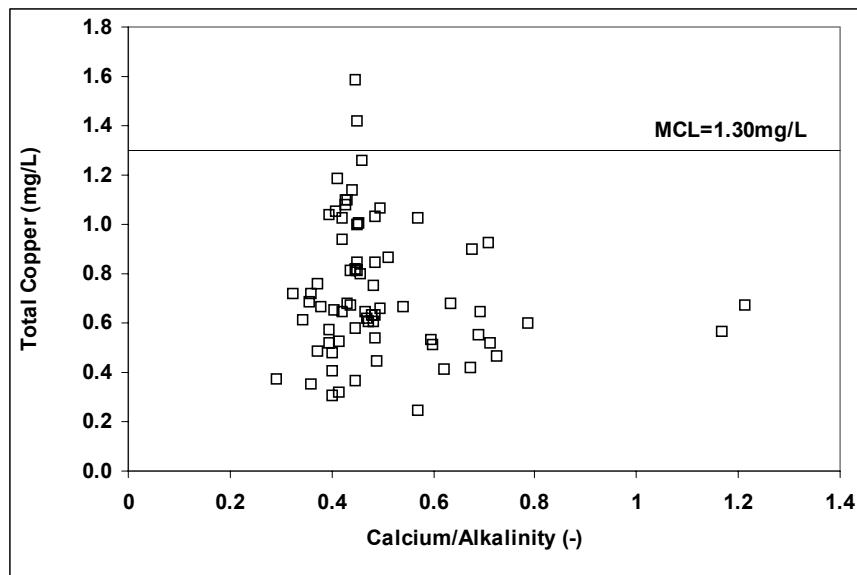


Figure 0.8 Normalized calcium effect on total copper release

Other Water Quality Parameter Effects

Silica is used as a corrosion inhibitor because it is surface active and can insulate metal surfaces from bulk water and reduce corrosion. Determining the effect of silica on copper required that the effect of alkalinity be removed from the effect of silica on copper release because like calcium, silica also came from the high alkalinity, high calcium groundwater. As shown in Figure 0.7, released copper increased as silica increased, which is opposite to what is expected of a material that is used to inhibit corrosion. However the plot of released copper versus the silica/alkalinity ratio clearly shows that total copper released decreased as the silica/alkalinity ratio increased, which is what would be expected of a material used for corrosion inhibition. This plot is shown in Figure 0.9.

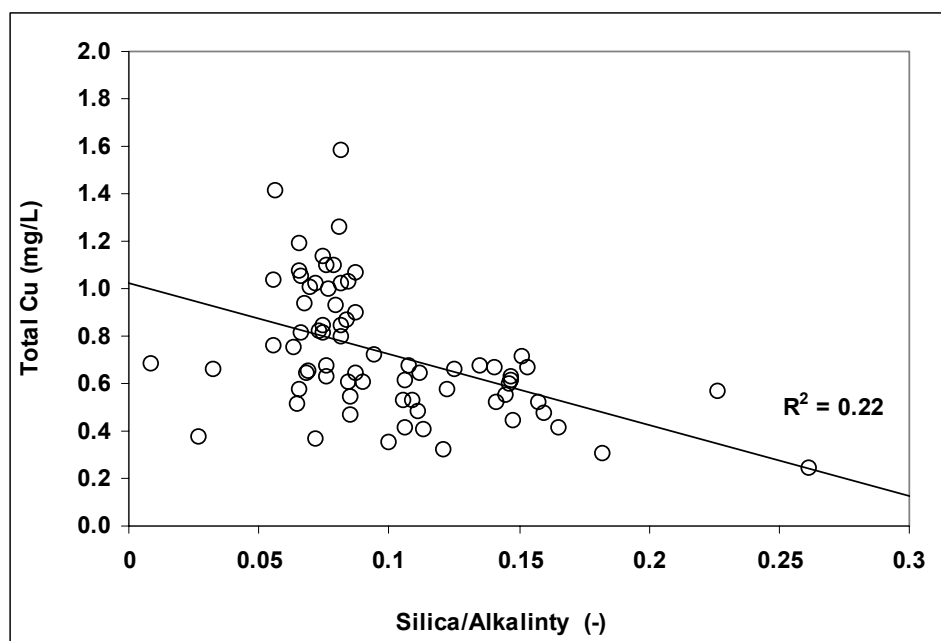


Figure 0.9 Normalized silica effect on total copper release

Other water quality parameters of interest did not show any impact on total copper release in this work. Dissolved oxygen (DO) can significantly affect copper corrosion processes, and has been studied extensively. However, the range of DO was very small in our work, as all waters were produced and staged before PDS discharge. DO was correlated to temperature but had no effect on total copper release. Chloramine residual and UV_{254} like DO did not impact total copper release. The lack of impact of these independent variable on total copper release may have been due to the limited range of the variable or the existing scale on the used pipes. Some relationships have been noted for residual and UV_{254} on new pipes.

Controlled Experiment Study-Isolation of the Anion Effect

A one-month study was conducted to determine the influence of chlorides and sulfates on the relationship of alkalinity and copper release. Selected PDSs were fed with varying alkalinity while varying chlorides and holding sulfates at $13.6 \text{ mg/L} \pm 2.3 \text{ mg/L}$ and then varying sulfates and holding chlorides constant at $32.7 \text{ mg/L} \pm 6.9 \text{ mg/L}$. PDS feed stream water quality was changed biweekly. The released total copper during the controlled sulfates and chlorides study versus alkalinity is shown in Figure 0.10. As seen in the previous work, copper release increased as alkalinity increased. pH increased from 8.09 to 8.44 as alkalinity increased during the controlled study. If alkalinity were held constant, total copper would have decreased instead of increased as pH increases. However the associated carbonate complexes with increasing alkalinity overcame the effect of increasing pH and the total copper increased.

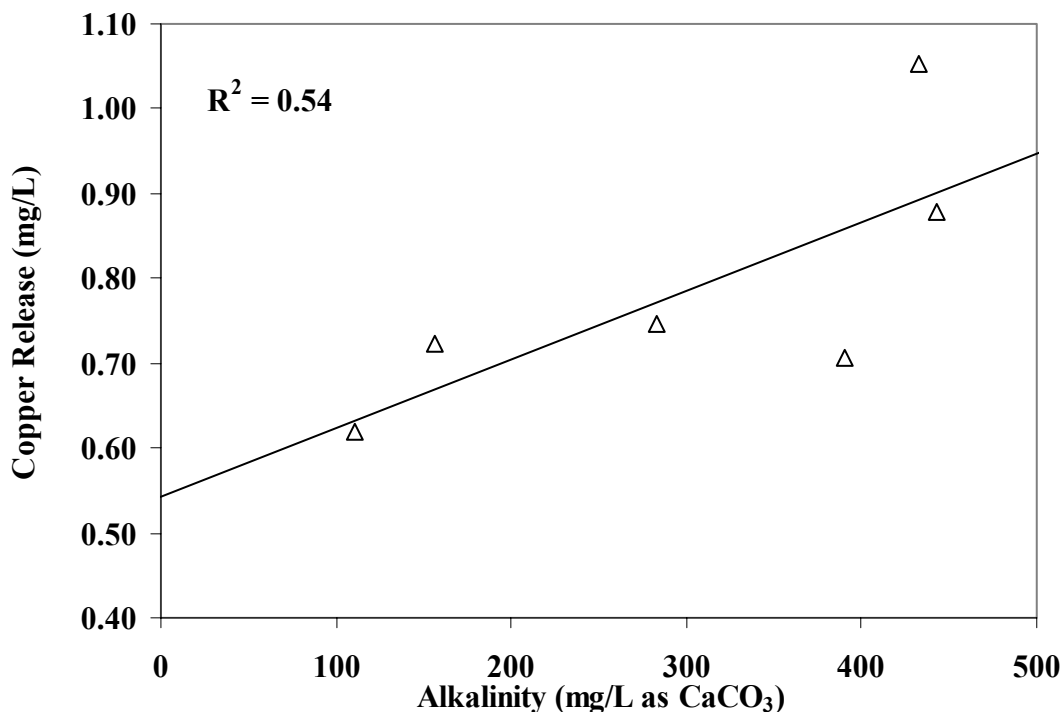


Figure 0.10 The effect of alkalinity on total copper release at constant chlorides and sulfates

In order to determine the effect of sulfates and chlorides on total copper release, additional controlled studies were conducted that held alkalinity and pH constant and varied chlorides while holding sulfates constant, and then varied sulfates while holding chlorides constant. The results of those studies are shown in Figure 0.11 and Figure 0.12. When chlorides were varied, sulfates, alkalinity and pH were 17.9 mg/L \pm 4.7 mg/L, 71 mg/L as CaCO₃ \pm 18 mg/L as CaCO₃, and 8.0 \pm 0.13 pH units. When sulfates were varied chlorides, alkalinity and pH were 32.9 mg/L \pm 4.6 mg/L, 81 mg/L as CaCO₃ \pm 7 mg/L as CaCO₃, and 8.0 \pm 0.16 pH units. As shown in Figure 0.11, the trend line indicates increasing chlorides decrease copper release. However the R^2 is low and the trend is not significant. One data point could be discarded using

outlier analysis, and a significant positive trend could be generated. The relationship of sulfate and total copper release for constant alkalinity, chlorides and pH is shown in Figure 0.12. Clearly a positive trend is shown that states increasing sulfates increase the release of total copper. Generally increasing sulfates or chlorides are thought to increase soluble copper to some extent because of complexation. The one outlier in Figure 0.11 may have been largely due to the release of particulate copper and independent of the variation in chlorides. An argument can be made that the data supports increasing chloride increases total copper release, which agrees with the view that chloride complexes and associated redox enhancement increases copper corrosion. The data clearly shows increasing sulfate increased total copper release.

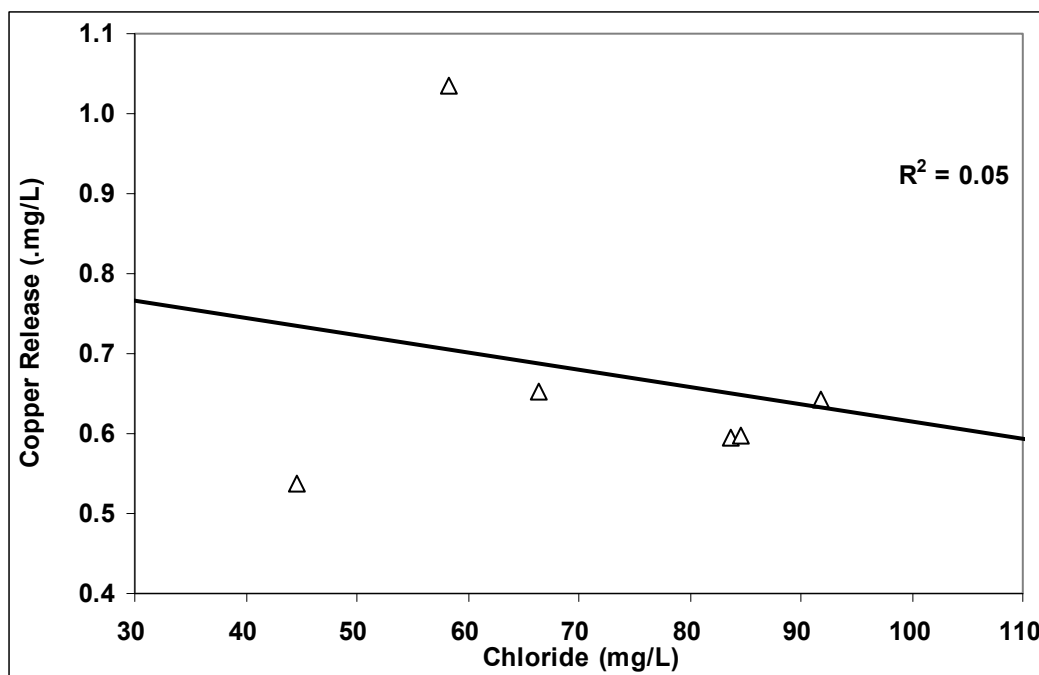


Figure 0.11 The effect of chloride on total copper release at constant pH, alkalinity and sulfates

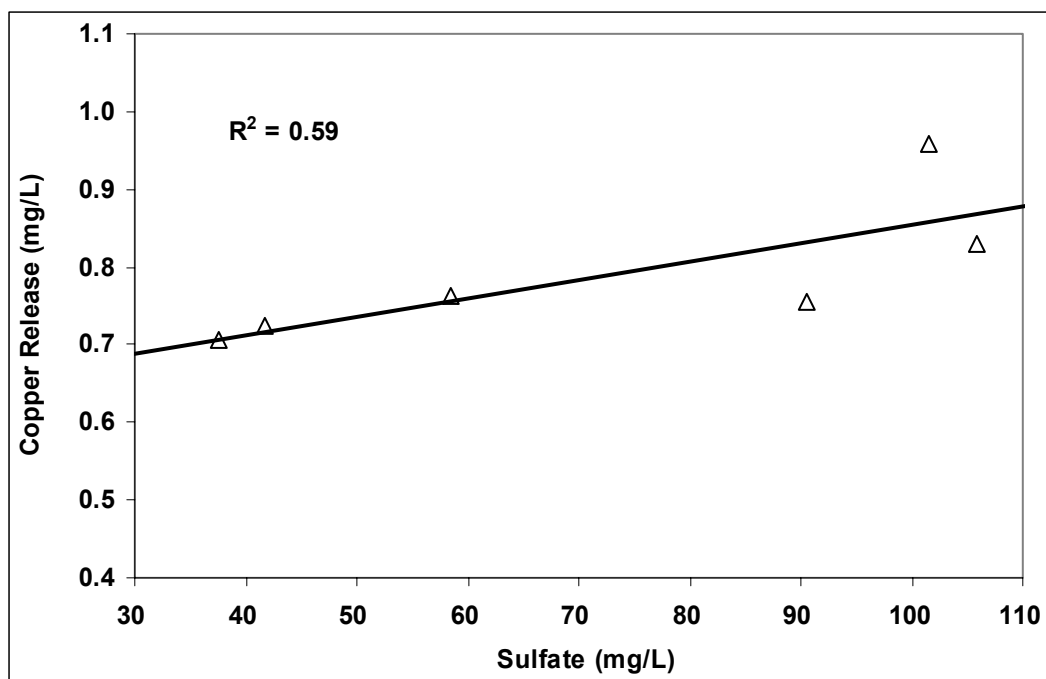


Figure 0.12 The effect of sulfates on total copper release at constant pH, alkalinity and chlorides

Empirical Model Development

Linear Regression

The precipitation/dissolution mechanisms controlling the release of total copper level in the bulk solution leads to the development of a predictive model for copper release. However, the difficulty of identifying specific controlling solids and related thermodynamic constants makes the development of a theoretical solubility model for the release of total copper very difficult if not impossible. A theoretical model based on a $\text{Cu}(\text{OH})_2$ controlling solid phase has been widely accepted as the best approach to develop such models. Development and verification of a theoretical model from field data assumes equilibrium, which may not be the

case and has no means to compensate for the release of particulate copper. Regression of total copper to bulk water quality using a large data set is presently the only feasible approach to build a predictive model for total copper release in drinking water systems. Although this approach is empirical, the resulting model can provide valuable insight into the most important mechanisms and reactions. Hence the empirical approach using regression was implemented to develop a model relating total copper release to water quality.

A linear model was initially developed using regression. Total copper release was regressed against all water quality parameters initially. From the initial regression ten water parameters were considered potentially significant to total copper release. These parameters were alkalinity, pH, DO, chloride, sulfate, total dissolved solid (TDS), temperature, UV-254, calcium, and silica. Over the 12 month study period, 610 observation of total copper release were collected spanning 4 phases and 18 PDSs. As mentioned in experimental section, the water quality flowing through each PDS pipeline was changed at the beginning of every phase, and water quality was maintained as constant through each phase, thus 72 observations were generated by averaging the collected data from 18 PDSs over 4 phases. Outliers were eliminated using the sigma criteria from a student's t test. The linear regression model is shown in equation (0.1) along with the compared prediction with field observations as shown in Figure 0.13

$$[Cu] = 7.20 + 0.0034 \times Alk. - 0.85 \times pH \quad (0.1)$$

where: Cu = mg/L Total Copper
 Alk. = mg/L as CaCO₃
 pH = -log (H⁺)

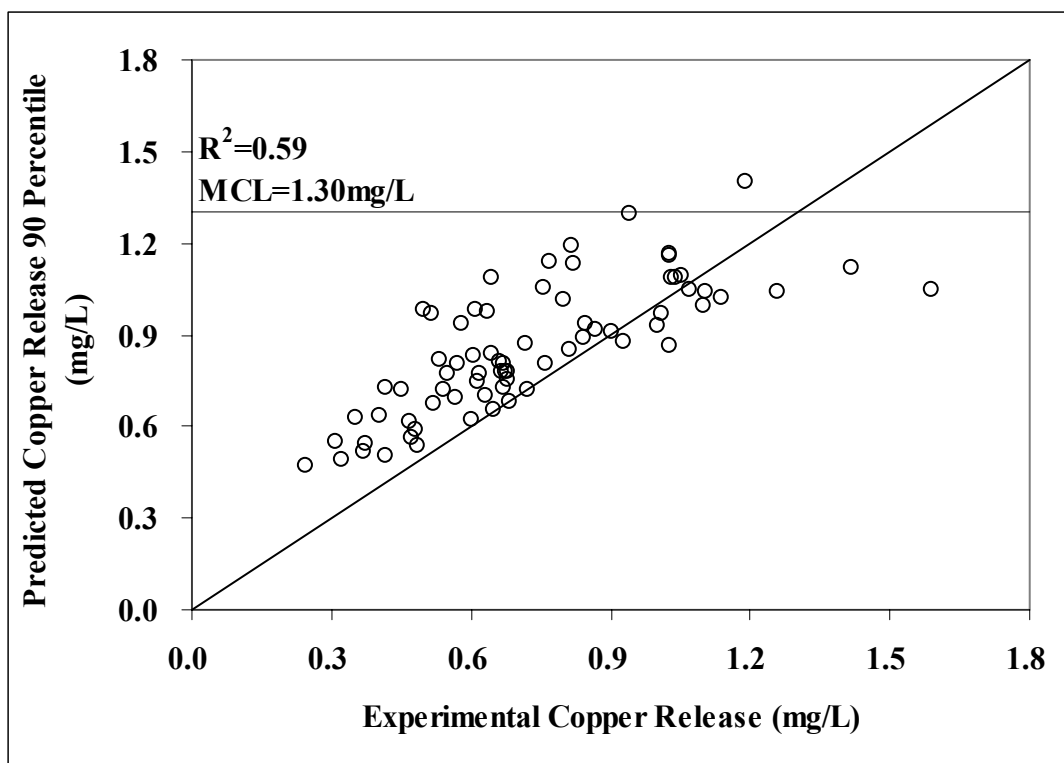


Figure 0.13 Actual and predicted total copper by linear regression

The linear model predicts that total copper released will increase as alkalinity decreases and pH increases for the conditions of this study. As shown in

Table 0.3 , Alkalinity varied from approximately 1 to 4 meq/L and pH varied from approximately 7.8 to 8.2. As with any regression model, using this linear model to predict total copper released outside of the developmental data range should be done with caution. Note, the predicted copper release underestimated the actual copper release for the highest actual released total copper observations. The absence of sulfates and silica from the regression equation is also noted. While sulfate and silica were visually related to total copper, the corresponding relationship was not significant at a 0.95 confidence interval (CI). However, the predicted total copper and effects of pH and alkalinity were highly significant and as shown in Figure 0.13 accurately predicted total copper released.

Nonlinear Regression

Equilibrium constants for chemical reactions are the basis for prediction of soluble species at equilibrium and are non-linear. Such relationships can be easily analyzed by non-linear regression, which was done. The resulting non-linear model relating total copper released to water quality is shown in equation (0.2), comparison with field data is shown in Figure 0.14. Unlike linear regression, the nonlinear regression has no fixed format, thus indefinite equations could be developed. However, that was not the case in this work.

$$[Cu] = Temperature^{0.72} \times Alk.^{0.73} \times pH^{-2.86} \times Sulfate^{0.10} \times Silica^{-0.22} \quad (0.2)$$

where:

Cu	=	mg/L Total Copper
T	=	°C Temperature
pH	=	-log (H ⁺)
Alk.	=	mg/L as CaCO ₃
Sulfate	=	mg/L SO ₄

Silica = mg/L Si as SiO₂

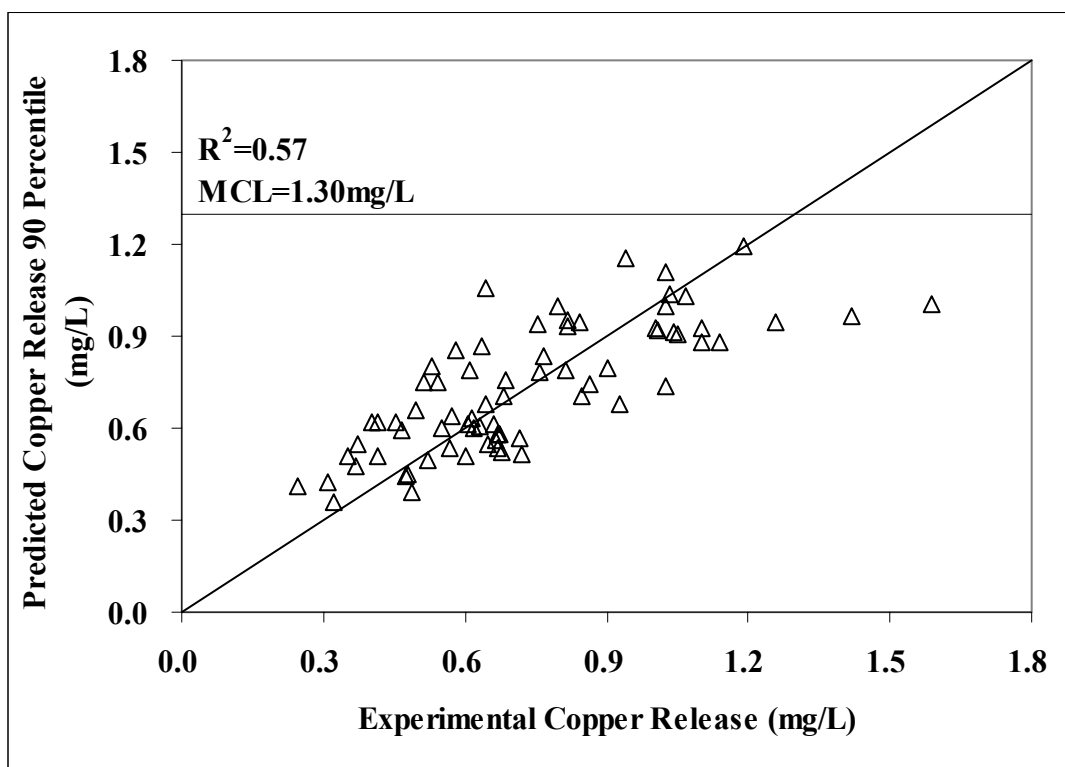


Figure 0.14 Actual and predicted total copper by non- linear regression

The trend from this non-linear prediction is quite consistent with the experimental data. The temperature coefficient indicates the release of total copper will increase in the summer, which was observed in our work. However, the non-linear model supports what was observed in the field observations and the general opinion of the water community. Alkalinity and pH were strongly related to copper release. Increasing alkalinity and decreasing pH increased total copper release supporting what was seen in the literature, field and linear model. Increasing sulfates increase total copper as predicted by equilibrium and the literature. Increasing silica decreases total copper as expected by silica inhibition of copper release and field experience. As shown in

Figure 0.14, statistically equation (0.2) is no better than equation (0.1). However, equation (0.2) is a better fundamental representation of the expected effects of water quality on copper release based on theory. However, either model could be used accurately in similar environments. Both models underestimated copper release at high concentrations of released copper..

Conclusions

Pilot-scale experiments indicated that copper corrosion by-product releases depended heavily on water quality, especially on alkalinity and pH, and also to a lesser extent on sulfates, silica and temperature for the conditions of this investigation. The findings in this study are:

- The release of total copper from home plumbing systems can be adversely affected by blending finished waters from surface, ground and saline sources. Adverse effects on total copper release can be mitigated by controlling water quality of blended finished waters primarily by controlling alkalinity and pH.
- The ratios of finished waters produced from blending ground, surface and saline sources can be monitored in drinking water distribution systems using key water quality variables common to each source. In this work, the percent of finished groundwater in blended distribution system water could be estimated by the percentage of alkalinity and calcium in the blend. The percent of finished surface water in the blend could be monitored by the percent of sulfates in the blend. The percent of RO water in the blend could be monitored by the percent of silica or chlorides in the blend.

- The release of total copper was primarily dependent on pH and alkalinity for the conditions of this study. Total copper release increased as alkalinity increased and pH decreased.
- Visual inspection of total copper release versus sulfates or chlorides and separation of the corresponding data into Euclidian groups indicated there was no relationship between chloride or sulfate concentrations and total copper release for the conditions of this study.
- Normalization of calcium and silica with respect to alkalinity was necessary to determine the effects of calcium and silica on total copper release. The Concentrations of calcium in the blended PDS water did not affect total copper release. Silica did affect total copper release, total copper release decreased as silica increased indicating naturally occurring silica was function like a corrosion inhibitor.
- Linear and nonlinear regression produced total copper release models as a function of water quality confirmed observed trends. The non-linear model was more representative of theoretical expression of chemical equilibrium and showed that alkalinity, pH, temperature, calcium, and sulfate were statistically significant to the release of total copper. Either model could be used to predict copper release in distribution system for similar conditions as were used for this study.

References

- (1) Pehkonen, S.O., A. Palit, and X. Zhang. 2001 Effect of Specific Water Quality Parameters on Copper Corrosion *Corrosion* 58(2):156-165
- (2) Edwards. M, J.F. Ferguson, S.H. Reiber. 1994 The Pitting Corrosion of Copper Journal of AWWA. 86(7):74-90
- (3) Michael R.S., A.L. Darren. 1995 Effect of DIC, Orthophosphate an Sulfate on Drinking Water Cuprosolvency *EPA/600/R-95/085*
- (4) Edwards, M., R.S. Michael, T.E. Meyer 1996 Alkalinity, pH, and Copper Corrosion by-product Release. *Journal of AWWA* 88(3):81-94.
- (5) Merkel, T.H., H.J. Gross, W. Werner, T. Dahlke, S. Reicherter, G. Beuchle, and S.H. Eberle. 2002. Copper Corrosion By-product Release in Long-term Stagnation Experiments. *Water Research*, 36(6):1547-1555
- (6) Boulay, N., and M. Edwards. 2001 Role of Temperature, Chlorine, and Organic Matter in Copper Corrosion By-product Release. *Water Research*. 35(3):683-690
- (7) Broo, A.E., B. Berghult, and T. Hedberg. 1997 Copper Corrosion in Drinking Water Disrtibution Systems-The Influence of Water Quality *Corrosion Science*. 39(6):1119-1132
- (8) American Water Work Association Research Foundation 1994 Internal Corrosion of Water Distribution Systems. AWWA Research Foundation DVGW Forschungsstelle, Denver, CO.
- (9) Hamann, C.H., A. Hammett, and W. Vielstich. 1998. *Electrochemistry*. New York: Wiley-VCH

- (10) Froning, M.H., M.E. Shanley, E.J. Jr. Verink. 1976 An Improved Method for Calculation of Potential-pH Diagrams of Metal-Ion-Water System by Computer *Corrosion Science*. 16(6):371-377
- (11) Pankow, J.F. 1991. *Aquatic Chemistry Concept*. Chelsea, Mich.: Lewis Publishers
- (12) Ugorets, M.Z., E.A. Buketov, and K.M. Akhmetov. 1968. Thermographic Study of the Dehydration of Copper Hydroxide in Alkaline Solutions. *Russ. Jour. of Inorganic Chemistry*, 13(6):1525-1529.
- (13) Dousma, J., and P.L.De. Bruyn 1978 Hydrolysis-Precipitation studies of Iron Solutions *Journal of Colloid and Interface Science* 79(2):314-320
- (14) Patterson, J.W., E.B. Richard, and D. Marani. 1991. Alkaline Prediction and Aging of Copper from Dilute Cupric Nitrite. *Environmental Science and Technology*, 25(10):1780-1787.
- (15) Marani, D., J.W. Patterson, and P.R. Anderson. 1995. Alkaline Precipitation and Aging of Cu(II) in the Presence of Sulfate. *Water Research*, 29(5) 1317-1326.
- (16) Robert, I.J. 1995 *An Introduction to Computational Statistics – Regression Analysis* New Jersey Prentice Hall
- (17) Rencher, A.C. 2002 *Methods of multivariate analysis* New York : J. Wiley
- (18) Edwards, M. 2002 Protecting your distribution system and maintaining finished water quality by corrosion control Proceeding ACE02 AWWA
- (19) Edwards, M., and J.F. Ferguson. 1993 Accelerated Testing of Copper Corrosion *Journal of AWWA*. 85(10):105-113

- (20) Zhang, X.H., S.O. Pehkonen, N. Kocherginsky, A.E. Grant. 2002 Copper Corrosion in Mildly Alkaline Water with the Disinfectant Monochloramine *Corrosion. Science* 44(11):2507-2528
- (21) Stumm, W., R.L. Champlin. 1967 Technical and Legal Aspects of Copper Tube Corrosion *Journal of AWWA*. 59(3):401-406
- (22) Adeloju , S.B., and H.C. Hughes. 1986. The Corrosion of Copper Pipes in High Chloride-Low Carbonate Mains Water. *Corrosion Science*, 26(10):851-870.
- (23) Atlas , D.C., and O.T. Zajicek. 1982. The Corrosion of Copper by Chlorinated Waters. *Water Research*, 16(5):693-658
- (24) Edwards, M., S. Jacobs, and R.J. Taylor. 2000. The blue Water Phenomenon. *Jour. AWW.*, 92(7):72-82.
- (25) Standard Methods for the Examination of Water and Wastewater 1999 APHA-AWWA-WPCF 18th Edition

Chapter 4 Simulation of Copper Release in Pipe Distribution System and Copper Rule Compliance

Introduction

Historically, groundwater has been the major water source for municipal use in Florida (1). However the capacity of groundwater to meet future demands is inadequate and alternate sources (brackish water, ocean water, and surface water) are needed. The different treatment techniques for these sources produces different finished water quality that can adversely impact distribution system water quality when these waters are blended or are distributed as a sole source in distribution systems that have only experienced finished groundwater. This paper discusses the effect of variable finished water quality on distribution system water quality. Such variations can cause regulatory violation of copper and lead action levels (2-8).

The current maximum contamination level (MCL) for copper is 1.30 mg/L at the 90 percentile of sampling sets collected from homes with copper plumbing after 6 hours of stagnation (9). Extensive research has been conducted on mechanisms of copper corrosion (2-7, 10-20). The primary controlling factors for copper corrosion are alkalinity and pH. Dissolved copper speciation primarily consists of free Cu (I) and Cu (II), hydroxyl complexes, and carbonate complexes. The CuCO_3^0 complex accounts for 80% of total dissolved copper speciation. The remaining 10% to 20% consists of mostly hydroxyl species. Temperature affects copper release and generally increases particle and decreases dissolved copper release (2). Particulate copper can account for a significant fraction of total copper.

Although the specific effects of anions, cations and physical parameters on copper corrosion have been studied, the confounding impacts of these factors are unknown and require

extensive pilot plant or system investigation. Accurate prediction of copper concentrations in full scale distribution systems is best done using models which are statistically based on theoretical mechanisms and extensive field data.

Copper corrosion was investigated as affected by varying water quality using a large pilot facility over one year. The varying water quality was produced by blending finished groundwater, surface water, and desalinated water in eighteen pilot distribution systems (PDSs) and copper loops. The blends were changed quarterly. The PDSs were made from PVC, lined cast iron (LCI), unlined cast iron (UCI) and galvanized steel (G) pipes taken from actual distribution systems. Models were developed using linear and non-linear statistical regression that correlated total copper concentration to water quality.

Experiments and Methods

Pilot Unit Design

Varying water quality was produced from seven different finished waters, which were blends of finished waters produced from groundwater (G1, G2, G3, G4), surface water (S1, S2), and reverse osmosis (RO). Blended waters are shown in Table 0.1.

Table 0.1 Treatment systems and blending scenarios

No.	I. D.	Source Water	Unit Processes
1	G1	Groundwater	Aeration, Disinfection, pH stabilization
2	G2	Groundwater	Softening, Sedimentation, Sand Filtration, Disinfection, pH stabilization
3	G3	Groundwater, RO and S1	Softening, Sedimentation, Sand Filtration and Disinfection, pH stabilization
4	G4	Groundwater, RO and S1	Nano-filtration, pH stabilization
5	S1	Surface Water	Coagulation, Flocculation, Sedimentation, Ozone, GAC bio-reactor, Disinfection, sand filtration, pH stabilization
6	S2	S1 after sedimentation	Nano-filtration, pH stabilization
7	RO	Groundwater	5 um cartridge pre-filtration, RO, Disinfection, pH stabilization

Post treatment for all finished waters included aeration, stabilization and disinfection. The G1 process consisted of only post treatment, which is typical for Florida groundwaters. Water was transported weekly from the Hillsborough River, stored in two 7,000 gallon tanks and treated by ferric sulfate coagulation, settling, cartridge filtration (CSF), ozone and GAC filtration before post treatment. Some of the S1 process water was diverted to a NF membrane pilot unit for the S2 process. RO water was produced by high pressure membrane filtration of groundwater and addition of sea salt to simulate the TBW RO finished water. G4 was a nanofiltered blend (62 % G1, 27 % S, 11 % RO), which was of interest of one of the member governments of TBW. G2 was softened water. G3 was a softened blend of partially treated waters, and like G4 was of interest to a TBW member government.

The PDSs receiving the blended waters were 100 feet long and made from pipe taken from MG distribution systems. Fourteen PDSs were made from PVC, lined cast iron (LCI), unlined cast iron (UCI) and galvanized steel (G) pipes. Four PDSs were made with a single material. As shown in Figure 0.1, The PDSs were covered by a roof for temperature control. The finished waters were stored in separate tanks before blending and distribution.



Figure 0.1 Pilot-scale distribution system research site. Left side is the whole site picture, right one is the 18 PDSs consisted of 14 hybrid and four single materials

Lead and Copper Loops

PDS effluent was fed to eighteen identical copper loops which is shown in Figure 0.2, which contained one each 50:50 tin: lead coupon. Thirty feet of 0.25" copper tubing was used in each loop. The samples for copper and lead monitoring were taken from the first twenty-two

feet. All other fittings and materials were polymer materials, typically PVC. The coupon surface area was 3.38 square inches, and was equivalent to 17 joint-ends or 7 to 8 fittings given a 0.125" bead on the inside of each 0.5" diameter joint, which is a reasonable assumption for a home plumbing site required for compliance with the Lead and Copper Rule.

Samples were collected after a 6 hour standing period once a week. Dissolved oxygen, pH, alkalinity, calcium, magnesium, silica, copper and lead were monitored in and out of each loop.



Figure 0.2 Copper loops connecting with individual PDSs effluent for LCR compliance study

Statistical Model Development

Water quality was changed every three months and 611 data points were collected over one year. The data was averaged by phase for each of the eighteen loops and regressed to

determine the influence of changing water quality on copper and lead concentration. SigmaPlotTM software was used to develop linear and non-linear models at a 0.95 confidence interval (CI). The most insignificant water quality parameter as determined by largest alpha value greater than 0.05 was discarded, and the regression was repeated until all parameters meet a 0.95 CI. The same procedure was used for non-linear models. Dixon's Q test was used to decide the outlier pickup [21].

Results and Discussions

Statistical Model Development

Empirical models were developed using linear and non-linear regression that related total copper to water quality using the parameters listed in

Table 0.2. Initially the most insignificant parameter as determined by the highest alpha value over 0.05, were dropped and the regression was repeated until only significant parameters remained. The resultant linear and non-linear predictive models for ninetyth percentile copper concentrations (copper violation) as a function of water quality are shown in equations (0.1) and (0.2). The units for the independent variable are: [Cu] total mg/L copper, mg/L alkalinity as CaCO₃, temperature as °C, mg/L sulfate, and mg/L silica as SiO₂. The range of the independent variables used to develop these models is shown in

Table 0.2. Caution should be taken when applying these models outside the range of the significant variables shown in these models.

Table 0.2 Finished groundwater (G1), surface water (S1) and desalinization (RO) water quality

Variable	Unit	Range	Concentration	Linear Model Prediction- Cu mg/L	Non-Linear Model Prediction- Cu mg/L
Alkalinity	mg/L as CaCO ₃	Maximum	225	1.74	1.54
		Minimum	50	1.15	0.70
pH		Maximum	8.30	0.96	1.05
		Minimum	7.60	1.56	1.28
Temperature	° C	Maximum	35		1.52
		Minimum	15		0.96
Sulfate	mg/L	Maximum	120		1.33
		Minimum	10		1.10
Silica	mg/L	Maximum	15.05		1.28
		Minimum	0.59		2.32
Chloride	mg/L	Maximum	19		
		Minimum	104		
Calcium	mg/L	Maximum	25		
		Minimum	89		
DO	mg/L	Maximum	1		
		Minimum	11		
TDS	mg/L	Maximum	204		
		Minimum	507		
UV ₂₅₄	mg/L	Maximum	15.05		
		Minimum	0.59		

Linear Model

$$[Cu] = 7.48 + 0.0034 \times \text{Alkalinity} - 0.85 \times \text{pH} \quad (0.1)$$

Non-linear Model

$$[Cu] = 0.28 + \text{Temp}^{0.72} \times \text{Alkalinity}^{0.73} \times \text{pH}^{-2.86} \times (\text{SO}_4^{2-})^{0.10} \times \text{SiO}_2^{-0.22} \quad (0.2)$$

As shown in the above equations, pH and alkalinity are statistically significant in both models, Temperature, sulfate, and silica are statistically significant in the nonlinear model. Traditionally, calcium is considered as a corrosion inhibitor because of CaCO_3 formation. In this work, calcium and alkalinity primarily come from groundwater, was confounding with alkalinity and was insignificant relative to copper release. DO was not statistically significant for copper release. DO can theoretically oxidize copper and could possibly be significant to copper release. However DO is typically not significant to copper release in aged pipe because the precipitation/dissolution is the controlling mechanism, and was not significant here. Ionic strength and conductivity will increase as TDS increases, and will increase corrosivity. However the range of TDS variation in this work was slight and the corresponding effect of TDS on copper release was insignificant. The same conclusion can be reached for UV_{254} and chlorides as for TDS. There was not enough range or concentration to make a difference in copper release. That might not be the case for all drinking waters as five fold higher UV_{254} absorbance's and chlorides concentrations are possible in drinking water.

Temperature, sulfate and silica were statistical significant in the non-linear model but not in the linear model. A possible reason for this difference is that the non-linear regression more closely resembles the equilibrium product for a chemical reaction involving copper release. The non-linear model is in the form of a ratio of products over reactants, and is more fundamentally representative of chemical reactions.

The linear and non-linear models both indicate that copper will increase as alkalinity increases and pH decreases. Temperature, sulfate and silica were not significant in the linear model but were significant in the non-linear model. The non-linear model predicted copper

concentration increased with increasing temperature and sulfate, and decreasing silica. Increasing pH and silica were observed to decrease copper concentration for the conditions of this investigation. As noted previously, these predictive equations should be used with caution outside the experimental range of the independent variables in equations (0.1) and (0.2). These variables undoubtedly affect dissolved copper concentration but their effect on total copper is difficult to theoretically predict because of the effects of particulate copper. Hence, there was not much statistical difference between these two models. The predicted copper release using the linear and non-linear models versus the actual copper released is shown in Figure 0.3 and Figure 0.4. The coefficient of error (R^2) for the linear and non-linear models was 0.59 and 0.57 respectively. While R^2 is not high for these models, the independent variables shown to increase copper in these models have been shown to increase copper in the TBW MG copper samples and in other national works, and can be used by the MGs to proactively control copper release. (2, 5, 7)

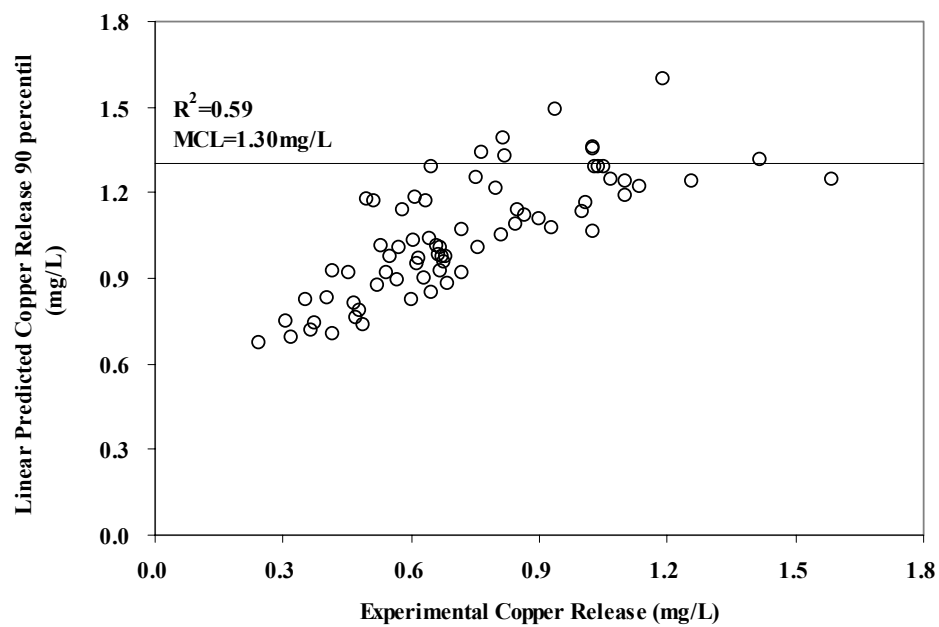


Figure 0.3 Actual versus predicted ninetyth percentile copper concentrations using linear mode

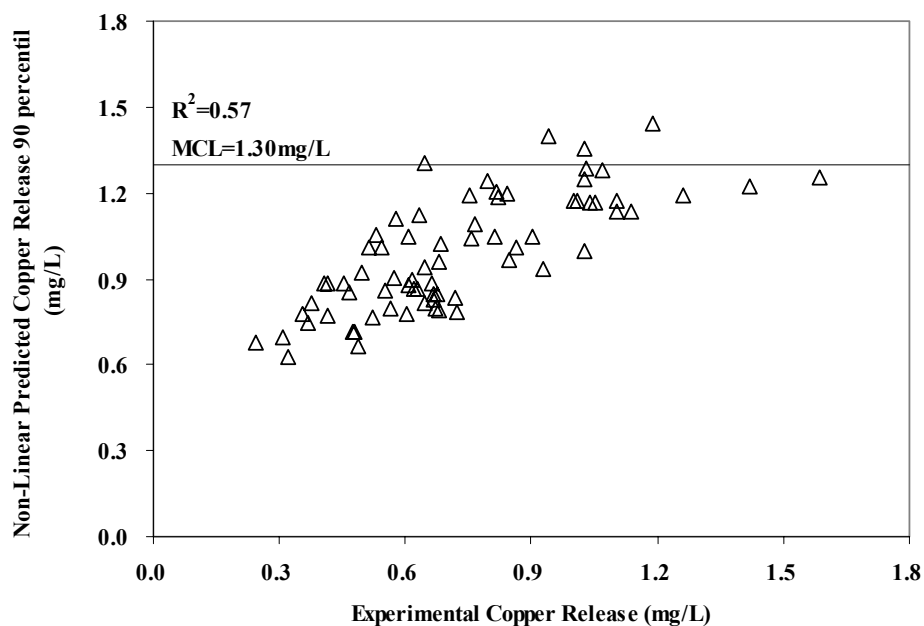


Figure 0.4 Actual versus predicted ninetyth percentile copper concentrations using non-linear model

Verification of Predictive Models

Model verification was done using data that was not used for model development. This data was collected over a six month period following the one-year period of data collection. The predicted versus the actual copper concentrations during the verification phase are presented in Figure 0.5 and Figure 0.6 for linear and non-linear models, respectively.

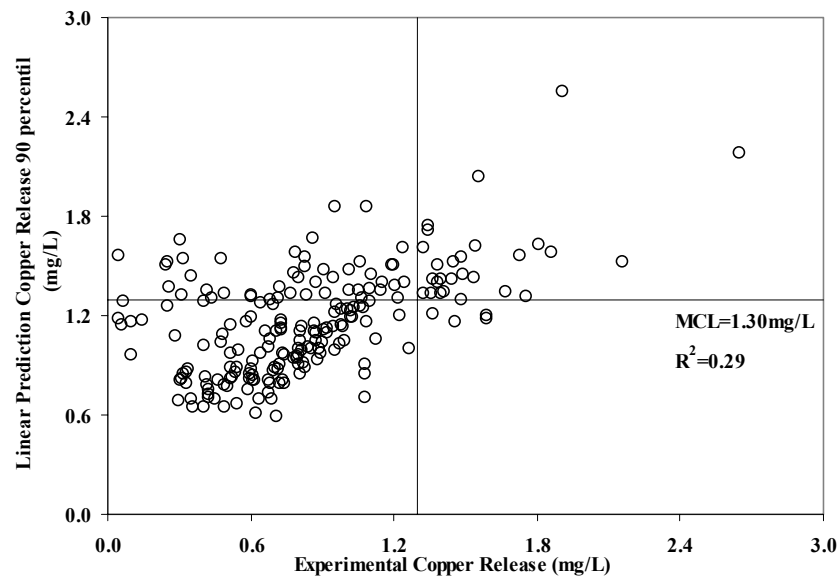


Figure 0.5 Verification plot of linear model

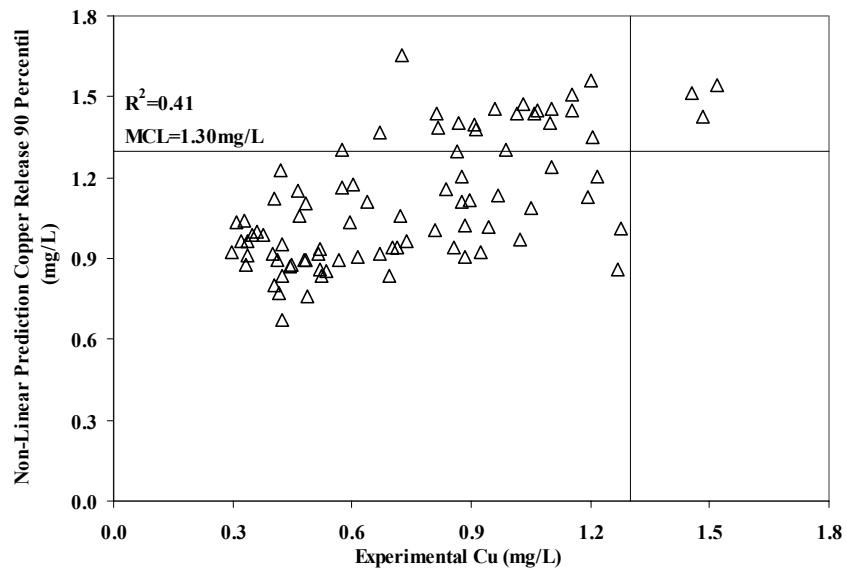


Figure 0.6 Verification plot of non-linear model

The non-linear model error (predicted Cu minus actual Cu) was less than the error for the linear model. As shown in Figure 0.5, the linear model over predicted actual copper concentrations in the lower range of the data set, and under predicted in the higher range. There was no such deviation for the predicted copper concentrations using the non-linear model. There was no statistical difference between the predicted and actual values for both models, consequently both models were verified statistically.

Simulation of Copper Rule Compliance

The effect of blended water quality on copper concentration was assessed graphically for blends of G1, S1 and RO. The resulting ternary plots are shown in Figure 0.7 and Figure 0.8 using the linear and non-linear Cu models. These plots provide a desktop estimation of ninetyth

percentile copper concentrations for any combination of ground, surface or RO finished water based in the water quality in Table 0.3. The Ternary plots can be read as follows:

- (1) Within the ternary plot region, the summation of three source water ratio is 1.0, and any point represents a unique blend.
- (2) Assume a blend of 62 % G1, 27 % S1 and 11 % RO.
- (3) Locate 0.62 on the G1 Ratio axis
- (4) Draw a line parallel to the S1 axis that passes through the 0.62 G1 Ratio point.

(Note the parallel axis will always be the first axis that is clockwise to the axis containing the blend ratio point. Circular arrows have been inserted in Figure 0.7 to illustrate the location of the reference axis for drawing the parallel line. Hence, S1 is clockwise from G1 and is the parallel axis of reference for this line.)
- (5) Locate 0.27 on the S1 Ratio axis.
- (6) Draw a parallel line to the RO Ratio axis that passes through the 0.27 S1 Ratio point. The intersection of these two lines defines the predicted ninetyth percentile copper concentration for this blend using the linear model to be 1.51 mg/L, which violates the copper action level.
- (7) Locate 0.11 on the RO Ratio axis
- (8) Draw a parallel to the G1 axis through the 0.11 RO Ratio axis point. (The intersection of this line passes through the 1.51 mg/L point found in step 6 and confirms the graph was used correctly).

This procedure can be used to develop and predict singular water quality parameters for any combination of blended water quality from three sources given the models for prediction of water quality are available. The desktop technique can easily be used by engineering scientific, operational, regulatory and managerial personnel to proactively manage water quality.

Table 0.3 Water quality range and predicted ninetyth percentile copper concentrations

Parameter	Unit	Ground Water	RO Water	Surface Water
pH		7.6	8.3	8.3
Alkalinity	mg/L as CaCO ₃	225	50	50
Cl ⁻	mg/L	15	50	10
SO ₄ ⁻²	mg/L	10	30	180
TDS	mg/L	400	150	300
Conductivity	us/cm	560	340	470
Calcium	mg/L as CaCO ₃	250	50	50
Silicate	mg/L as SiO ₂	20	20	10

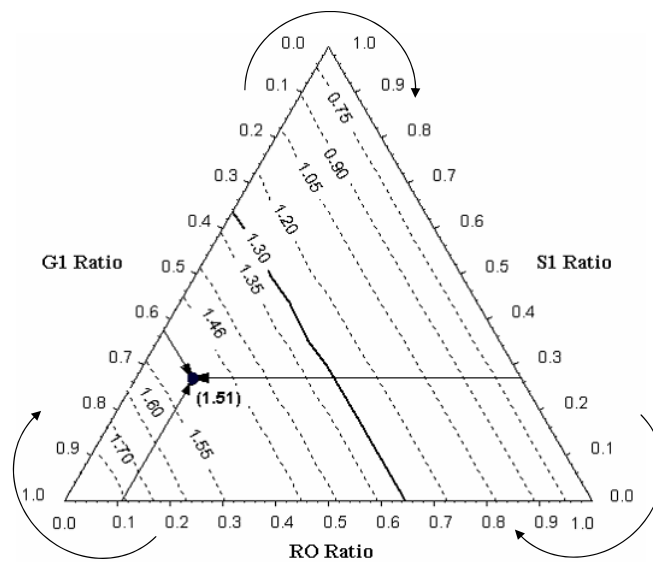


Figure 0.7 Ternary diagram showing predicted ninetyth percentile copper concentration for blends of finished ground, surface and desalinated water using linear model

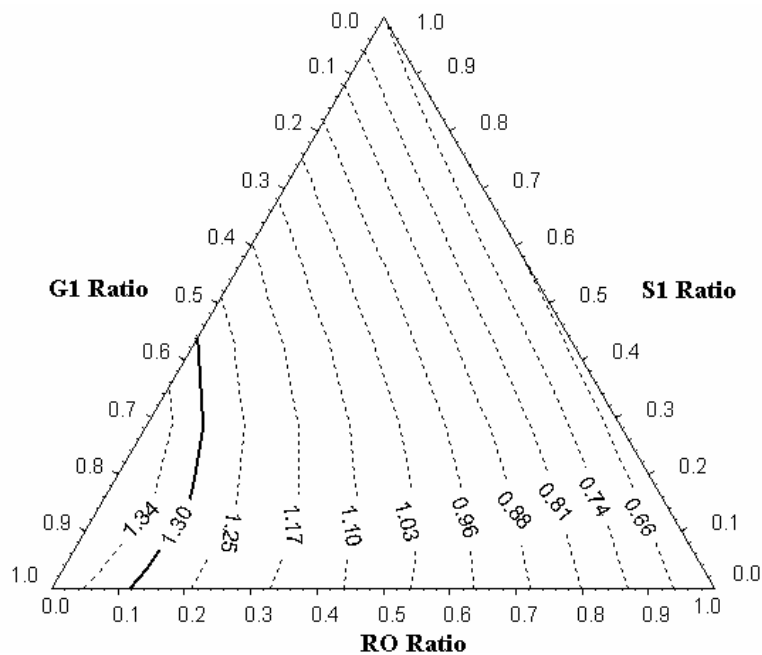


Figure 0.8 Ternary diagram showing predicted ninetyth percentile copper concentration for blends of finished ground, surface and desalinated water using non-linear mo

Conclusions

- Linear and non-linear models for predicting the ninetyth percentile copper concentrations were developed for varying water quality produced by blending finished groundwater, surface water and RO water.
- Both linear and non-linear models revealed lower pH enhance copper release, higher alkalinity produce higher copper release.
- The non-linear model indicated high sulfate and temperature corresponds to higher copper release, while silica can inhibit the copper release.
- Sensitivity analysis indicated the copper action level would be violated for some blends. The predicted violation was due primarily to high alkalinity.

References

- (1) Dietz, J.D., J.S. Taylor, L.A. Mulford, C.J. Cullen., and C.A. Owen. 2002. Assessment of Source Water Blends on Distribution System Water Quality. *In Proc. of 31st annual AWWA Water Quality Technology Conference. Seattle, Wash: AWWA*
- (2) Schock, M.R., and J.A. Clement. 1995. *Effect of pH, DIC, Orthophosphate and Sulfate on Drinking Water Cuprosolvency.* Cincinnati, Ohio. EPA/600/R-95/085
- (3) AWWARF Internal Corrosion of Water Distribution Systems DVGW-TZW 1996
- (4) Boulay, N., and M. Edwards. 2001 Role of Temperature, Chlorine, and Organic Matter in Copper Corrosion By-Product Release in Soft Water. *Water Research.* 35(3):683-690.
- (5) Edwards, M., M. Schock, and T.E. Meyer. 1996. Alkalinity, pH, and Copper Corrosion By-Product Release. *Jour. AWWA.*, 88(3):81-94.

- (6) Atlas, D.C., and O.T. Zajicek. 1982. The Corrosion of Copper by Chlorinated Waters. *Water Research*, 16(5):693-658.
- (7) Pehkonen S.O., A. Palit, and X. Zhang. 2002. Effect of Specific Water Quality Parameters on Copper Corrosion. *Corrosion* 58(2):156-165.
- (8) Rehring, J.P., and M. Edwards. 1996 Copper Corrosion in Potable Water Systems Impacts on Natural Organic Matter and Water Treatment Processes. *Corrosion*, 52(4):307-317
- (9) Lead and Copper. Final Rule Correction. 1992. *Federal Register*. 57:125:28785.
- (10) Marani, D., J.W. Patterson, and P.R. Anderson. 1995. Alkaline Precipitation and Aging of Cu (II) in the Presence of Sulfate. *Water Research*, 29(5) 1317-1326.
- (11) Merkel, T.H., H.J. Gross, W. Werner, T. Dahlke, S. Reichert, G. Beuchle, and S.H. Eberle. 2002. Copper Corrosion By-product Release in Long-term Stagnation Experiments. *Water Research*, 36(6):1547-1555.
- (12) Cheielova, M., J. Seidlerova, and Z. Weiss. 2002 X-Ray Diffraction Phase Analysis of Crystalline Copper Corrosion Products after Treatment in Different Chloride Solutions. *Corrosion Science*. 45:883-889.
- (13) Nassau, K., A.E., Miller, and T.E. Garedel. 1987. The Reaction of Simulated Rain with Copper, Copper Patina, and Some Copper Compounds. *Corrosion. Science*. 27(7):703-719
- (14) Reiber, S.H. 1989. Copper Plumbing Surfaces: An Electrochemical Study. *Jour. AWWA*, 81(7):114-122.
- (15) Broo, A.E., B. Berghult, and T. Hedberg. 1997 Copper Corrosion in Drinking Water Distribution Systems-The Influence of Water Quality. *Corrosion Science*. 39(6):1119-1132

- (16) Edwards, M., L. Hidmi, and D. Gladwell. 2002. Phosphate Inhibition of Soluble Copper Corrosion By-product Release. *Corrosion Science* 44(5):1057-1071
- (17) Pankow, J.F. 1991. *Aquatic Chemistry Concept*. Chelsea, Mich.: Lewis Publishers.
- (18) Cotton, F.A., and G. Wilkinson. 1988. *Advanced Inorganic Chemistry. Fifth*. New York: John Wiley and Sons, Inc.
- (19) Fronning, M.H., M.E. Shanley, and E. D. Jr. Verink. 1976. An Improved Method for Calculation of Potential-pH Diagrams of Metal-Ion-Water System by Computer. *Corrosion. Science*. 16(6):371-377
- (20) Edwards, M., S. Jacobs, and R.J. Taylor. 2000. The blue Water Phenomenon. *Jour. AWWA.*, 92(7):72-82.
- (21) Miler J.C., and J. N. Miler. 2001 Statistics for Analytical Chemistry the 4th edition. Prentice Hall.

Chapter 5 Comparison of Corrosive Potential by Source and Process

Introduction

Increasingly, nanofiltration (NF) has been used to remove DBP precursors and hardness. Integrated systems like lime softening and GAC filtration can serve the same purpose. A lime softening-GAC process will produce similar water quality as a NF process when treating the same source. Both can remove natural organic matter (NOM) and hardness. Other than HCO_3^- , Ca^{++} and Mg^{++} , NF will remove more ions than a lime softening-GAC. Although these processes have been studied extensively, but the iron and copper corrosion potential is not well defined (1-4).

In the past several decades, mechanisms of copper and iron corrosion in distribution systems (1, 2, 3, 4, 5, 6) have been studied. Theoretically, the majority of dissolved copper species is carbonate and hydroxide complexes, and significantly affected by alkalinity and pH (5, 6). Copper release increases as alkalinity increases and pH decreases. Sulfate and chloride weakly impact copper release relative to alkalinity and pH in typical drinking water conditions. However, actual copper release is best determined in field studies under varying water quality conditions.

Sulfate, chloride, and DO are the major factors affecting iron release. Alkalinity has also been reported to affect iron release but to a lesser degree than sulfate, chloride, and DO (5,7,8,9). Unlike copper, pH is not a controlling factor for iron release in typical drinking water conditions. High sulfate, high chloride and DO can cause high iron release. High alkalinity reduces iron release.

The qualitative and quantitative impact of varying water quality on distribution system water quality was investigated in this work as a part of a large-scale project funded by AWWARF and Tampa Bay Water (Florida, US). Qualitative and quantitative assessment of copper and iron corrosion by process water quality was assessed for year in a field study using finished waters produced from seven different treatment process and 18 pilot distribution systems (PDSs) that were made from unlined cast iron (UCI) and galvanized steel (G) pipes, and lined cement cast iron (LCI) and polyvinyl chloride (PVC) pipes taken from actual distribution systems. . Corrosion potential was compared qualitatively and quantitatively for all seven waters by monitoring copper release from copper loops and iron release from the PDSs. In particular, the corrosion potentials from finished water treated by nanofiltration, lime softening, and GAC treatment processes for different source waters were examined and compared.

Experimental Methods

Pilot Plant

Seven different waters made from blends of finished waters produced from treated groundwater, surface water, and desalinated water were distributed to eighteen pilot distribution systems for one year. The identification, source and treatment systems used to produce these waters are shown in Table 0.1.

Table 0.1 Water source and treatment systems

No.	I. D.	Source Water	Unit Processes
1	G1	Groundwater	Aeration, Disinfection, pH stabilization
2	G2	Groundwater	Softening, Sedimentation, Sand Filtration, Disinfection, pH Stabilization
3	G3	Groundwater, RO and S1	Softening, Sedimentation, Sand Filtration and Disinfection, pH Stabilization
4	G4	Groundwater, RO and S1	Nanofiltration, pH Stabilization
5	S1	Surface Water	Coagulation, Flocculation, Sedimentation, Ozone, GAC bio-reactor, Disinfection, sand filtration, pH Stabilization
6	S2	S1 after sedimentation	Nanofiltration, pH Stabilization
7	RO	Groundwater	5 um cartridge pre-filtration, RO, Disinfection, pH Stabilization

All finished waters were treated by aeration, stabilization and chloramination. The G1 process consisted of only aeration, stabilization and chloramination, which is typical for Florida groundwaters. Water was transported weekly from the Hillsborough River, stored in two 7,000 gallon tanks and treated by ferric sulfate coagulation, settling, cartridge filtration (CSF), ozone and GAC filtration before post treatment. Some of the S1 process water was diverted to a NF membrane pilot unit for the S2 process. RO water was produced by high pressure membrane filtration of groundwater and addition of sea salt to simulate the RO finished water. A blend of finished water of 62 % G1, 27 % S1 and 11 % was further treated by nanofiltration, which was G4. G2 was softened water. G3 was a softened blend of partially treated waters, and like G4 was of interest to a TBW member government.

The PDSs consisted of fourteen hybrid lines and four single material lines as shown in Figure 0.1. PDSs were 100 feet long and made from pipe taken from MG distribution systems. Fourteen PDS were made from PVC, lined cast iron (LCI), unlined cast iron (CI) and galvanized steel (G) pipes. Four PDSs were made with a single material. Water quality was changed every three month by changing the influent PDS blend, hence the project was conducted in four phases over one year.



Figure 0.1 Pilot-scale pipe distribution system research site. Fourteen hybrid material pipes and four single material pipelines

Lead and Copper Loops

The PDS effluent was fed to eighteen identical copper loops as shown in Figure 0.2, which contained one each 50:50 tin: lead coupon. Thirty feet of 1/4" copper tubing was used in

each loop. The samples for copper and lead monitoring were contained in the first twenty-two feet. All other fittings and materials were polymer materials, typically PVC. The coupon surface area was 3.38 square inches, and was equivalent to 17 joint-ends or 7 to 8 fittings given a 1/8th inch bead on the inside of each 0.5 inch diameter joint. This assumption was reasonable for a kitchen sink. Samples were collected occurred after a 6 hour standing period. Dissolved oxygen, pH, alkalinity, calcium, magnesium, silica, copper and lead were monitored in and out of each loop.

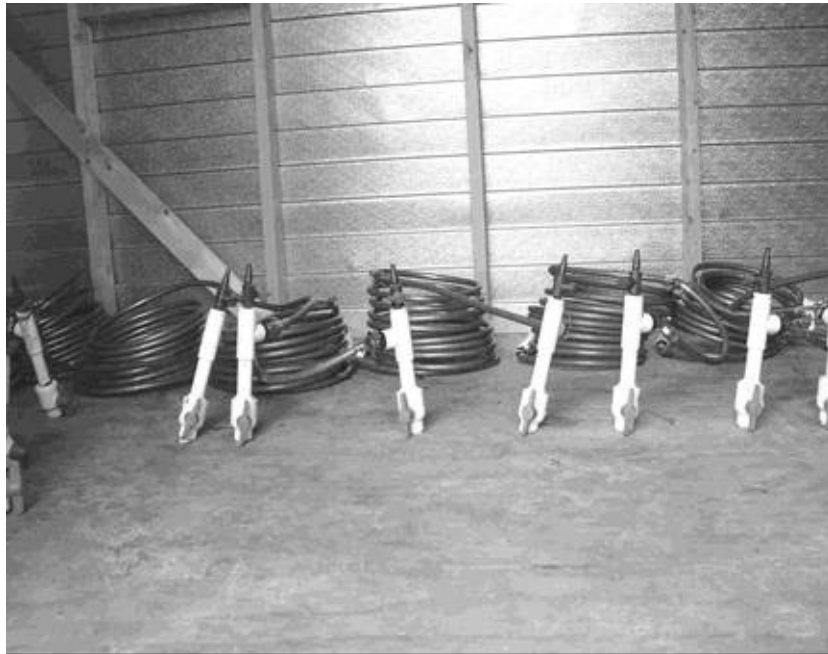


Figure 0.2 Eighteen identical copper loops connecting with eighteen PDSs for LCR study

Results and Discussion

PDS influent water quality is shown in Table 0.2. The finished groundwater (G1) had relatively high alkalinity, hardness, and TDS. Treated surface water (S1) had relatively high sulfate and TDS. Desalinated water (RO) had relatively high chloride. Blended water quality depended on blending ratio of finished waters. This work focuses on the water quality and corrosion potential comparisons to iron and copper by source and processes.

Water Quality of nanofiltration and conventional treatment processes

The average water quality for the one year of study is shown in Table 0.2. The water quality was divided into three groups for the purpose of comparing corrosion potential of the waters within a group. S1, G1 and RO are from group 1 representing different sources. S1 and S2 are group 2 representing the same source but different treatments. G3 and G4 are group 3 representing the same source but different treatments.

Table 0.2 Blending ratios and influent copper loop water quality

Blending Composition	Blending Ratio	Alkalinity (mg/L)	pH	Cl ⁻ (mg/L)	SO ₄ ²⁻ (mg/L)	DO (mg/L)	TDS (mg/L)	Ca ²⁺ (mg/L)	Si as SiO ₂ (mg/L)	Temp. (°C)	UV-254 (cm ⁻¹)
G1	100	207	7.87	28.9	26.1	6.5	421	84.8	13.7	24.2	0.060
S1	100	60	7.92	37.1	190.2	6.3	423	56.5	10.0	24.0	0.024
RO	100	69	8.06	91.7	5.8	5.2	267	28.7	3.5	24.1	0.028
G2	100	89	7.92	23.0	26.0	6.9	227	34.1	13.7	24.2	0.057
G3	100	61	8.13	49.7	79.0	6.2	306	35.4	10.4	23.9	0.043
G4	100	88	8.17	43.9	6.8	6.3	233	35.0	10.0	24.0	0.028
S2	100	66	8.13	68.5	12.7	5.6	239	28.0	8.8	23.9	0.029
G1-S1-RO	62-27-11	147	7.91	40.1	77.4	5.5	394	66.4	10.8	24.2	0.046

Corrosive Effect of Typical Ions on Iron and Copper

Alkalinity and pH have been identified as the most significant factors affecting copper release. Sulfate is a secondary factor that enhances copper release by forming a CuSO_4^0 soluble complex. This complex is much weaker than carbonate and hydroxide complexes, which compose more than 80% total soluble copper speciation. Chloride ions can increase soluble copper release by forming soluble CuCl_2^0 and CuCl^+ complexes, but these complexes account for less released copper than carbonate and hydroxide complexes. Sulfates and chlorides may inhibit the formation of particulate copper, which may offset the contribution of their associated complexes to total copper release. Based on equilibrium, the species shown in equation (0.1) account for more than 99% of the soluble copper in drinking water assuming equilibrium and $\text{Cu}(\text{OH})_2$ or CuO is the controlling solid phase.

$$\begin{aligned} [\text{Cu}]_T = & [\text{Cu}^{2+}] + [\text{CuOH}^+] + [\text{Cu}(\text{OH})_2^0] + [\text{Cu}(\text{OH})_3^-] + [\text{CuHCO}_3^-] \\ & + [\text{CuCO}_3^0] + [\text{Cu}(\text{CO}_3)_2^{2-}] + [\text{Cu}(\text{OH})_2\text{CO}_3^{2-}] \\ & + [\text{CuCl}_2^0] + [\text{CuCl}^+] + [\text{CuSO}_4^0] \end{aligned} \quad (0.1)$$

Iron chemistry is different from copper chemistry. Except for bicarbonate, chloride and sulfate are the two most important ions affecting the release of soluble iron. Our experiments demonstrated that high chloride and sulfate produce more iron release, but high alkalinity will inhibit iron. Thermodynamic models developed describing the soluble iron is shown in equation (0.2) assuming the equilibrium has been reached and FeCO_3 as controlling solid phase in water[10]. As shown by the mass balance in (0.2), soluble iron increases as chloride and sulfate

increases. Increasing bicarbonate alkalinity inhibits soluble iron release because FeCO_3 is the controlling solid phase.

$$Fe_T = [Fe^{+2}] + [FeOH^+] + [Fe(OH)_2^0] + [Fe(OH)_3^-] + [FeHCO_3^+] + [FeCO_3^0] + [FeSO_4^0] + [FeCl^*] \quad (0.2)$$

Group 1 water quality

G1 had relatively high alkalinity, calcium, silica, and organic content (UV-254). G1 water quality was very close to the raw water quality except for pH and residual changes from stabilization and disinfection. Sulfates were relatively higher in S1 due to ferric sulfate coagulation. S1 and G1 treatment processes do not remove dissolved polyvalent ions effectively, thus their TDS was relatively higher. RO rejects all ions effectively but because of high chlorides in saline sources, finished chlorides are relatively high and were relatively high as shown in Table 0.2.

Group 2 water quality

Water quality variation in group 2 was caused by treatment since both S1 and S2 had the same raw water source. Relative to GAC filtration, NF filtration rejects ions, is shown by the S1 and S2 TDS in Table 0.2. Sulfates are added to S1 during coagulation; however sulfates are highly rejected by NF so there is a large TDS difference between S1 and S2. This All waters were stabilized before blending; consequently the S1 pH is slightly lower than the S2 pH because of the difference in calcium.

Group 3 water quality

Alkalinity and sulfate varied more than other water quality parameters. The difference in alkalinity of the source water was due to the high alkalinity in the ground water. As noted, the difference in sulfates was due to ferric sulfate coagulation. Nanofiltration removes all ions where softening only removed calcium and alkalinity in this work.

Corrosion Potential Comparison

G1, S1 and RO

Physical Factor Impact

The total iron and copper released for group 1 is shown in Figure 0.3 and Figure 0.4. Temperature has been shown to increase metal release (15). Although metal release did increase with temperature, the increase was the same for the group 1 waters. Temperature was equal for each sampling event and was not a factor comparing metal release among the waters in each group. These results were consistent during the calendar year of operation.

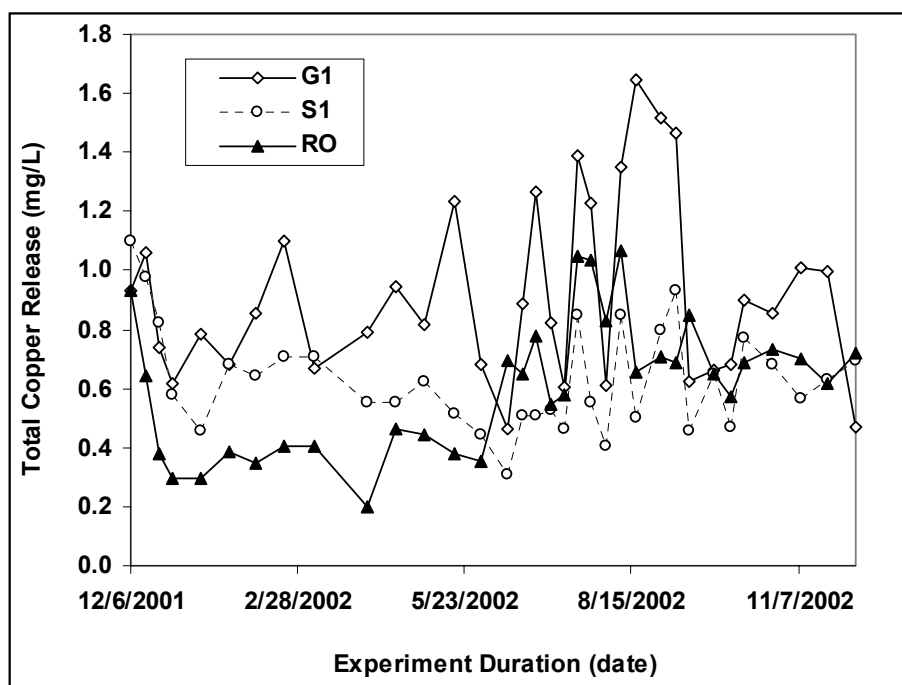


Figure 0.3 G1, S1 and RO total copper release

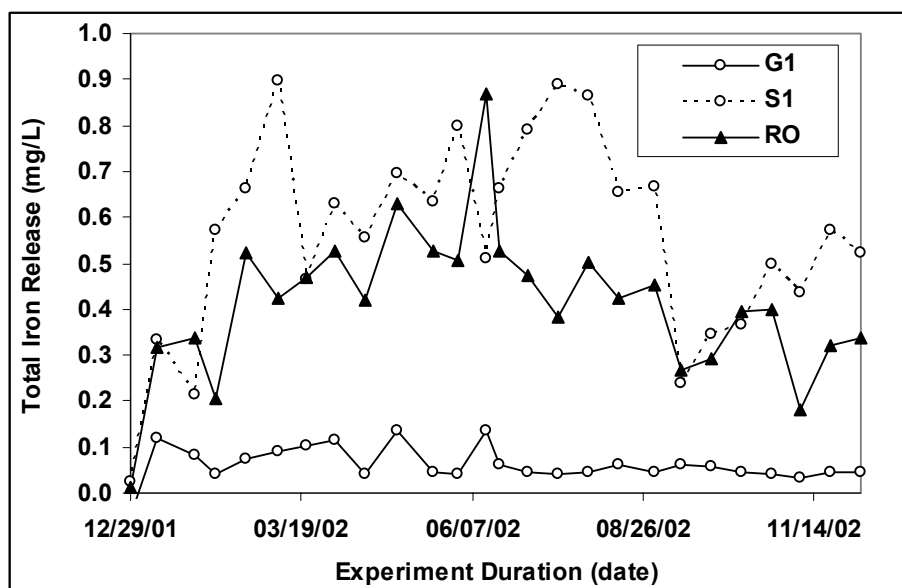


Figure 0.4 G1, S1 and RO total iron release

Chemical Factor Impact

As shown in Figure 0.3 and Figure 0.4 the most copper was released from G1. As noted there were large alkalinity differences in the G1, S1 and RO waters and alkalinity significantly affects copper release. Conventional treatment does not change alkalinity and G1 has the highest alkalinity (4 meq/L). Enhanced coagulation was used to produce S1 and has the lowest alkalinity (1 meq/L), which was the same alkalinity of RO finished water. S1 and RO pH_s was higher than G1 pH_s, which reduced RO and S1 copper release relative to G1 copper release. RO alkalinity can be adjusted to the raw water alkalinity using alkalinity recovery, which significantly reduces the corrosivity of RO finished waters. The average alkalinity for G1, S1 and RO finished waters was 207 mg/L, 60 and 69 mg/L as CaCO₃ respectively. Even though chloride was much higher in RO finished water, the potential for total copper release was not adversely affected as previously noted. Sulfates in the G1, S1 and RO waters were 26.1 mg/L, 190 mg/L and 5.8 mg/L. Sulfate complexes slightly increase soluble copper release.

Obviously, the lowest iron release was for G1 finished water because of the relatively high alkalinity. RO total iron release was lower than total S1 iron release at similar alkalinities. Both sulfate and chlorides have been identified as contributing factors for iron release, these results suggest sulfate has more impact on total iron release than chloride. However, there was no apparent difference in copper release for sulfate and chloride. Generally speaking, copper release was always higher for G1, while there was no significant difference between S1 and RO.

Comparison of Nanofiltration and GAC filtration

Figure 0.5 and Figure 0.6 present total iron and copper releases produced from S1 (GAC) and S2 (NF) waters, respectively. It is clearly noted that copper out of GAC water was higher

than that of NF except in short period. For iron, however, the difference went through the entire experiment period except two data pairs. More interestingly, for both copper and total iron, the metallic release appeared as analogous trend within each phase with respect to S1 and S2.

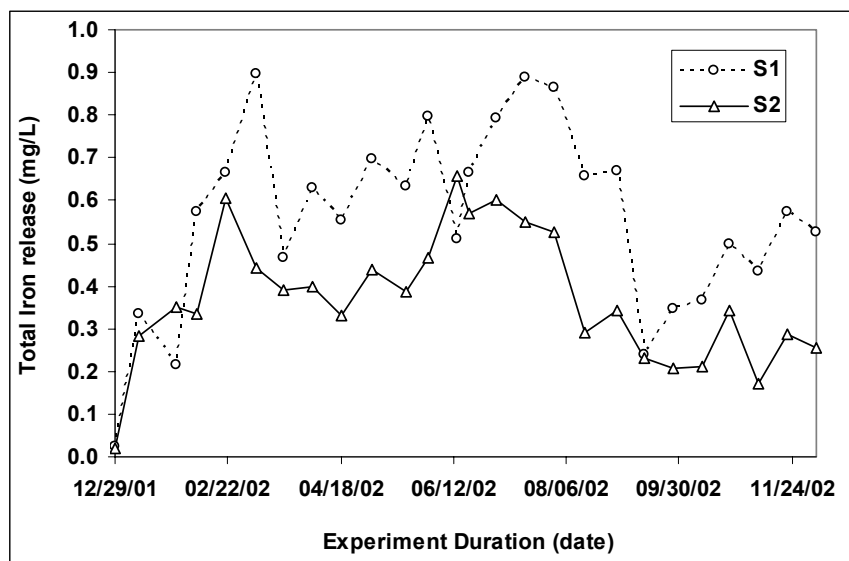


Figure 0.5 S1 and S2 iron release

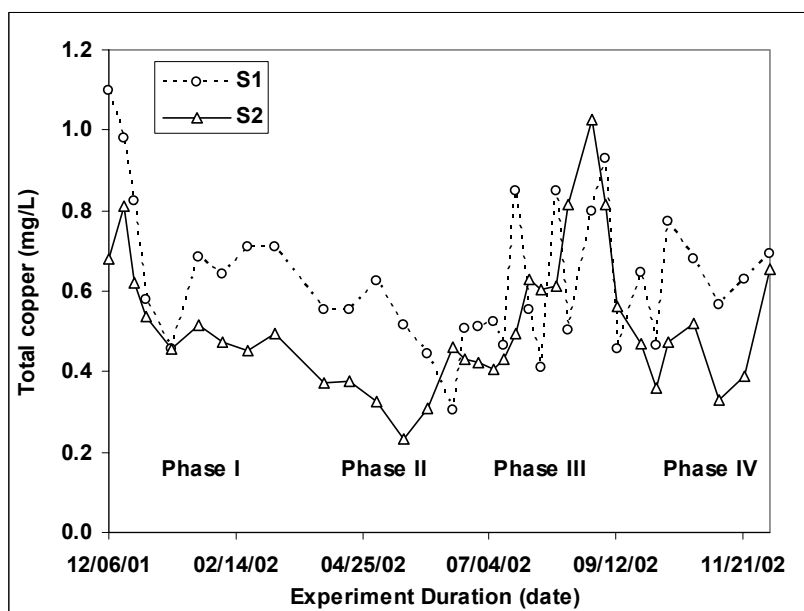


Figure 0.6 S1 and S2 copper release

Physical Factor Impact

As noted previously, all samples were collected at the same time so differences between S1 and S2 metal release due to temperature and calendar time can not be identified. However there is a difference between S1 and S2 during some time periods. These differences have to be due to other than physical factors.

Chemical Factor Impacts

Iron and copper release increases as pH decreases based on solubility. Since pH is a log function, a small pH decrease will enhance metal release. Lower pHs resulted in higher metal releases in this work. Through the entire year, more than 90% of S1 pHs were lower than S2 pHs, and more than 90 % of the released total copper and iron for S1 were higher than for S2.

Chloride and sulfate also affected S1 and S2 metal release. Alkalinity and pH were most the most significant water quality parameters affecting copper release. Since alkalinities were similar for S1 and S2, the difference in total copper release from S1 and S2 is due to the smaller difference in pH. For Iron, there were other factors than pH and alkalinity.

Chloride and sulfate can accelerate metal oxidation by providing negative ions to neutralize the positively charged metal ions. Hence removing them from a free state and causing more impetus for oxidation of elemental iron. Chlorides in S2 were higher than in S1, but sulfates were higher in S1 than in S2. Chlorides were inadvertently added during post treatment of S2, which is the reason chlorides are higher in S2 than S1. This was a process error and has nothing to do with treatment; in fact the chlorides should be slightly lower in S2 than S2 as NF does remove some chlorides. S2 pH is 0.2 units higher than S1. The increased S2 metal release was due to higher sulfate and lower pH relative to the S1 water. There is no clear evidence illustrating the single sulfate effect on total iron release. However, the narrow pH range and associated iron sensitivity will not cause such obvious differences without sulfate assistance. Additionally, the higher S2 chloride did not greatly affect iron release, which indicates pH and sulfate are more important to iron release. For these waters, S1 was more corrosive with respect to the total iron release than S2. NF finished waters will typically release less copper and iron in distribution that enhanced coagulation finished waters when alkalinity recovery is controlled. Calcium rejection, alkalinity recovery, higher pH₂, lower sulfates and lower TDS will typically result in less metal release in NF treated waters relative to waters treated by enhanced coagulation.

Comparison of Nanofiltration and Softening

The total iron and copper released from the PDSs by G3 (lime softening) and G4 (nanofiltration) finished waters is shown in Figure 0.7 and Figure 0.8. Total iron release was higher in phase I and III for G3 than G4, and equivalent in phase II and IV. Copper release from G3 and G4 was not erratic, but did exhibit periods when G4 copper was higher and lower than G3.

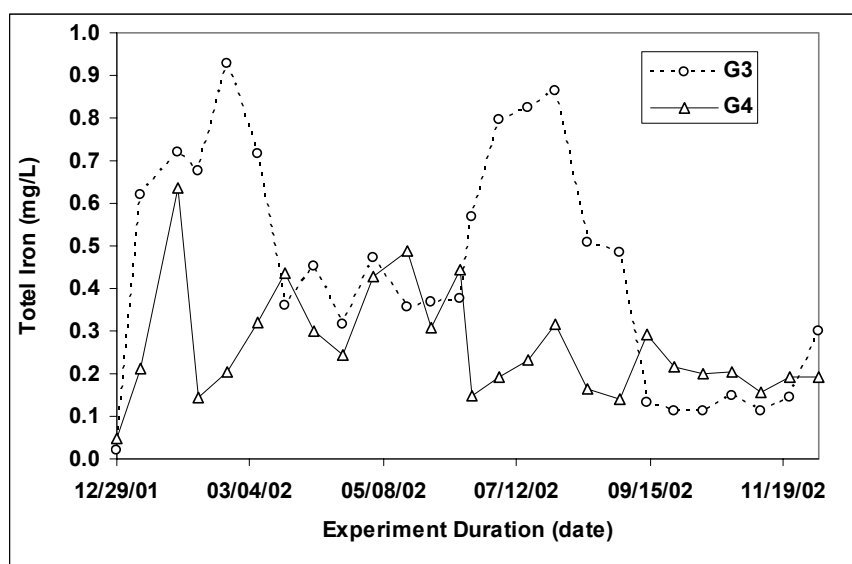


Figure 0.7 G3 and G4 iron release

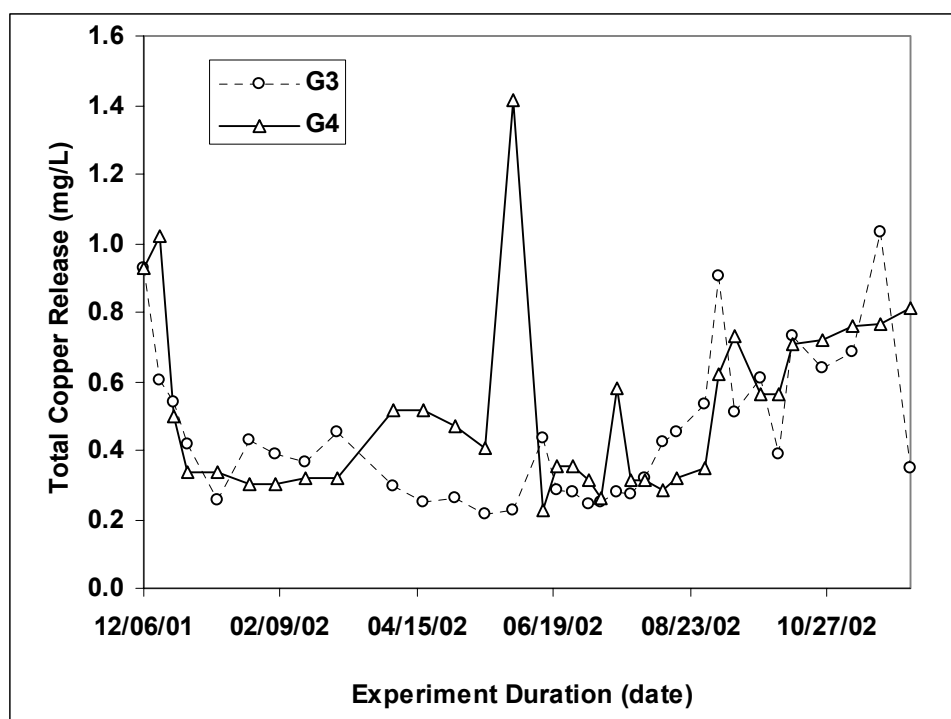


Figure 0.8 G3 and G4 copper release

Physical Factor Examination

As previously stated, it was not possible to detect any temperature effects among treatment processes because all samples were taken simultaneously. The hydraulic residence time in the PDS and the stagnation time in the copper loops were constant for the first year of study and incubation time effects could not be analyzed.

Chemical Factor Consideration

Softening produces lower alkalinity water than NF which need alkalinity recovery and or addition. Hence, alkalinity in these two finished water is quite similar. As expected, their corrosive potential is not much different because of their similar alkalinity values, which is 61 and 88 mg/L as CaCO_3 , respectively. However, there is a obvious higher copper release in NF

water in the period between earlier April and earlier June than that of GAC water. Data check shows that alkalinity was large different in G3 and G4 water between Apr.10,2002 and June 10,2002 (in Phase II). The average alkalinity within that period for G3 and G4 was 52mg/L and 103mg/L as CaCO_3 , respectively. G3 and G4 pH was 8.27 and 8.20, which were almost identical. Hence, the difference in released copper in that period is due to alkalinity differences. Copper was not impacted by sulfates. Average sulfate through the entire experiment period in soften water was 79.0mg/L but only 6.8 mg/L in NF water. Such large differences in sulfate produced negligible differences in copper release in other phases.

General Process Comments

As shown in

Table 0.3, some general comments concerning the effect of the investigated processes on total copper and iron release can be made. Conventional treatment did very little to change source water quality and did produce low iron and high copper release. Additionally, removal of hydrogen sulfide by conventional aeration and chlorination produces sulfur turbidity, which will produce iron and copper sulfides and increase iron and copper release. Softening reduces TDS and alkalinity which reduced total Cu release and had a variable effect on iron release as the higher pH_s somewhat offset the lower alkalinity. Nanofiltration will remove almost everything from Fresh Water, which benefits copper release and increases iron release and produces a very non-corrosive water from ground or surface sources. Enhanced coagulation of surface water produced a low alkalinity, high sulfate finished water. Hence pH_s and sulfates were high but alkalinity was low, which had somewhat offsetting effects on copper release and iron release. RO has similar effects on iron and copper release as NF except the high TDS will typically produce high chlorides in the finished water will adversely affected iron release and requires alkalinity recovery to control copper release. As shown in

Table 0.3, no process is perfect and any process could be modified to offset unwanted copper and iron release.

Table 0.3 Relative ranking of processes on copper and iron release for blending project

Process	Source	Factors				Release	
		pH _s	HCO ₃	SO ₄	Cl	Cu	Fe
Conventional	Ground	Low	High	Low	Low	High	Low
Softening	Ground	High	Low	Low	Low	Neural	Neutral
Nanofiltration	Ground or Surface	High	Low	Low	Low	Neutral	Neutral
Coagulation	Surface	High	Low	High	Low	Low	High
Reverse Osmosis	Sea	High	Low	Low	High	Neutral	Neutral

Conclusion

- Enhanced coagulation followed by ozonation and GAC filtration produced water that released more total iron and copper than finished water produced by nanofiltration. The higher sulfate concentration and lower pH of the coagulated water resulted in greater metal release from the unlined cast iron pipes and copper loops than for the nanofiltered water. Alkalinity addition to coagulated waters could make the coagulated waters non-corrosive with respect to iron. However, inhibitor addition is recommended for control of copper release for both waters.
- The release of total iron in the cast iron pipes in the pilot distribution system for lime softened waters was slightly higher than nanofiltered water. There was no statistical difference for copper between the softened and nanofiltered waters.
- Nanofiltration produced the least corrosive water in these studies.

References

- (1) Thompson, M.A., B. Azar. 1998 Evaluation of conventional and membrane processes for softening in a North Carolina groundwater. *Desalination*. 118(1-3):229-238
- (2) Bergman, R. 1995 Membrane softening versus lime softening in Florida: a cost comparison update. *Desalination*. 102(1-3):11-24
- (3) Duran, F.E., and G.W. Dunkelberg. 1995 A comparison of membrane softening on three South Florida groundwaters. *Desalination*. 102(1-3):27-24
- (4) Yeh, H.H., I.C. Tseng, S.J. Kao, W.L. Lai, J.J. Chen, G.T. Wang, and S.H. Lin. 2000 Comparison of the finished water quality among an integrated membrane processes, conventional and other advanced treatment processes. *Desalination*. 131(1-3):237-244
- (5) AWWARF “Internal Corrosion of Water Distribution Systems” DVGW-TZW Second Edition 1996
- (6) Michael R.S. and A.L. Darren. 1995 Effect of pH, DIC, Orthophosphate and Sulfate on Drinking Water Cuprosolvency. EPA/600/R-95/085
- (7) Evans, and U. Richardson c1960. The corrosion and oxidation of metals; scientific principles and practical applications. London, E. Arnold
- (8) McIntyre, P., and A.D. Mercer. 1993 Corrosion and related aspects of materials for potable water supplies London : Institute of Materials
- (9) Montemor, M.F., A.M.P. Simoes, and M.G.S. Ferreira, 2003 Chloride-induced corrosion on reinforcing steel: from the fundamentals to the monitoring techniques. *Cement & Concrete Composites*. 25(4-5):491–502
- (10) Zhijian Tang Dissertation 2003 1University of Central Florida